UAV (drone) aerial photography and photogrammetry and its utility for archaeological site documentation

2017

Scott Hamilton
Jason Stephenson
Lakehead University.

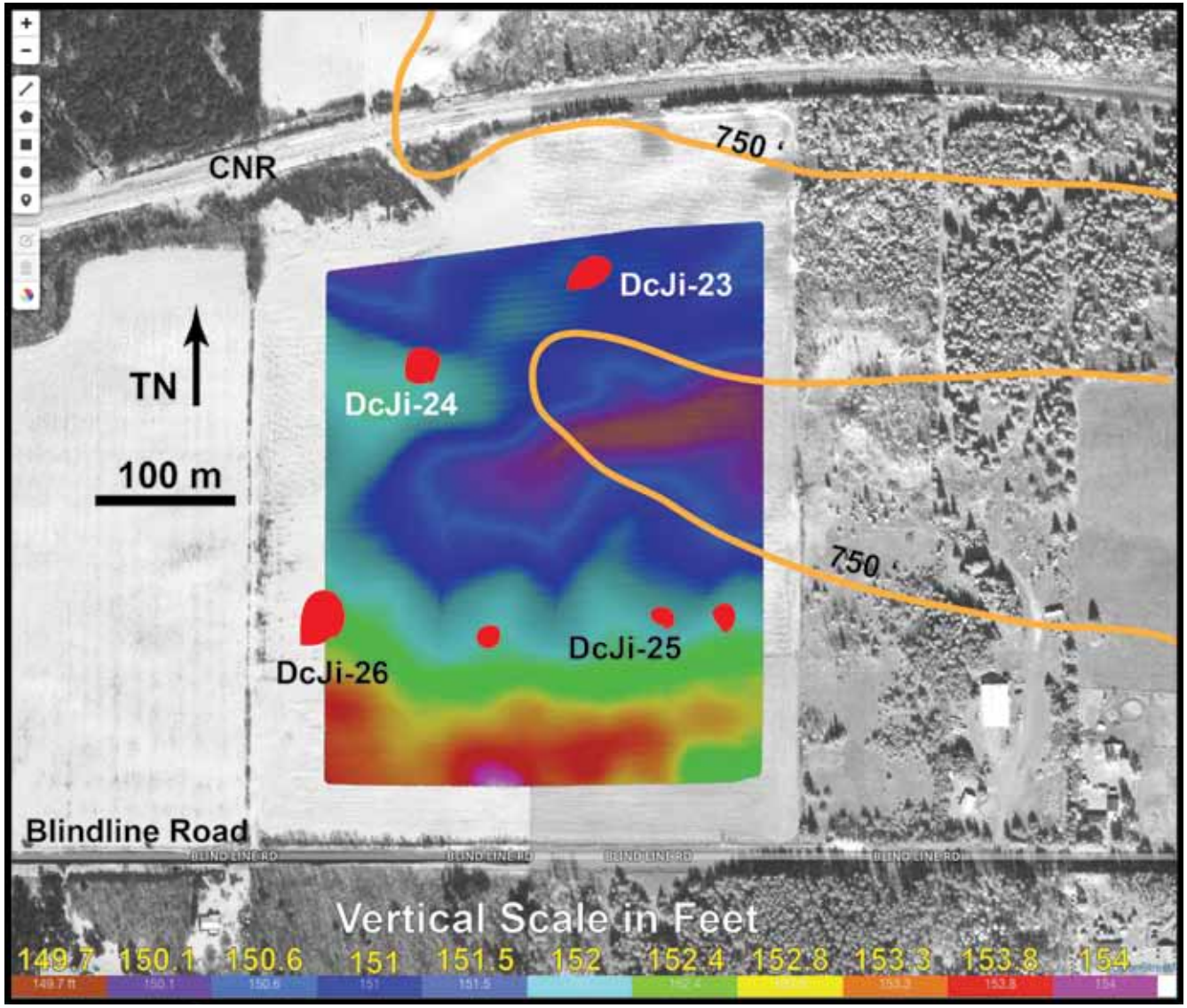

Ontario Association of Professional Archaeologists
Occasional Paper #2

Abstract

The technological development of Unmanned Aerial Vehicles (UAVs or drones) and their marketing as recreational devices offers considerable potential for field documentation and research in a number of disciplines, including archaeology. Early experimentation with UAVs is reviewed, outlining strengths and limitations of the technology using several case studies. This includes evaluation of data resolution and precision under different conditions compared to conventional maps and satellite imagery, and also consideration of equipment purchase and operational costs relative to cost-effectiveness of drone-assisted site mapping. The utility of UAVs for archaeological mapping is considerably enhanced when used with semi-autonomous flight planning software, photogrammetric data processing, and refinement and analysis of output within Geographic Information Systems. One important constraint upon widespread use of UAV-assisted air photography as an archaeolgoical research tool is the increasingly complex regulatory environment, coupled with the requirement for insurance coverage.

Table of Contents

List of Figures

UAV (drone) aerial photography and photogrammetry and its utility for archaeological site documentation

2017
Scott Hamilton
Jason Stephenson
Lakehead University.

Preface

Since an earlier version of this paper was first distributed as an internet resource (Hamilton and Stephenson 2016), we have continued experimentation with low elevation aerial photography and photogrammetry at archaeological sites in s. Manitoba and n.w. Ontario (Hamilton 2017, Hamilton in press, Hamilton and Stephenson 2017). We have shifted from equipment evaluation, developing flying skills and generating imagery, and towards the application of photogrammetry and 'value-added' output deriving from GIS manipulation. We have documented comparatively small-scale earthworks, ruins and standing structures, and natural and anthropogenic features important for contextualizing archaeological sites. We have compared UAV image resolution to conventional satellite imagery, horizontal and vertical precision of geo-referenced drone maps, and cost-effectiveness of UAV mapping as an alternative to conventional methods. More recently the UAV photogrammetric output has been processed and augmented within Geographic Information Systems (GIS). Examples of this latter output has been added here to the original paper (Hamilton and Stephenson 2016).

Ironically, as the technology continues to improve, we note the greatest impediment to routine research application is the increasingly complex regulatory environment coupled with insurance liability. This paper summarizes some of the research outcomes, reviews new efforts at data processing, and the challenges of employing such disruptive new technology in applied and academic archaeological research.

Introduction

Over the past several years Unmanned Aerial Vehicles (UAVs or drones) have rapidly advanced through improved flying ease, and high quality still and video photography. They have become prominent consumer products, and offer potential for low elevation aerial photography to support research and commercial applications. Most such applications feature visible light photography, but we anticipate that future remote sensing applications will include thermal and near-infrared imagery and beyond.

Consumer-grade UAVs reflect three general categories: 1) comparatively inexpensive entry-level drones used for casual hobby flying; 2) so-called 'prosumer' machines that have significant technical capacity, and good quality integrated cameras and gimbals; and 3) high capacity units intended for professional users. The professional machines have sufficient payload capacity to carry extra batteries, sophisticated gimbals, and high quality interchangeable cameras and lens. This third class of machines already have capabilities beyond visible light photography. The equipment discussed here falls in the intermediate category that feature significant technical capacity, but are marketed primarily for serious hobbyists.

The dynamism of the consumer drone market results in rapid obsolescence as new features and capacities are introduced. We also note a recent shift in UAV development, with increased focus on professional applications. Despite this, we continue to use a prosumer model as a research tool. This reflects 'price point' issues, as well as the comparatively high quality and ease of use of such devices.

Figure 1 The Blade 350 QX3 quadcopter. It lacked sufficient telemetry control and image quality to support archaeological research.

The issue is no longer whether these machines can support aerial archaeology. Rather, how can they be used for more than novelty or orientation images, and become tools for mapping, spatial analysis and other heritage documentation.

Early Efforts

In the fall of 2014, Hamilton purchased a UAV (quadcopter) to address its utility for archaeology. This was stimulated by Stephenson's HBA Honours thesis research, and in anticipation of his 2015 admission into a Lakehead University graduate program.

The first purchase was a Blade 350 QX3 equipped with a camera capable of 16 MP still photography and 1080p/60 frames per second video (Fig. 1). Imagery is stored on a mini SD card inserted into the unit, with camera and drone controlled through Wi-Fi interface to a tablet or smart phone. We used an early generation iPad tablet. Communication range between the drone and radio controller is only several hundred metres (visual line of sight). The Blade also features a compass, GPS, accelerometer and barometric altimeter, and a battery life that permits about 16-20

minutes of flight time.

While fixed wing radio-controlled aircraft offer considerable capacity, we chose the quadcopter to enable stationary photography, and vertical take-off and landing. This is important for work in forested regions, but fixed wing craft offer significant advantages through extended flight times to document larger areas, higher payload capacity, and more diverse camera choices.

The Blade was assessed through the fall and winter of 2014-15. It demonstrated good GPS lock and precise automatic 'return to home' capability. However the limited flight telemetry control and 'fish eye' distortion of the camera limited its utility for archaeological documentation.

In the spring of 2015 Hamilton crashed the machine, damaging the camera, gimbal and airframe. While the fragile camera assembly could not be repaired, the drone body was fixed using epoxy glue, and is again air-worthy. In light of the relatively high replacement cost (and inadequate imagery), it was decided to not replace the camera and gimbal, and to await technological developments that overcome the Blade's limitations. The risk of crash damage, sometimes resulting in a loss of initial investment, is a serious consideration for potential users. One must think about drones as 'consumable supplies' that is mitigated by the strategic gain in data/mapping quality, and time saved in site documentation.

Ironically, the ease of machine operation may contribute to marginally trained flyers making mistakes during flight, or operating in sub-optimal conditions. Users should invest significant time in developing skills using simulation software, studying often cryptic manuals, and practising with the controls. These issues also help explain the increasingly strict regulations regarding UAV operation. In increasingly crowded airspace, UAV operators must be aware of their responsibilities and take measures to prevent flying in restricted airspace, near other aircraft, or in ways that risk harm to property or individuals.

The Blade's limitations constrain its utility for research, and it rapidly became obsolete. The current state of drone technology is consistent with the mid 1980s development of micro-computers, and the late 1990s development of GPS technology. While initially expensive and with limited capacity, the technology rapidly developed through recreational and commercial application. In our view, consumer-grade UAV technology is at the early 'breakout' stage that will lead to widespread application.

Evaluation of the Blade drone

Despite the limitations of the Blade drone, the testing outcomes remain useful. The most serious limitation was the 'fish-eye' distortion of the wide angle fixed focus camera. This is dramatically evident in Figure 2, a winter view of an art installation on the Lakehead University campus. This photograph was taken at a 45° angle, and at a comparatively low elevation. The sunlight reflecting off the snow resulted in exposure problems, with dark surfaces and the background being relatively 'featureless'. This could not be sufficiently corrected using image processing software, nor did the camera permit adjustment to accommodate difficult lighting conditions. The optimal lighting conditions are overcast days with few shadows. Waiting for the right light conditions is seldom realistic during field operations, and we have begun experimenting (with good results) using filters attached over the camera lens.

When examining Figure 2, it is clear that the wide-angle lens severely distorted the outer two thirds of the image. A white horizontal line was drawn on the unmodified image to mark the upper roof corners of a flat-roofed building in the background. The photographed roof line is distorted to form an upward arc in Figure 2:arrow. If such aerial images are to be used for photogrammetric processing, they must be processed using algorithms in image processing software. Given the number of images that would re-

Figure 2 Photograph of art installation using Blade quadcopter. It generated 16 megapixel images, but the limited aperture, shutter speed, white balance and exposure control limited image quality. Note the over-exposure caused by snow reflection, and the severe 'fisheye' distortion.

quire individual correction, this is a major time consideration. Since the lens profile for the Blade camera is not known, correction often required repeated iterations until the image 'looked right'. This is hardly satisfying, and is dependent upon some sort of 'control grid' in the image to provide a reference.

To assess the magnitude of this distortion, we used painted lines in a parking lot to provide the control grid (Fig. 3). Sixty metre tapes and metre poles provided a scale, and to document the dimensions of the parking lot. This control grid was sufficient to assess the apparent dimensions represented in the air photographs compared to the actual measured distances. While the gimbal was fully depressed to achieve a downward vertical orientation, it appears that it was not fully vertical. This resulted in more coverage to the north than to the south, and exaggerated the fish-eye distortion (Fig. 3).

Figure 3 reveals that significant differences exist between the 'real' versus 'apparent' linear distances represented by the rudimentary grid. The superimposed red solid and dashed lines also illustrated the complexity of the image distortion as one moves away from the centre of the frame. Without a grid superimposed on the ground, it is difficult to assess when lens correction filters have sufficiently addressed the distortion. A vertically oriented image taken with a different drone camera that features no fish-eye distortion is presented later to offer a point of contrast to Figure 3.

Fish-eye distortion is common with most aerial photography, and efforts at photogrammetry require closely spaced flight transects and significantly overlapping photographs. This overlap minimizes the problem because the most distorted outer edges of each image can be ignored. The slight differences in 'point of view' between overlapping images is also the basis of traditional air photo interpretation using stereo-paired images. It is also key to computer-assisted photogrammetry.

Achieving sufficient overlapping photo coverage using the Blade drone was difficult because of the limited telemetry control. One must rely on the camera 'Point of View' that is transmitted back to the iPad screen. While this might be viable if only a few photographs are taken of a specific point of interest, it is not effective to achieve systematic coverage of larger areas.

Our efforts involved one person flying the drone while the second took the photographs using the iPad. The iPad operator gave verbal instructions to the drone operator to place the machine in the proper position, and to adjust the gimbal. This was slow and frustrating as we worked out effective communication protocols. More seriously, such maneuvering expended significant battery power, thereby shortening the effective flight time.

The iPad/camera operator was forced to rely on his own judgement when to take successive pictures to achieve the required spatial overlap of images. In

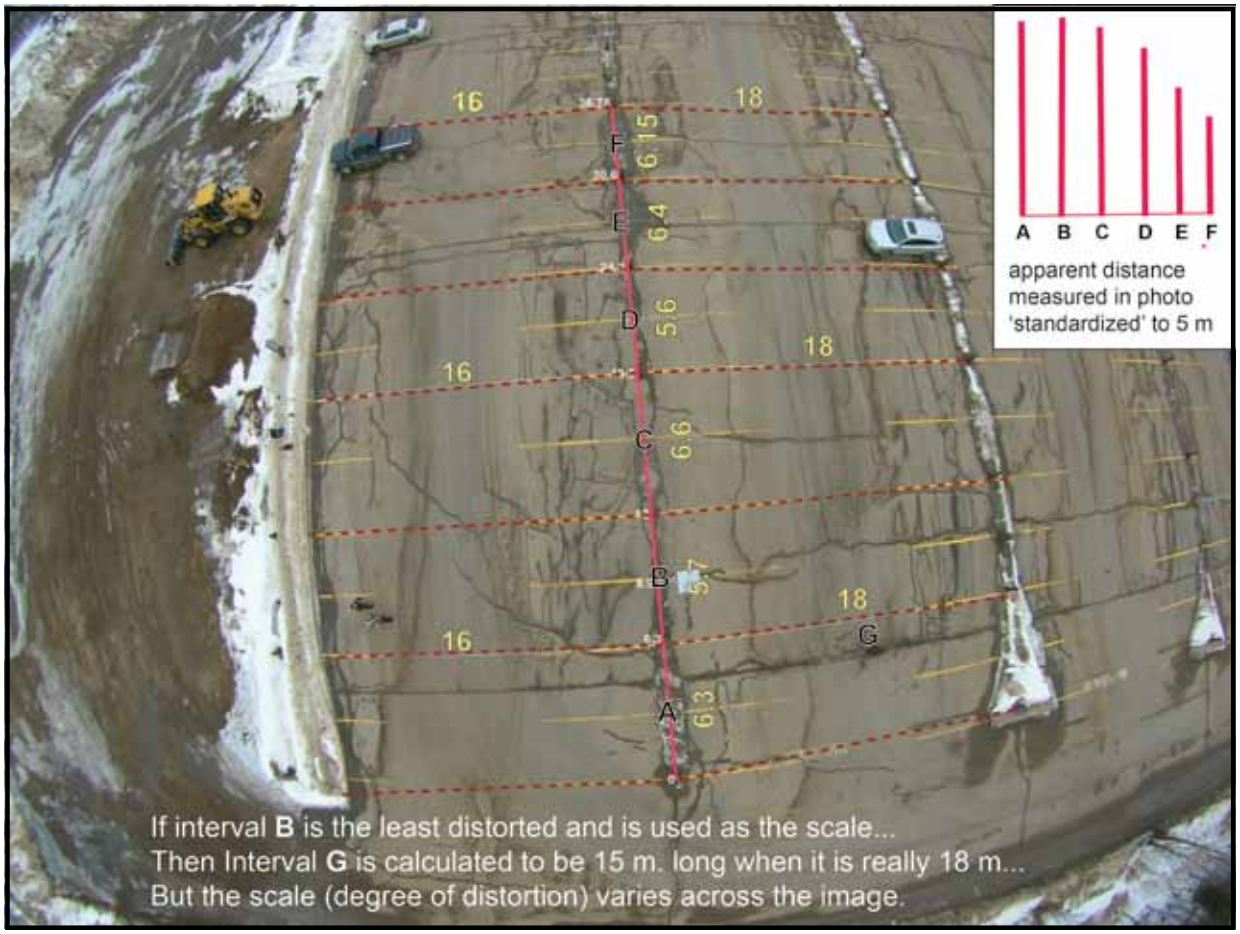

Figure 3 A test of the 'fish eye' camera distortion of the Blade drone. It was conducted using a 'grid' defined by parking lot lines. Sixty metre tapes were laid out to measure distances between painted lines. The yellow letters measure distances between the lines and the parking stalls. Note that the image is distorted disporportionately across the frame. While 'fisheye' can be 'corrected' using image processing software, the severity of the distortion in this image is problematic.

reality this was more a matter of chance than survey design. While practise might have improved our performance in achieving overlapping imagery at a standard height, technological improvements rendered this approach (and the Blade drone) obsolete, and it is now discontinued.

As the Blade drone did not transmit elevation information or remaining battery charge back to the operator, we had to estimate the height of the machine (while striving to maintain a constant elevation). Also problematic was the need to monitor time in flight using a wrist watch or stop watch. This can be difficult if the operator's hands (and attention) are fully engaged with the radio-controller and the drone. While the machine is programmed to emit flashing warning lights as battery power declines to a low level, such lights are hard to interpret if the machine is distant, or obscured by vegetation or sun glare.

Despite the ease of flight, drone operation is stressful, particularly while maneuvering around trees or other obstructions. Operators risk sensory overload while simultaneously monitoring the drone's flight, manipulating the controls, receiving verbal instructions, and monitoring flight duration. With this in mind the machine is programmed to unilaterally return to its start point (HOME) and automatically land if the pilot fails to heed the low power warning lights. Failure to properly monitor flight time was the primary cause of the Blade drone crash.

Another important consideration was addressing image resolution at various elevations, and determining whether objects of various sizes can be detected. We addressed this with photography at two estimated flight elevations. A small grid was established, and then large lithic flakes and bones were distributed around it. These objects exhibited maximum visibility since they rested on a mowed lawn. While not reflecting archaeological reality, the objective was to determine what object size could be reasonably detected at various flight elevations. The first image was taken at an estimated 30 m elevation in order to provide broader context to the grid (Fig. 4). The second image was taken at ca. 5 m elevation to only focus on the area where objects had been deposited (Fig. 5).

In Figure 4 the rudimentary grid defined with 60 metre tapes is faintly visible at ±30 m elevation, but the fish-eye distortion likely affects realistic representation of the spatial patterning of the objects, certainly more than 10-15 metres distant from the centre of the frame. The original image is too large (5.8 MB) to effectively illustrate (55 inches or 139.7 cm wide). It was processed within Adobe Photoshop to adjust its resolution from 72 DPI to 300 DPI, and then reduced to page size. This was calculated to balance acceptable image resolution with file size, while rendering it for printing. A portion of the original image was cropped and processed at a larger scale to reflect the actual resolution of the objects (inset in Fig. 4). While the larger bones were visible and somewhat interpretable, even the larger lithic pieces were not readily detectable. This is a consequence of the high elevation calculated to capture the whole area of interest, but at the cost of comparatively poor resolution of individual objects on the ground.

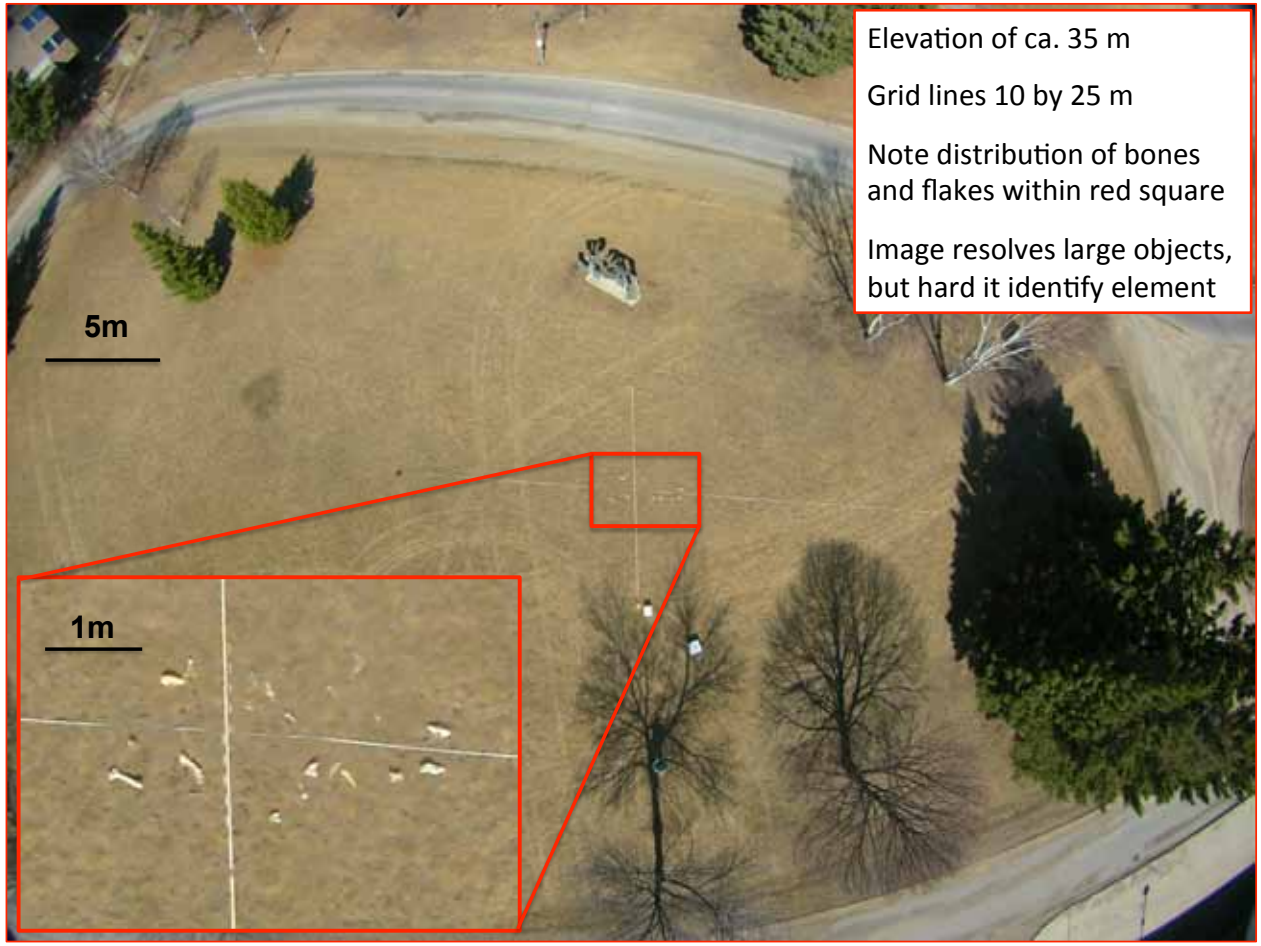

Figure 4 Documenting mock artifact scatters using the Blade drone. The 16 megapixel camera offered comparatively good resolution, even at significant height. At issue is whether image resolution allows identification of objects, and whether image distortion compromises interpretation of spatial relationships.

Figure 5 is an overhead photograph of the artifact distribution at an estimated 5 m height. This was initially quite encouraging as an area of 18 to 25 m^2 can be photographed at a relatively low elevation directly over the point of interest. This has obvious implications for documenting block excavations or surface features, particularly if the fish-eye distortion can be dealt with. Again, the original JPEG image was rendered at 300 DPI, and then reduced to page size. The individual large mammal bones are now readily identifiable (often permitting element identification), and the larger of the lithic debitage fragments can be seen (see two inset photos in Fig. 5). While yielding encouraging results, the image quality of objects is largely dependent on chance to achieve the right light exposure. This is as good as can be reasonably expected from this camera with very limited adjustability. Also of concern is whether the 'fish-eye' effect is distorting the spatial relationship between objects. Again, a control grid is required to determine whether lens correction filters have sufficiently addressed the problem. To confirm scale and image precision, it is wise to always include scales in the photograph. This is particularly important when individual images are re-scaled and cropped for different illustrative purposes.

Finally, we tested whether low elevation drone photography offers sufficiently improved interpretative resolution of site localities over readily available satellite imagery such as Google earth or Birdseye. That is, does drone-derived image quality and resolution justify the associated costs, or is it more cost-effective to utilize freely available satellite imagery or other cartography available for download? Of course, for consulting archaeologists such considerations are also tempered by the data quality expectations of the regulatory agency that reviews the reports. If comparatively coarse-grained satellite imagery is deemed sufficient and acceptable for reporting, then there is little immediate incentive to seek better quality cartographic data. At issue here is whether improved resolution through UAV photography significantly improves site interpretability with manageable costs. The first case study addresses the image resolution achieved using the Blade UAV, with subsequent discussion addressing output from a more sophisticated UAV (see section titled 'The Second Try').

Comparison of UAV with satellite imagery was first addressed at archaeological sites located along the McIntyre River on the LU campus (Fig. 6). While known since the 1970s, it was assumed that they had been destroyed by development of the campus. Site inspection by Clarence Surette and several students revealed lithic debitage exposed intermittently along walking trails that bisect the wooded banks of the McIntyre River. Surette then investigated these sites during the 2015 LU archaeological field school.

The sites of interest (Fig. 6, DcJh-13, 14, 15) coincide with a break in slope that may represent mid-Holocene shorelines of Lake Superior (Nipissing Transgression). The original 1970s archaeological survey suggested a possible Archaic cultural affiliation on the basis of the recovery of processed copper objects. This was reinforced with the recovery of a copper projectile point in 2015. In contrast, sites located at or near Glacial Lake Minong shorelines are thought to represent late Paleoindian occupation (Lakehead Complex) (Fig 6).

Surette sought to relocate the known sites (DcJh-13, 14, 15) that had been originally (and rather

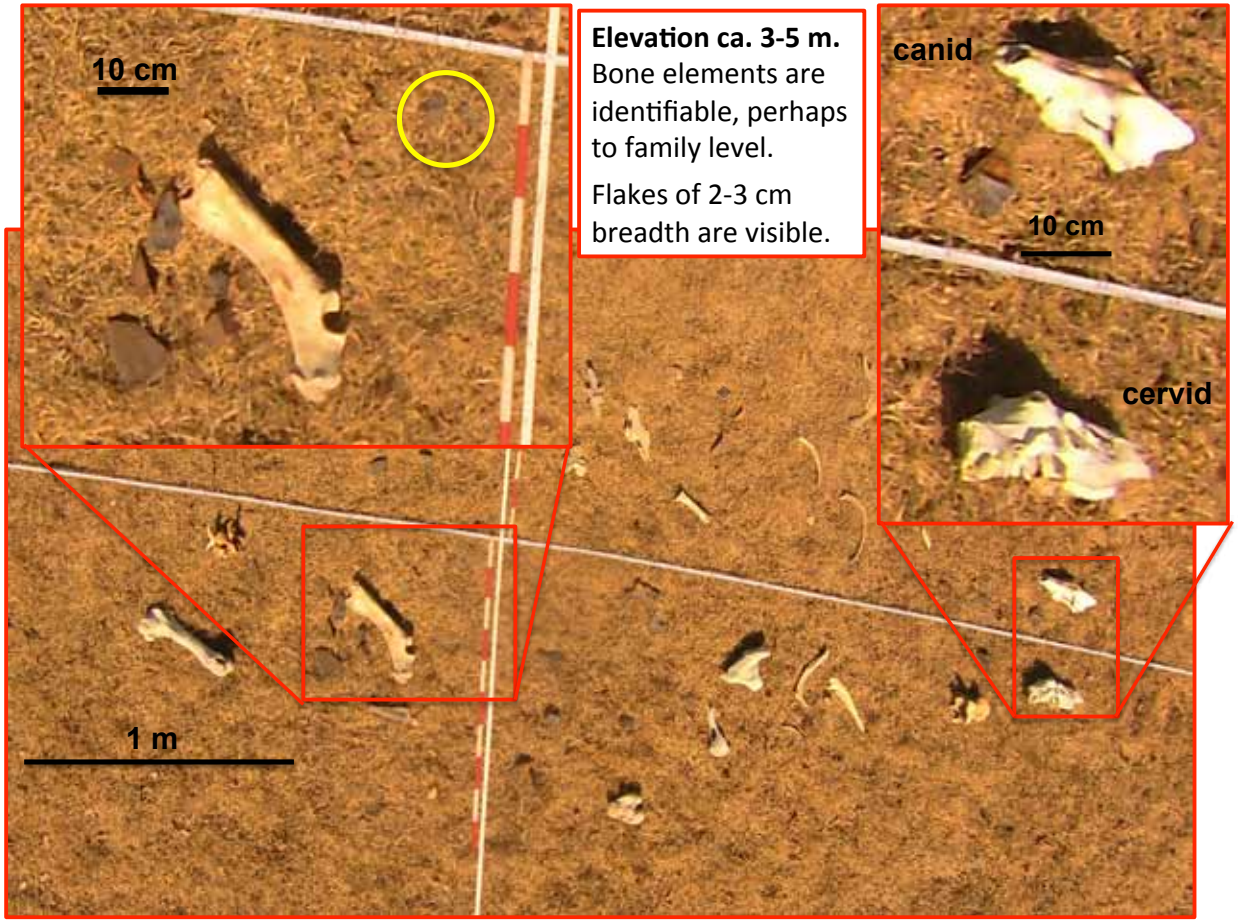

Figure 5 Air photo taken at ca. 5 metre elevation.

imprecisely) recorded using 1:50,000 NTS maps. GPS-supported documentation of the lithic scatters suggest several additional sites, and also natural landscape features relevant to possible mid-Holocene deposition. To this end conventional topographic mapping and UAV air photography were used to evaluate the supposed landscape associations.

Figure 7 contains a Google earth image of the locality. It contains several discrete lithic scatters along the McIntyre River, often near bedrock-controlled breaks in slope (marked in part by rapids) (Fig. 7). While affected by landscaping of the campus grounds, ground observation of local relief (coupled with sediment texture exposed in the test excavations) supported the notion that some of the deposits remain intact, and may represent the mid-Holocene (i.e. Nipissing Transgression) shoreline of Lake Superior.

The satellite image in Figure 7 dates to the spring of 2010 prior to deciduous leaf emergence, thereby offering maximum visibility of the ground surface. While appearing to be good resolution, a larger-scale inset illustration reveals that it is insufficient to detect and interpret surface details observed during the ground inspection. At issue is whether the Blade drone offered useful imagery to confirm ground observations.

Figure 8 is a contour map of the site locality with choropleth plots of the artifact density deriving from the shovel tests. The inset photograph is a detail of a Blade drone photograph taken shortly before it crashed. It shows individuals and equipment within one of the test excavation areas, and when enlarged (Fig. 9), ground details are readily interpretable. An enlarged portion of the Google earth satellite image for the same area is presented to offer a point of contrast (Fig. 9 inset).

Figure 9 reveals details of the ground surface despite the tree cover, and suggests the utility of low-elevation photography. This might enable detection of archaeological surface features, vegetation patterns and other landscape features relevant for interpretation. While such photography offers significant advantages over the satellite imagery, we emphasize that pilot error caused the drone to crash while taking these images. At issue is whether useful imagery can be collected with manageable risk. These issues are explored more fully with the evaluation of the replacement drone.

The Second Try

The DJI Phantom 3 series was released for sale in the summer of 2015, but was superseded, and replaced by new models by the middle of 2016. The Phantom 3 and 4 machines have overcome most of the limitations identified during our experiments with the Blade. Hamilton purchased the Phantom 3 Advanced model (Fig. 10) that differs from the Professional model primarily through the higher quality video capability of the latter. At the time these machines offered comparatively high technical capacity, but significantly less cost than the professional grade machines. The built-in 'Lightbridge' signal streaming feature significantly improved communications capacity, but necessitated the purchase of a 4th generation iPad mini.

DJI currently dominates the consumer drone market, particularly the upper consumer and professional grade. It has been aggressively developing its technical capacity, and appears to be moving into commercial applications. This is signalled by the integration of thermal imaging cameras, user-customizable drones, and equipment intended for 'precision farming' (agricultural herbicide spraying).

DJI products (along with other brands) are now being marketed by major electronics retailers, and DJI's current market dominance is encouraging third party software developers to produce Apps specifically for its products. A remaining issue is the comparatively short battery life that constrains flight to about 20-23 minutes. This is consistent with the balance of consumer-grade drones and likely reflects the current state of development of micro-processors and the lithium polymer batteries.

Since the fall of 2016 we have continued testing and experimentation using the Phantom 3 machine on archaeological sites in Manitoba and northern Ontario. These tests focused on assessing the drone's ability to characterize the geographic and topographic context of site localities. Notably, we have not suffered further serious crashes or any damage to the

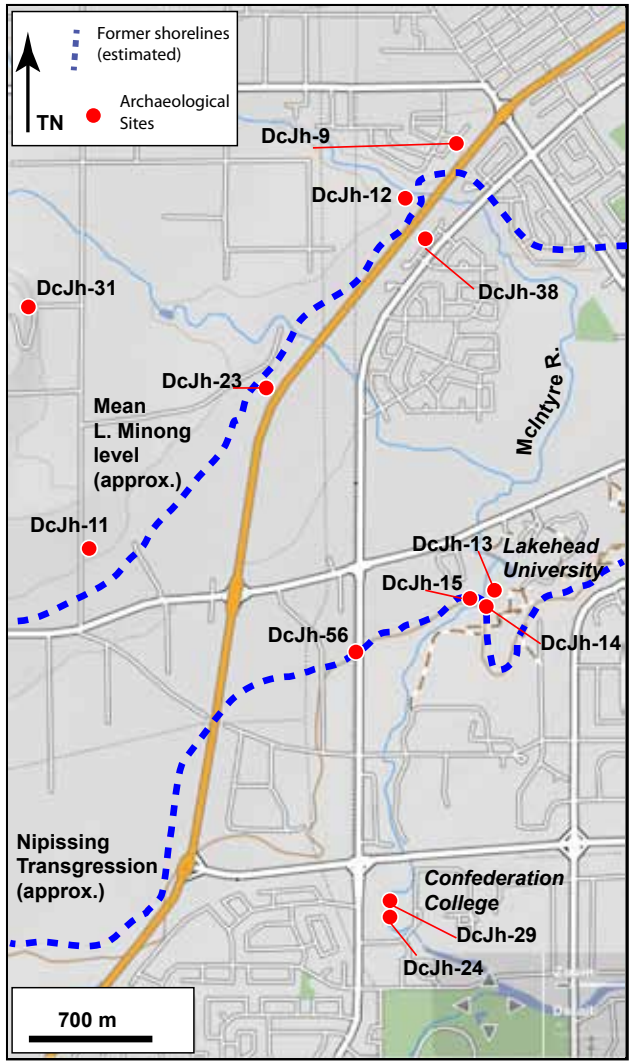

Figure 6 Probable early and mid Holocene archaeological sites along ancient shorelines near Lakehead U. and Confederation College, Thunder Bay.

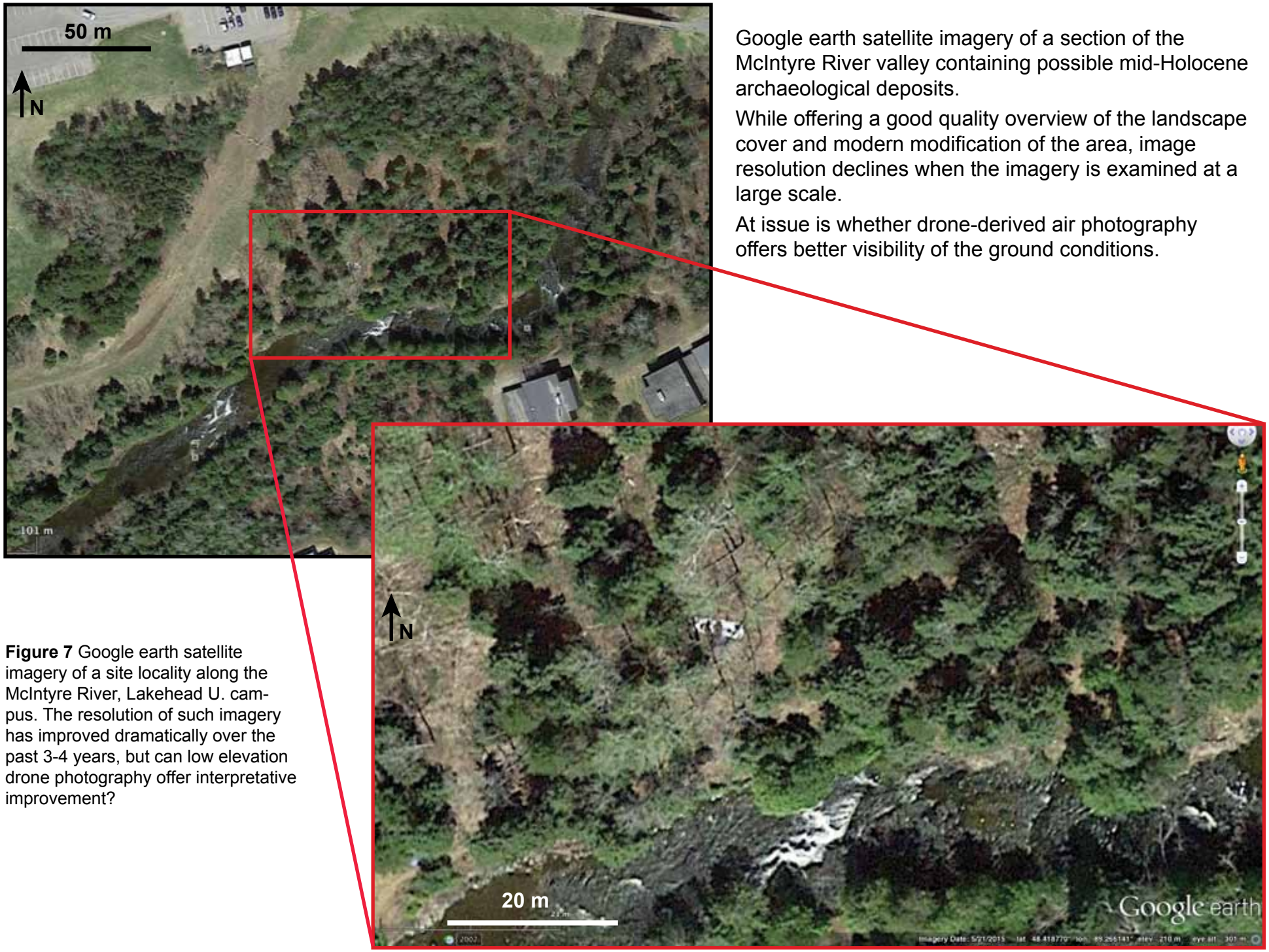

Google earth satellite imagery of a section of the McIntyre River valley containing possible mid-Holocene archaeological deposits.

While offering a good quality overview of the landscape cover and modern modification of the area, image resolution declines when the imagery is examined at a large scale.

At issue is whether drone-derived air photography offers better visibility of the ground conditions.

Figure 7 Google earth satellite imagery of a site locality along the McIntyre River, Lakehead U. campus. The resolution of such imagery has improved dramatically over the past 3-4 years, but can low elevation drone photography offer interpretative improvement?

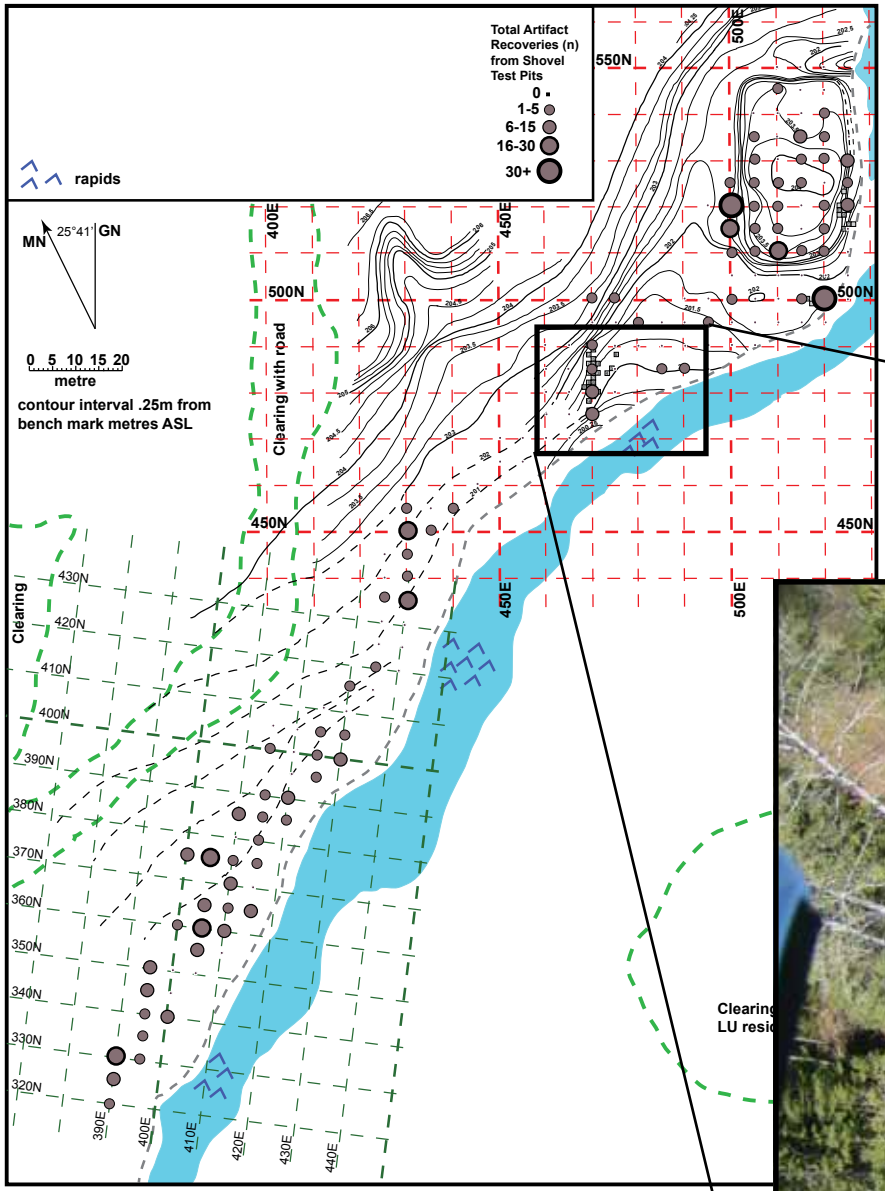

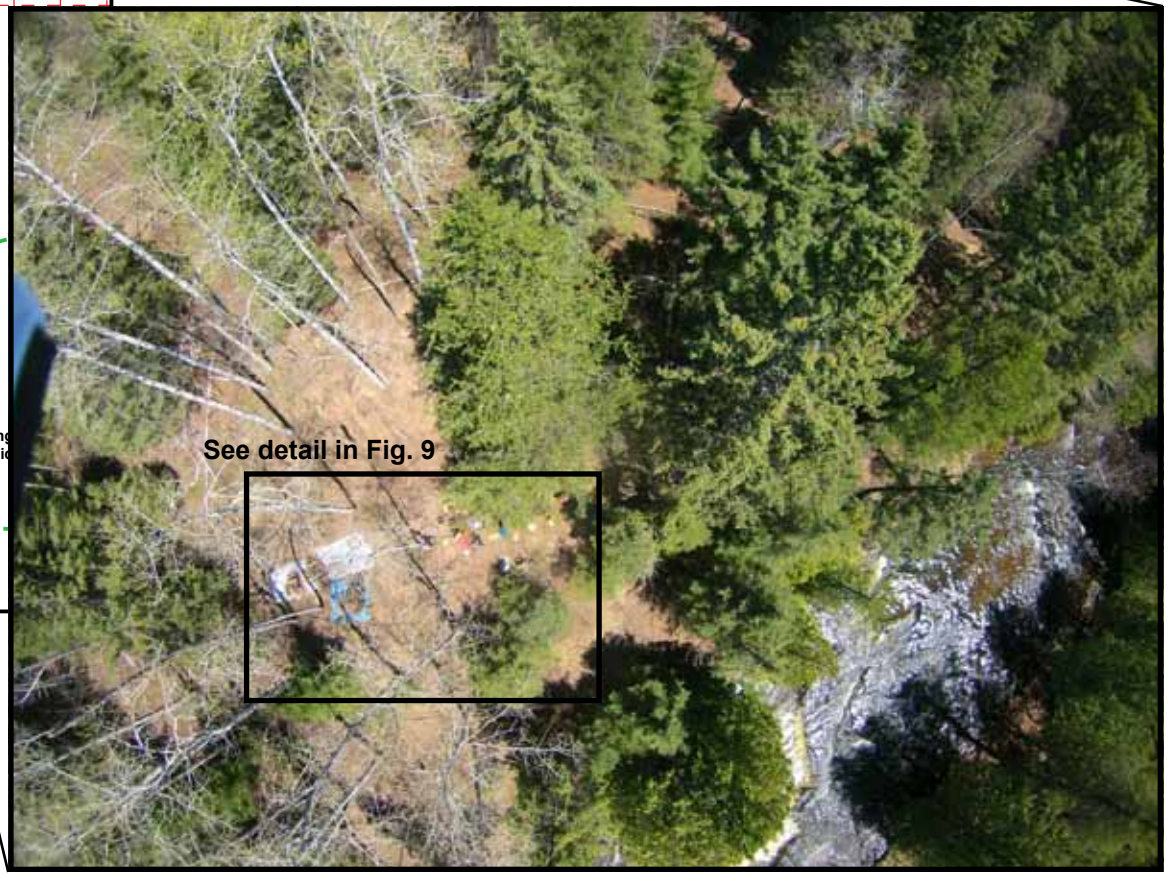

Figure 8 Map of Lakehead University 2015 archaeological field school site. A series of lithic scatters were located along the McIntyre River. Conventional mapping and choropleth plots of test excavation yield were supplemented with aerial photography using the Blade drone.

This air photo was captured above one of the excavation zones where possible Archaic-age lithic debitage was encountered near the estimated shore of the Nipissing Transgression relic shoreline. This required a flight above the tree line, but as Hamilton became preoccupied with the photography, he forgot to monitor the 'time in air' carefully enough with his wrist watch. The drone had insufficient battery power to return to a safe place to land, and crashed into the tree tops.

This resulted in damage that was compounded with a second crash that destroyed the camera assembly. This emphasizes the importance of telemetry controls to monitor flight elevation, battery life and other prompts to warn the operator of flight conditions.

Figure 9 Detail of area specified in Figure 8. The original image was reprocessed to increase DPI while reducing page size to permit presentation. Scale is approximate. While obscured by vegetation, objects on the ground are readily identifiable even when flying at ca. 35-40 metres elevation to avoid the tree canopy. Compare to the inset (deriving from the Google earth imagery from spring of 2010 presented in Figure 7) that shows approximately the same area.

Figure 10 The DJI Phantom 3 Advanced drone. It communicates with the radio-controller with telemetry information viewed on iPad 4 tablet.

aircraft. This likely reflects the consequences of improved telemetry and control software.

The DJI Phantom 3 Advanced offers high quality still and video imagery through its gimbal-mounted camera. It is capable of 12 megapixel stills and 2.7 K video at 30 frames per second. These are lower specifications than the Blade, but the camera lens has features that overcome the weaknesses observed with the Blade. The Phantom 3 is equipped with GPS, accelerometers, a compass and barometric altimeter. It also features better telemetry controls and much improved radio communication range. This is up to 2 km, but given the limited flight duration, a flight range of 200 to 500 metres is much more prudent.

The camera on the Phantom series does not exhibit fish-eye distortion, and the gimbal enables 90° downward photography. This is evident in Figure 11 that illustrates a soccer field. The chalk lines marking the field corner appear straight and form a 90° angle, and are unwarped across the breadth of the frame. These features greatly facilitate its use as a mapping tool since lens correction filtering of every image is unnecessary.

The Phantom 3 and 4 models are equipped with a visual and ultrasonic positioning system on the underside of the drone that detects the ground and augments the GPS in stabilizing flight. This is important for indoor flying, and to mitigate the loss of GPS signal while flying close to obstructions and tree cover. This does not represent true collision avoidance capacity (a feature common with the DJI Phantom 4, Mavic, Spark models as well as the professional machines), but rather, improves the stability with which the machine will hover with minimal sideways or vertical drift. This is particularly important in situations where GPS satellite geometry might be inadequate. We discuss this further in the context of our investigation of the Dog Lake Effigy site.

As was the case with the Blade, the Phantom imagery is stored on a micro-SD card installed on the side of the gimbal. This allows ready transfer of imagery to a computer using a SD card reader. Like those produced with the Blade, these images are large (5.4 to 6.1 MB), and are 41.4 by 55.5 inches (105.2 by 141 cm) in size at 72 DPI. This offers quite high image resolution, much of which is retained when images are reprocessed to 300 DPI, and then reduced to more manageable sizes for presentation. Extended field work might require several mini SD cards, particularly when collecting dozens or even hundreds of images while flying transects over large sites. As we have been generating upwards of 1 GB of imagery on each flight, cards can fill up quickly and fresh (empty) ones should be on hand for successive flights over

Vertical imagery of one corner of a soccer field. Note that the red dashed lines superimposed on the image are straight lines arranged at right angles to one another. Very little fish-eye distortion affects this image, even at the edges of the frame.

For scale, please note the white 3/4 ton truck on the road side in the photo below.

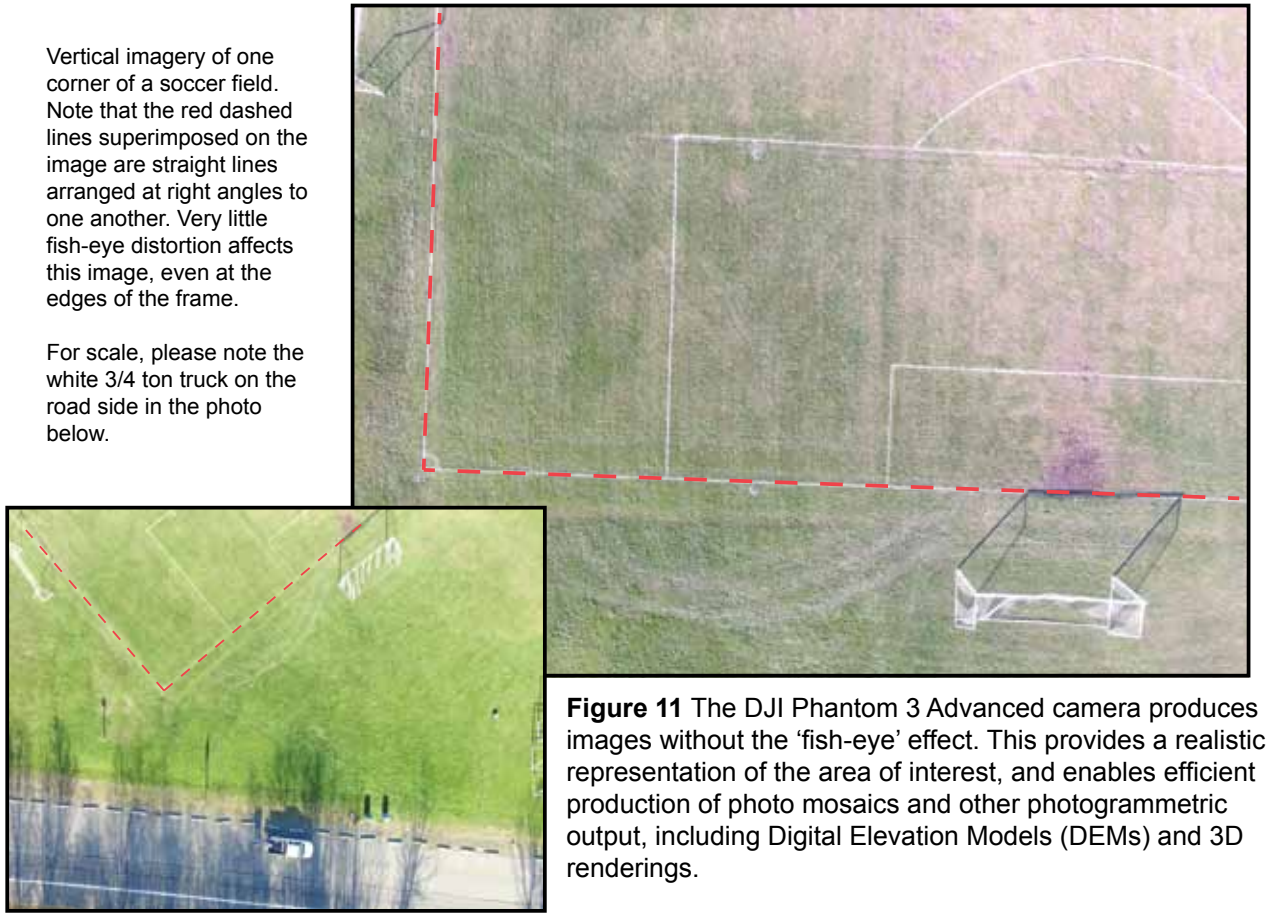

Figure 11 The DJI Phantom 3 Advanced camera produces images without the 'fish-eye' effect. This provides a realistic representation of the area of interest, and enables efficient production of photo mosaics and other photogrammetric output, including Digital Elevation Models (DEMs) and 3D renderings.

the course of the day, or in case a card develops a fault. Undertaking successive flights in one day also assumes several spare batteries, and the means to recharge them.

Recharging drone batteries, those in the radio-controler and also the ipad is an important consideration when working in remote situations. This recharging might be undertaken with an AC inverter from a 12 V battery, or through a portable generator or solar panel. The ideal situation is to have sufficient spare batteries for multiple flights during the work day, with recharging occurring in the evening. While conducting flights in far northern Manitoba in the spring of 2017, we noted problems with rapid battery depletion in cold weather (ground temperature of ca. 10-14° C, with much colder air at flight elevations). Not only did this affect the drone battery, but also resulted in rapid depletion of the ipad battery. We sought battery recharge using a portable generator, but the one used was of rather low amperage, requiring extended recharging times. In remote contexts, such issues represent a significant logistical challenge.

Remote field work also require careful planning of machine servicing and repairs. Given the risk of damage during transport and use, drones should be stored in hard shell transport cases, and field work should include carrying replacement parts (engines, propellers, propeller guards, landing legs, repair epoxy and fine tools). Clearly, significant additional capital is required beyond the initial UAV purchase cost.

Perhaps the most immediately obvious improvement in capabilities is evident with the proprietary software used with many of the DJI products. The DJI Go software is available in Apple iOS and Android versions, and can be downloaded and regularly updated through AppleStore or Google Play. UAV firmware updates also need to be regularly done. Web-published reviews of this software demonstrate its complexity, offering many features and settings for customizing flight, calibrating components, upgrading software, and collecting and editing of imagery.

While appearing overwhelming, this array of information and in-flight control significantly improves functionality, flight safety and image quality. It offers utility to both hobbyists and professionals, and we are still learning how to adjust the settings for optimal results under different conditions. One important feature for novice fliers is the flight simulation software that is integrated into the DJI Go App. Discussion, reviews and tutorials regarding DJI Go are widely available on the internet, and will not be discussed in detail here. Hamilton must confess to some confusion during early flights (or with long interludes between flight operations) in remembering which button does what, and which information tabs should be constantly monitored. Given the consequences of making a mistake in flight, repeated practice and review of the documentation is essential. The most useful learning tools are the array of online tutorials and Youtube videos.

In the fall of 2015, 'DronesMadeEasy' released an App (Map Pilot) specifically for DJI products. It is marketed to be installed on the iPad or other mobile device used to control the drone. It enables well-controlled semi-automated flights that maximizes efficient battery use and photographic coverage. While such automated flights increase the risk of aircraft loss, the efficiency of battery utilization, coupled with the precise control over elevation, photograph coverage, camera settings and orientation of flight lines justify the risk. Other semi-autonomous flight planning and execution software is available, but we focus this discussion upon Map Pilot.

We began experimenting with Map Pilot to plan flights and undertaking automated 'missions' shortly after purchasing the Phantom 3 Advanced. This planning requires an internet connection in order to access Google earth satellite imagery which acts as a geo-referenced 'backdrop' upon which to specify details of the flight plan (see Fig 12). Once the plan is completed, the geo-referenced flight paths, flight parameters and other relevant information (along with the map image) are saved on the smart device for later upload and use by the drone (without the need for internet connection). In circumstances where cell phone coverage is available, it is possible to use the phone to create a 'personal hotspot' that will enable internet access for flight planning. This solution may allow sufficient connectivity to develop or revise a plan in the field, albeit with decreased speed and efficiency of operations. In remote field conditions this is obviously problematic, perhaps requiring internet communications via satellite phone. We have not utilized the satellite approach, and instead have relied upon wholly manual flights in remote areas. This works sufficiently well when flying small areas of interest, but will be problematic when attempting to map larger site areas.

An example plan is offered in Fig 12 that illustrates a portion of Camp Hughes National Historic Site in southwestern Manitoba. This training facility was developed during World War I, and a number of military trenches remain intact within the open prairie. With availability of better quality Google earth satellite imagery, these features are readily evident when examined at large scale, particularly when snow accumulates in the trenches. A second satellite image dating to mid summer offers a point of contrast. As more freely accessible imagery becomes available for rural and remote Canada, one might ask whether UAV-derived low elevation aerial images are useful. Our experience demonstrates many subtle features that are either invisible or ambiguous when examined using conventional satellite images, but are rendered with surprising clarity using UAVs. More to the point, semi-autonomous flights to capture imagery at standardized height and image overlap offer enormous potential through the development of photomosaics and other photogrammetry products (digital elevation models and 3D models). Examples of this output are offered below.

The flight plans can be quickly and intuitively developed using the MapPilot app installed on the ipad. After launching the app to develop a new plan, one scrolls to the area of interest and zooms in to orient oneself on the Google earth image used as an orientation backdrop (Fig 12: image C). After opening

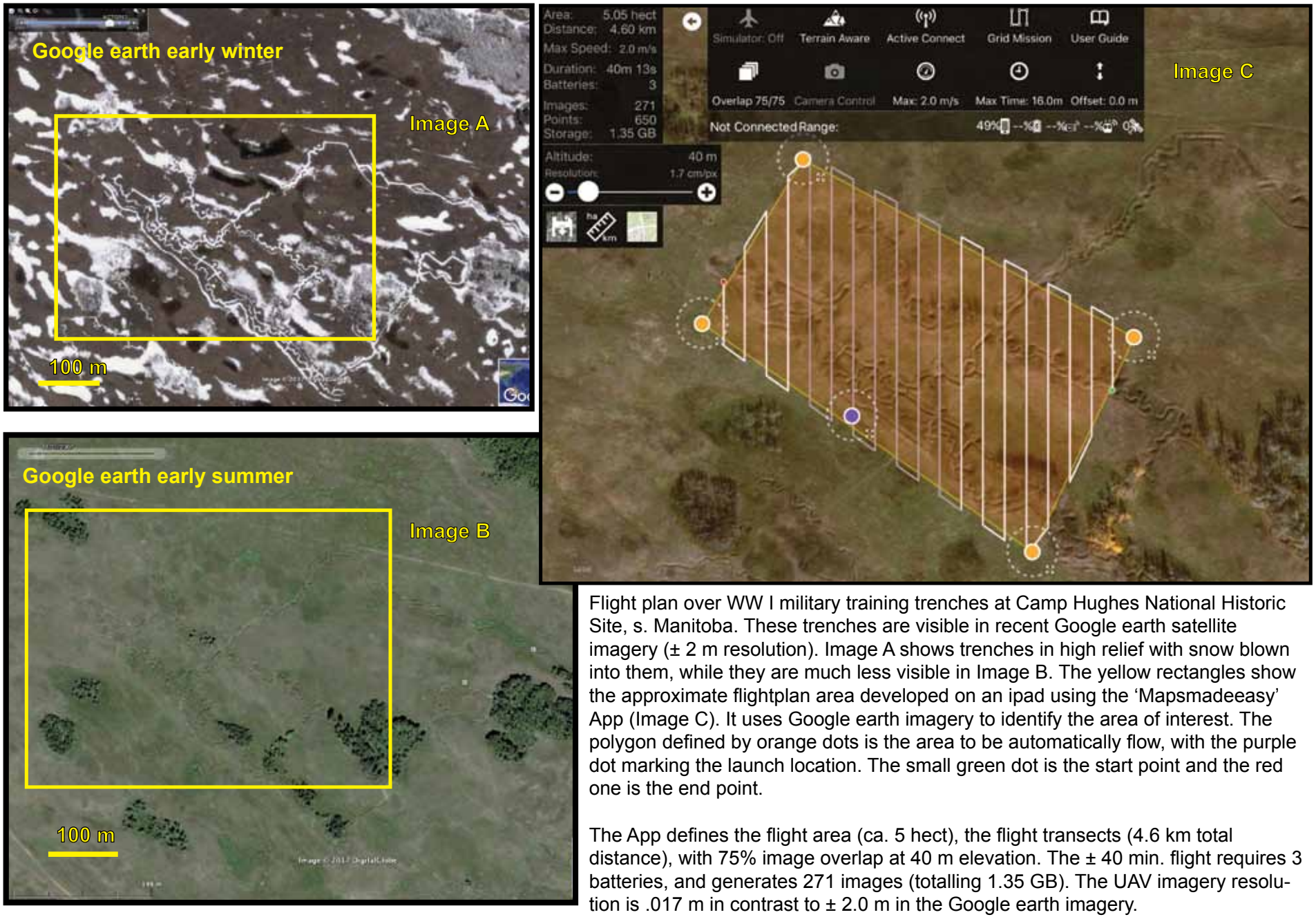

Flight plan over WW I military training trenches at Camp Hughes National Historic Site, s. Manitoba. These trenches are visible in recent Google earth satellite imagery (± 2 m resolution). Image A shows trenches in high relief with snow blown into them, while they are much less visible in Image B. The yellow rectangles show the approximate flightplan area developed on an ipad using the 'Mapsmadeeasy' App (Image C). It uses Google earth imagery to identify the area of interest. The polygon defined by orange dots is the area to be automatically flow, with the purple dot marking the launch location. The small green dot is the start point and the red one is the end point.

The App defines the flight area (ca. 5 hect), the flight transects (4.6 km total distance), with 75% image overlap at 40 m elevation. The ± 40 min. flight requires 3 batteries, and generates 271 images (totalling 1.35 GB). The UAV imagery resolution is .017 m in contrast to ± 2.0 m in the Google earth imagery.

Figure 12 Mock flight plan of WWI military trenches at Camp Hughes National Historic Site.

tabs around the top and left margins of the screen, the user can specify the flight speed, elevation and percentage of overlap between adjacent images to define the basic flight parameters. With single finger taps on the touchpad, the corners of the polygon (orange dots) are defined and adjusted to identify the area of interest. A double tap gesture is used to define the proposed UAV launch location, and the app automatically establishes the flight lines according to the flight specifications, calculates the flight duration, number of batteries required, and the number of images (and memory requirements) that will be collected. Finger gestures on the touch screen allow the planner to change the orientation of the flight lines to improve efficiency, and thereby change the start and end points of the flight. Our experience suggests it is wise to ensure that the flight end point is close to the HOME position (purple dot) to enable rapid descent and landing if the battery is getting low.

When the flight plan is actually launched, a red triangle appears on the screen representing the location of the drone, and once the mission is launched, the operator can monitor the progress of the automatic flight by noting the position of the red triangle along the flight lines. Figure 13 provides a view of a flight plan executed over a rock feature flooded by the Boulevard Lake headpond in Thunder Bay, Ontario. As the flight mission is executed, the software also places small black dots along the flight lines to mark the location where photographs were taken and stored on the mini-sd card. This is valuable to monitor performance and rate of completion of the flight mission relative to the remaining battery life that is also reported on the iPad screen.

Along the left side of the panel in Figures 12 and 13, is information about the area and linear distance being flown, the estimated duration of the flight and number of batteries required, the number and storage requirements of those images, and the estimated image resolution (i.e. 1.7 cm/pixel). This information derives from the specifications entered during planning. The camera can also be adjusted to address lighting conditions, either during flight planning, or when initiating the mission. Along the right side of the image (Fig. 13) are a series of tabs that provide in-flight information to ease monitoring, and to troubleshoot issues as they arise.

'DronesMadeEasy', also provides a photogrammetry service through its associated 'MapsMadeEasy' web site. During early stages of research we chose this strategy as a more cost-effective alternative to the purchase of photogrammetry software and

Figure 13 Photograph of flight planning window in the Map Pilot software. **1**) The four corners of the polygon specifing the flight area. **2**) The white lines define the flight path within the polygon intended to generate a 90% overlap between adjacent images. **3**) The planned launch location. The red triangle marks the identified drone location at beginning of the flight. **4**) The green dot marks the mission start point. Upon launch the drone will fly to this location and then initiate the mission. **5**) The red dot marks the flight end. After completing the automated flight, the drone is returned to manual control for landing.

a high-speed computer.

There are several online tutorials and Youtube videos available that detail Map Pilot, and its operational utility. We will not contribute to this growing body of information here aside from the above discussion, and focus the balance of this paper on archaeology outcomes of our tests.

Five localities in the Thunder Bay area are addressed here. Four are within the immediate Thunder Bay area, and the fifth is the Dog Lake Effigy, located near Dog Lake about 45 km northwest of Thunder Bay. Figure 14 illustrates the Thunder Bay area and also the approximate extent of Glacial Lake Minong compared to the current Lake Superior. While test localities 1, 2, and 4 are unrelated to these ancient shorelines, those within the purple square (3) may be related to the glacial lake levels.

Boulevard Lake rock ring

Due to maintenance of the Current River hydroelectric dam in the fall of 2015, the Boulevard Lake reservoir was drained, revealing a rock ring feature. This reservoir derives from the 1907 dam construction at rapids along the lower Current River (Fig. 14). A number of Paleoindian sites are located upstream along the Current River, and in the uplands beyond (Fig. 14), and Archaic period sites are reported in the area surrounding the dam headpond.

Given the early date of dam construction, no archaeological investigation occurred prior to development. However local residents have observed a large rock ring that periodically appears within the reservoir during times of low water. Figure 15 is a Birdseye satellite image captured during one of these periods of low water, and the rock feature is partially exposed. It appears to be constructed on a point bar terrace along the south bank of the original Current River channel about 300 to 400 metres upstream from the rapids (at the dam).

The rock feature became fully emergent in the fall of 2015 after reservoir drainage (Fig. 16), and it became our first serious test of the Phantom 3 drone and the Map Pilot flight planning software. Surface inspection revealed a large C-shaped rock ring located on a low point bar terrace within the shallow reservoir. The area surrounding the feature is at a lower elevation, and is wet and muddy (Fig. 16).

The area within and immediately around the rock feature retained its weathered (pre-flood) soil, and is mantled by sparse water-tolerant vegetation. Areas removed from the ring appear to be deflated by wave erosion, and the exposed surface consists of muddy lake bottom dotted with rocks. Water-saturated logs,

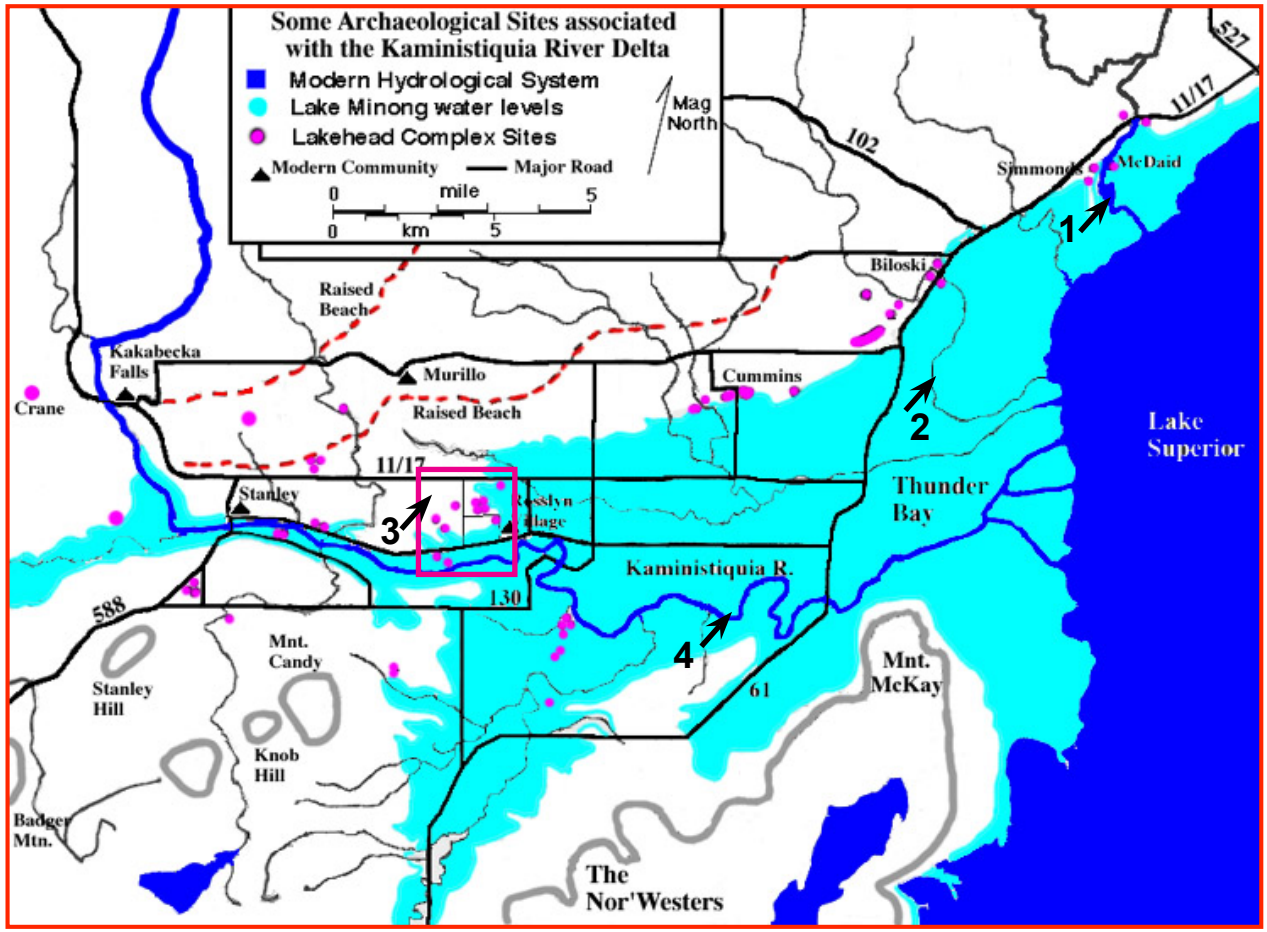

Figure 14 The Thunder Bay area with some Paleoindian sites along the relict shores of Glacial Lake Minong. The most prominent and well documented of these beaches coincides approximately with the 750 foot contour line, that is used here to represent the former lakeshore. This is rather coarse-grained, and much work is required to refine the both the paleo-landscape, and the range of site types defining the Lakehead Complex settlement system. Some sites featured in this report include **1**) the Boulevard Lake Rock Ring, **2**) the Lakehead University sites along the McIntyre River, **3**) several lithic scatter sites observed in cultivated fields in the Rosslyn Village area, and **4**) the site of the Fort William reconstruction.

and other debris was noted in the reservoir basin, but much of it seemed to be discarded into the water by lake users. That said, we observed a piece of broken asphalt near the rock ring, and also pieces of wood (tree roots, lower trunks) that protrude from under some of the rocks. Many of these rocks are large, and portions of the ring are upwards of 1.5 metres wide and composed of many rocks (Fig. 16).

The function and antiquity of this feature is not known. While it may be of 20th Century construction and built during a time of low water, it may be of Aboriginal origin and predates the 1907 dam construction. In any case, it has sparked considerable local interest, and we sought to assess whether the Phantom drone offered a cost-effective means of mapping it before water levels again rose.

Three flights were undertaken over two days. Each flight was about 18-20 minutes in duration, and the last two were flown in succession after swapping batteries. We estimate that the total field time was about 2 hours, while conventional mapping of the individual rocks of the feature could have taken two people at least 5 to 7 days.

The original flight plan is illustrated in Figure 13, but adjustments were made for the two subsequent flights to overcome identified flaws. Image A of Figure 17 is poorly exposed, and with washed out colour. When we zoomed in to examine image detail, the rock outlines were blurred and pixilated. The next two flights were undertaken the following day under similar overcast conditions, but with drone speed reduced from 4 m/sec (first flight) to 2 m/sec. Image B in Figure 17 shows output from flight 3. In this case the image is much brighter, with better colour contrast defining the rocks. Close examination of individual rocks indicated less motion blur, and much better definition and colour contrast of rock surfaces and edges.

The best photogrammetric interpretation of aerial imagery is achieved with flat overcast conditions (fewer shadows), but this results in lower light levels. This can be compensated for by making sure the camera lens is set for cloudy conditions, and by flying the drone sufficiently slowly to reduce motion blur effects. For short flights (i.e. smaller mapping areas) this is not an issue, but it can become a problem when mapping areas too large to safely fly using one battery. Fortunately the Map Pilot software calculates this at the planning stage, and can automatically suspend the mission when the battery

Birdseye satellite image of sw corner of Boulevard Lake Reservoir.

Water levels drawn partly down, exposing portions of former south bank of Current River immediately upstream from falls.

Note partially exposed ring of rocks on point bar terrace, with balance of the structure still fully submerged.

Figure 15 Partially exposed rock ring along the former banks of the Current River within the Boulevard Lake reservoir.

nears depletion. It then returns to the operator and lands, whereupon the battery is replaced and the drone is relaunched. It is programmed to fly to the point where the flight path was interrupted and resume the transects until the mission is completed.

The third flight over the rock ring feature was uploaded for processing using the MapsMadeEasy site. This involves establishing a credit account, uploading the images, and then specifying the product(s) sought. One can request (and pay for) urgent service, or accept standard product delivery time. Flight 3 generated about 312 images (each between 5.4 to 6.1 MB). Uploading this much information can be quite time consuming if using a wireless connection, so it is often wise to use a hard-wired ethernet connection. After providing basic information about the flight, and confirming that it is correct, the photogrammetry service accepts the job and debits the account upon completion. We found that MapsMadeEasy consistently produced output faster than their estimated 'time to completion', and we received an email indicating it was ready for viewing and download within 3 to 6 hours of submission. While the cost of this processing service varies with the mission size, in general each of the projects described below likely ranged from $10 to $25 CAD.

Several products derive from the MapsMadeEasy service. In the case of Flight 3 this includes:

1) a GeoTIFF mosaic (99.8 MB)

2) a full resolution JPEG version (6.0 MB)

3) a Digital Elevation Model (DEM) (12.2 MB)

4) a colourized DEM as a GeoTIFF (4.7 MB)

5) a colourized DEM as a JPEG (763 K)

6) a 3D KMZ (10.1 K)

7) several other 3D products.

The service has subsequently added addition output for download that likely reflects customer demand for more raw data that they can process to their own specifications. This includes estimations of the quality of aerial coverage, 'point cloud' (XYZ) data files and other useful products.

As the on-board drone gps unit 'tags' each image with the estimated coordinate of the photograph, these images can be used to produce a geo-referenced mosaic (the GeoTIFF mosaic). The most basic image output is illustrated in Figure 18, and includes a simplified version overlaid upon a Google earth satellite scene. This comparatively low resolution ver-

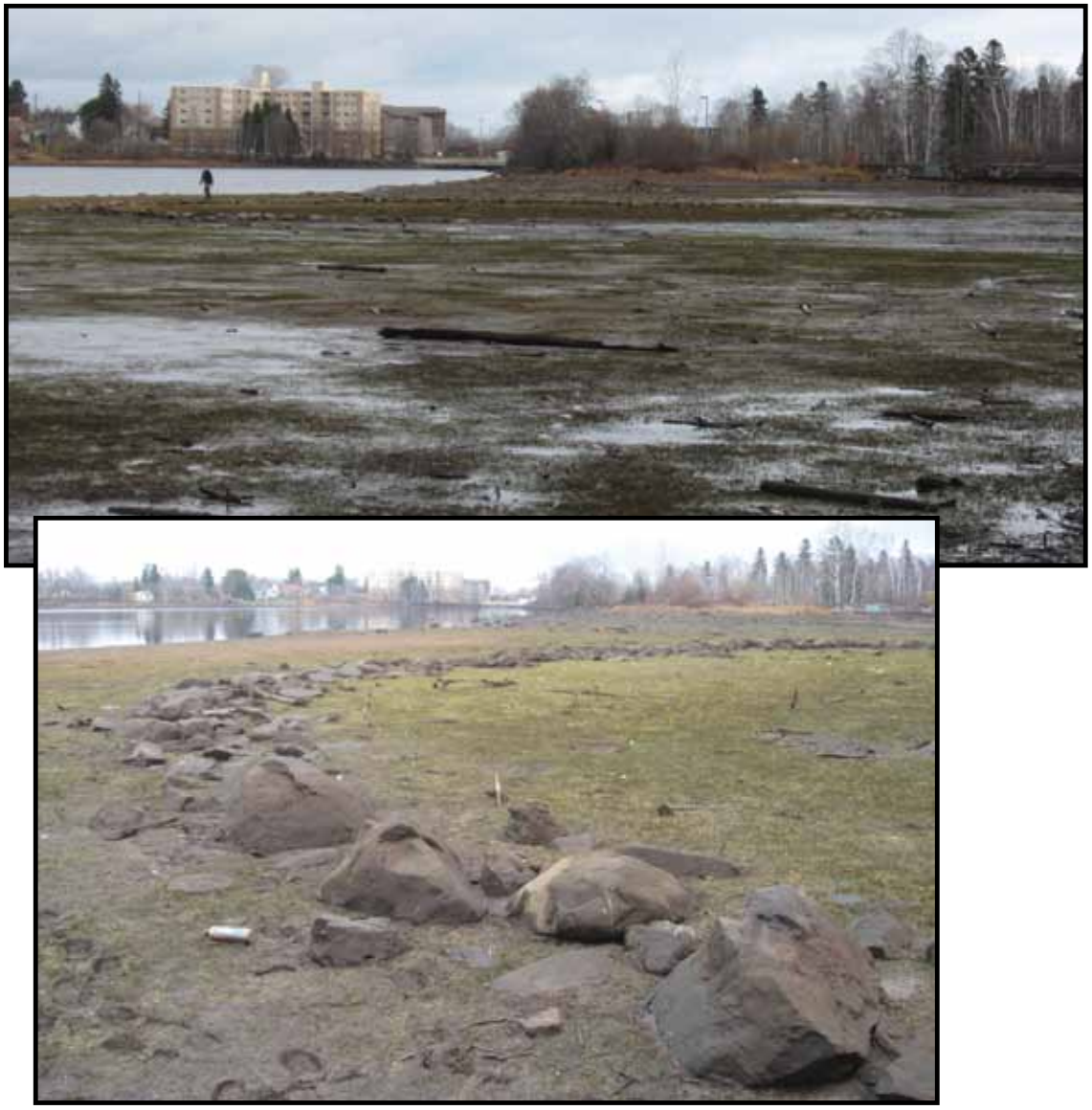

Figure 16 View from ground level of the rock ring usually submerged below the Boulevard Lake reservoir. Note the dam in the background along the treeline. The wet floodplain is overlooked by a point bar terrace upon which the C-shaped rock ring is located overlooking the former Current River channel.

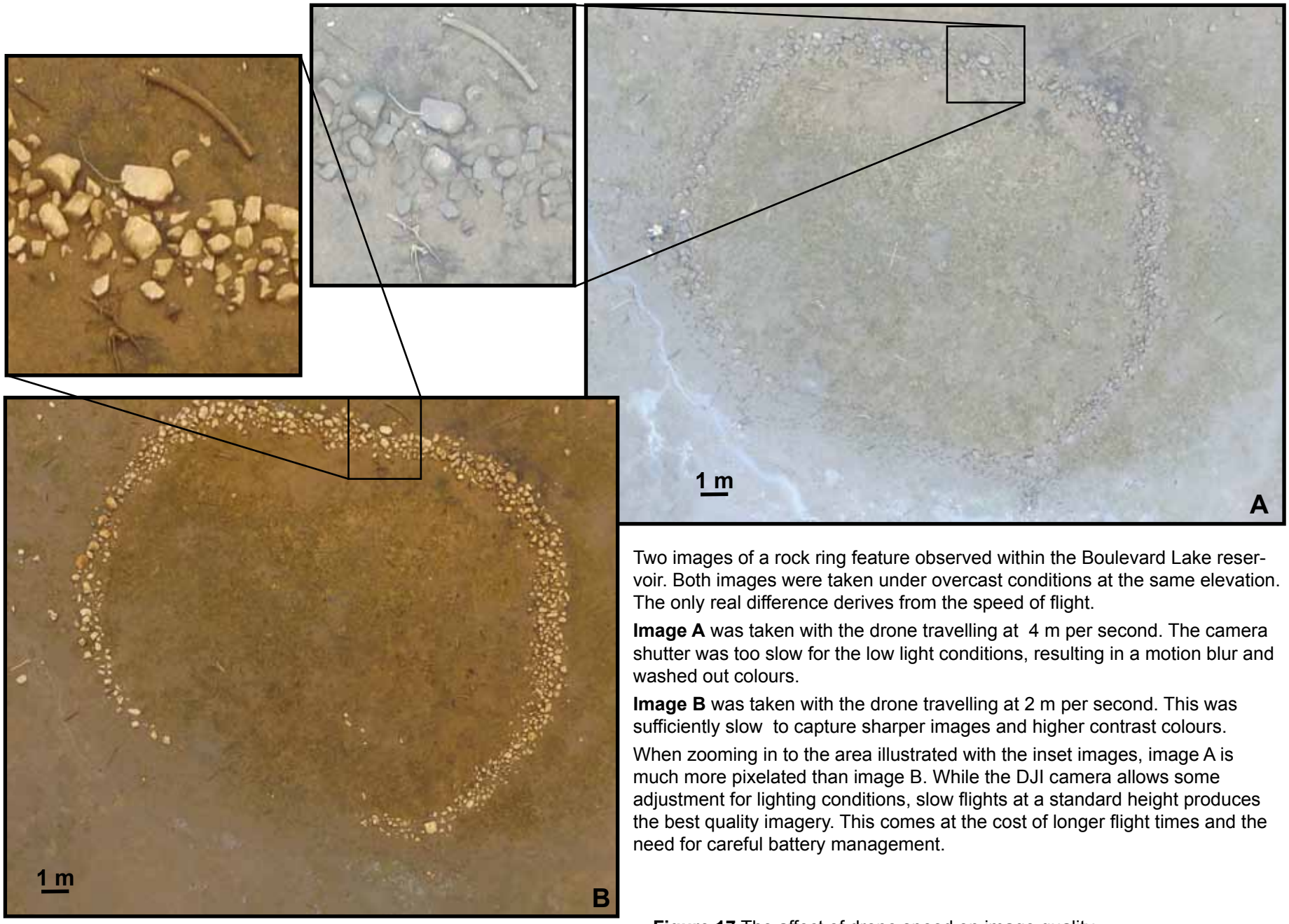

Two images of a rock ring feature observed within the Boulevard Lake reservoir. Both images were taken under overcast conditions at the same elevation. The only real difference derives from the speed of flight.

Image A was taken with the drone travelling at 4 m per second. The camera shutter was too slow for the low light conditions, resulting in a motion blur and washed out colours.

Image B was taken with the drone travelling at 2 m per second. This was sufficiently slow to capture sharper images and higher contrast colours.

When zooming in to the area illustrated with the inset images, image A is much more pixelated than image B. While the DJI camera allows some adjustment for lighting conditions, slow flights at a standard height produces the best quality imagery. This comes at the cost of longer flight times and the need for careful battery management.

Figure 17 The affect of drone speed on image quality.

sion was rendered to 300 DPI and reduced to page size. Hamilton then attached a scale, north arrow, labels and interpretative lines using vector graphics software (Adobe Illustrator).

The GeoTIFF mosaic (Fig. 19) is quite impressive, with the boundaries between individual images being imperceptible. It also seems to be well registered and integrated with the underlying Google Earth image. The full-scale original image mosaic is large (107 by 162 inches or 271.8 by 411.5 cm at 72 DPI), with the TIFF version being 104.6 MB in size.

Such large and cumbersome files are readily manageable within most image processing software, and discrete details can be enlarged and examined without becoming severely pixilated. For this report, the unmodified images are rendered to 300 DPI and then reduced down to a more manageable presentation size.

Figure 19 is a reduced version of the original GeoTIFF image mosaic. The original large image offers a detailed representation of the ground surface. It derives from photographs taken at 40 metres elevation (resolution of 1.7 cm/pixel). The upper inset image is a detail extracted from the original image to illustrate an isolated rock that appears as a tiny white dot in the reduced mosaic image (Fig. 19). Also note the white seagulls foraging upon the reservoir mud-

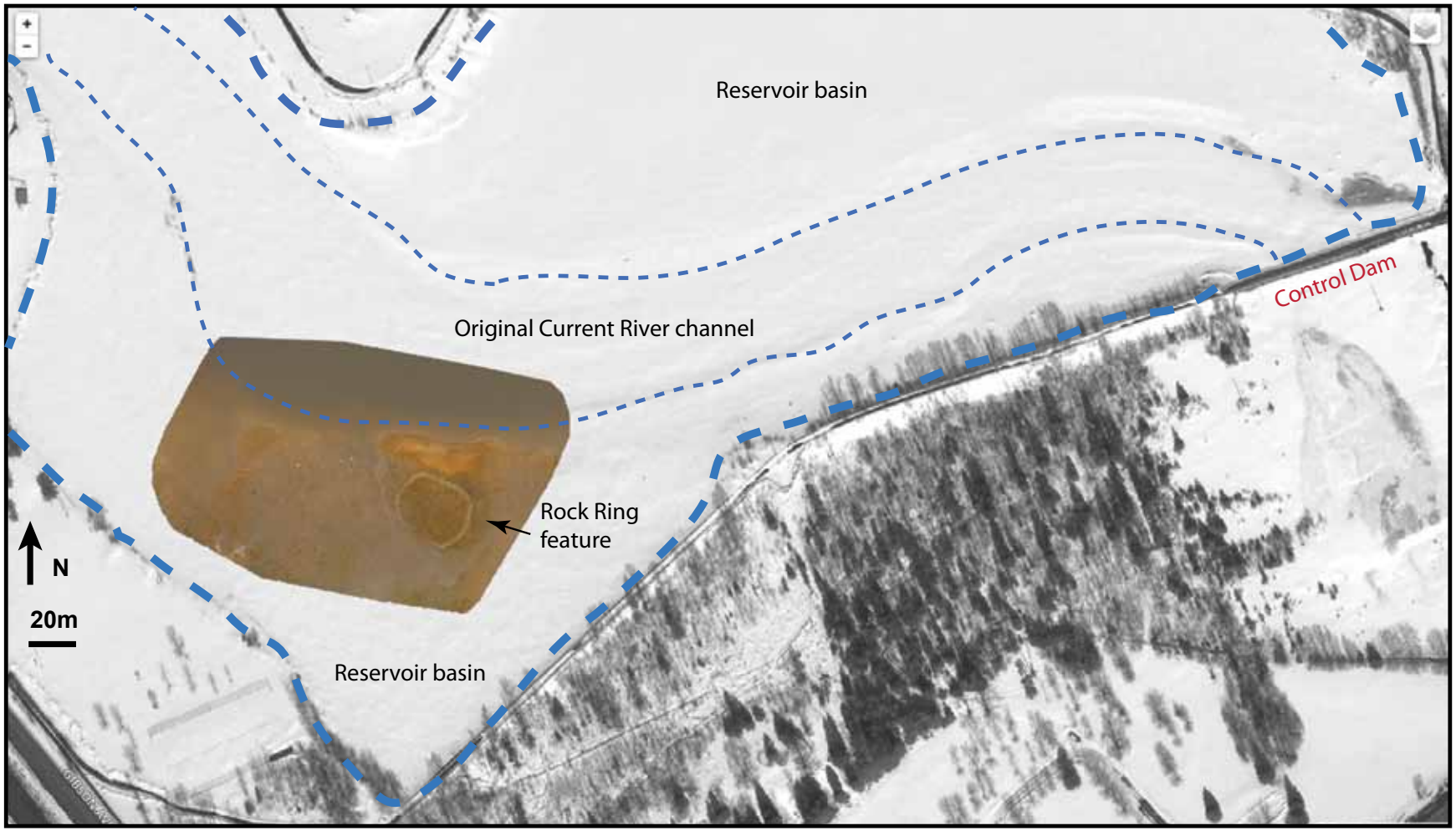

Figure 18 Georeferenced air photo mosaic of rock ring feature taken at 40 m elevation. It was exposed on the former river terrace edge overlooking Current R. a short distance upstream from the falls now contolled by the dam. Feature was photographed during low water in fall of 2015. Image is overlaid upon Google earth imagery (winter) during a time of low water levels, thereby showing the original river course.

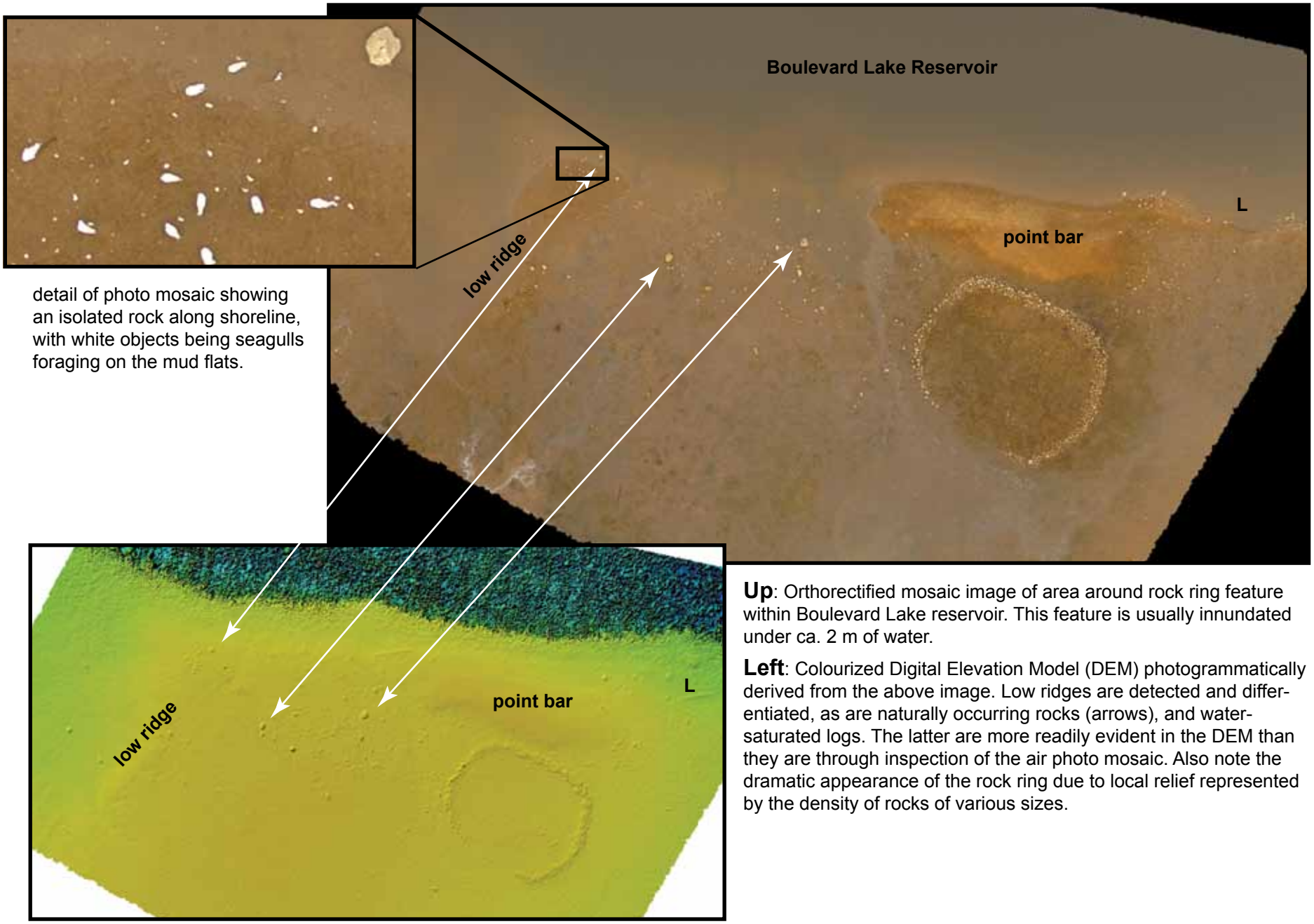

Up: Orthorectified mosaic image of area around rock ring feature within Boulevard Lake reservoir. This feature is usually innundated under ca. 2 m of water.

Left: Colourized Digital Elevation Model (DEM) photogrammatically derived from the above image. Low ridges are detected and differentiated, as are naturally occurring rocks (arrows), and water-saturated logs. The latter are more readily evident in the DEM than they are through inspection of the air photo mosaic. Also note the dramatic appearance of the rock ring due to local relief represented by the density of rocks of various sizes.

Figure 19 Boulevard Lake rock ring feature presented as a GeoTIFF image (upper). This is significantly reduced for presentation. See the inset photo that is a detail of the original image showing an isolated rock. The lower inset image is a colourized Digital Elevation Model (DEM) of the original mosaic. Note that the ring and isolated rocks are readily apparent in the DEM, drawing attention to subtle relief that was detected and documented.

flats nearby. The anatomical features of the birds are not readily visible (perhaps an exposure or white balance issue). If the mission had been flown at a lower elevation, the detail and image resolution would have been better, but with a greater cost in terms of flight time and image mosaic size. Planning flight missions over archaeological sites requires balancing factors revolving around required image resolution, intended data output, and safe flight management.

The lower inset image in Figure 19 is a reduced version of the colourized Digital Elevation Model (DEM). It represents relief change detected by the photogrammetry software. In this case the open water of the reservoir appears as a chaotic mix of colours suggesting abrupt and localized elevation changes. The software was 'confused' by light reflection off the water surface. We noted similar errant data when addressing tree cover. The reservoir bottom is quite flat, but relief is represented by a subtle colour range from light green (low elevation), through yellow, and on to yellow-brown (high elevation). Individual naturally occurring rocks as well as those making up the ring feature stand out in dramatic contrast on the DEM (Fig. 19). Even water-saturated logs half buried in the mud are detectable in the original large-format version of the DEM.

The DEM is created within the photogrammetry software. While being described as a DEM, it is created through photogrammetric interpolation, and not direct measurement of relief change as would be the case with LIDAR imagery. In this circumstance the relief modelling derives from interpretation of the same geographic area from several different perspectives provided by the overlapping photographs. To produce high quality results, a significant degree of overlap is required. In the case of Figure 19, the flight plan specified a 90% overlap, but good quality results have been achieved with 75 to 80 percent overlap. Errors should be expected if the mission was flown in bright sunlight, which might cast shadows, or reflections from wave surfaces. Ongoing research has been analyzing the DEMs to determine what relief change is actually being represented in the imagery. The DEM likely represents relative relief, and not actual elevation as measured Above Sea Level (ASL). Subsequent refinement of the MapPilot software allows for this relative relief to be calculated in reference to the elevation of a photograph (and altimeter reading) taken on the ground before flight launch that derives from coarse-grained global elevation models deriving from NASA data. While such estimations of 'starting elevation' may not be precise (horizontally or vertically), it more realistically links the calculated relief to ASL, thereby easing the process of linking data from discrete missions together.

Figure 20 represents a detail of one of the Flight 3 images that was taken directly above the rock ring. Orange plastic pylons and 1 metre range poles provide a scale. The averaged coordinates of the pylons were determined using a hand held GPS, with the distances between pylons measured with 60 metre tapes. Evaluation of this image suggests that Figure

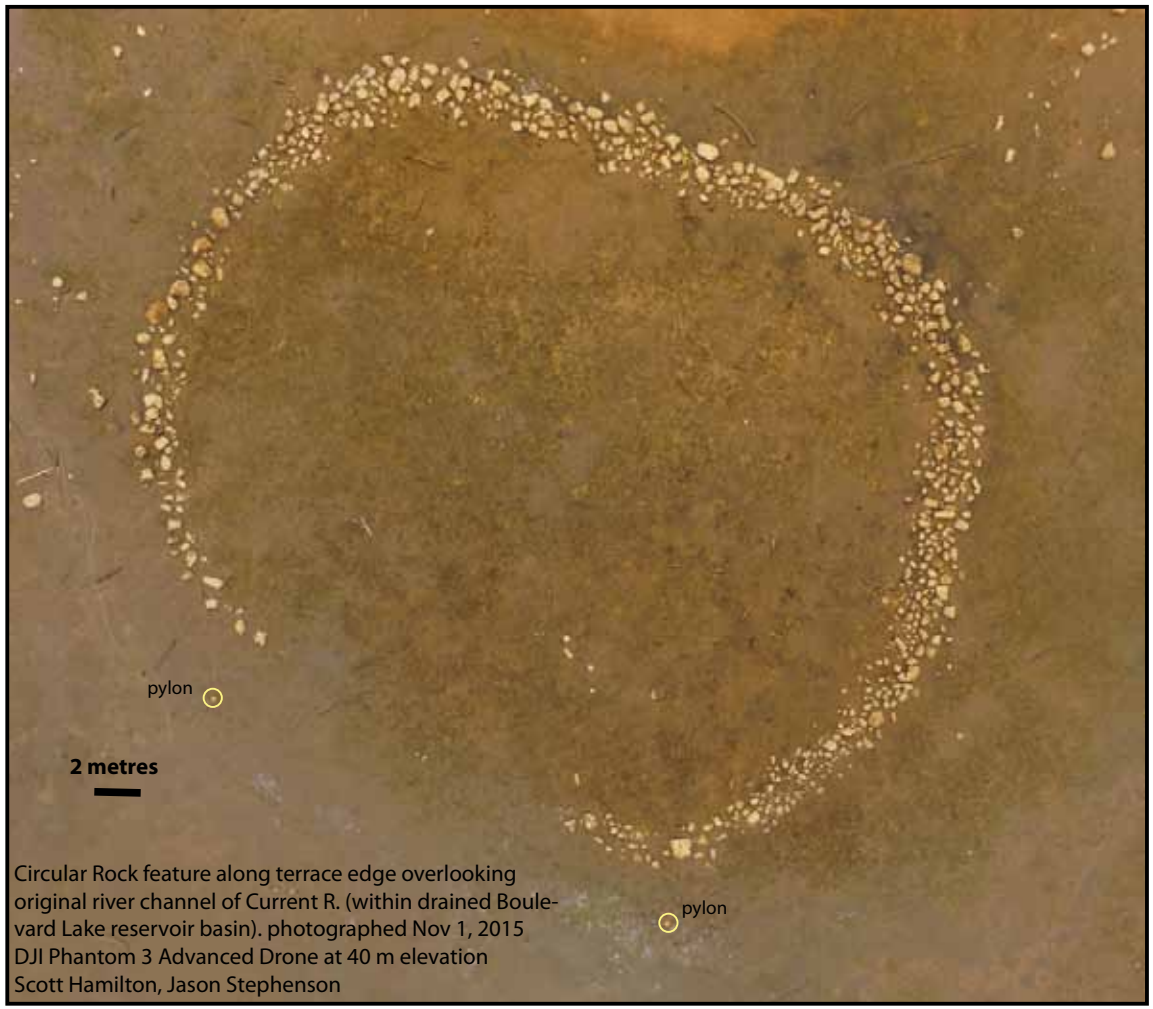

Figure 20 Detail image of rock ring feature within Boulevard Lake. This image does not suffer 'fish eye' distortion, and could be used as an archaeological site plan. It forms a dramatic contrast to the severe distortion apparent in Figures 2 and 3.

20 is sufficiently detailed and spatially undistorted for use as a feature/site map in an archaeological report. In these ideal conditions (exposed feature in a freshly drained reservoir with no obscuring vegetation), drone-assisted site documentation offers a cost-effective strategy. Ongoing research is assessing what map quality can be generated under less than idea conditions.

Another important consideration is that the drone flight plan can be saved and repeatedly used to produce duplicate maps of the same area under different conditions (i.e. lighting, weather or vegetation conditions). This might prove useful when documenting archaeological sites disturbed by cultivation, or to document successive phases of site investigation. Such flights are also useful if archaeological features remain intact below the plow zone and become evident through differential crop growth, or if micro-relief representing former structures or earthworks is evident. Repeated flights under different conditions are easily undertaken until imagery of optimal interpretative value is produced.

Dog Lake Effigy

Despite modest snow cover in November of 2015, we relocated and mapped a small zoomorphic earthwork originally reported by K.C.A. Dawson (1965). This site is located along the southern flank of the Dog Lake Moraine overlooking the Kaminsitiquia River valley (Figure 21). It is an intaglio earthwork interpreted to represent the outline of a dog or similar animal. Dawson noted some damage from soil test pits dug as part of hydro-electric development prior to his 1962 visit. Through limited subsurface investigation, Dawson recovered a triangular projectile point that he attributed to the Late Precontact period.

Figure 22 replicates images in Dawson's 1965 publication. He reports the effigy along the south-facing top edge of the Dog Lake Moraine, near where a portage trail climbs up and over the landform. This path may be one of the historically important portages that connected the Kaministiquia River to Dog Lake, a Aboriginal travel route that was also intensively used by the North West Company after 1804.

Dawson described the construction of the earthwork feature and provided a contour map of its configuration (Fig. 22). He also published a southwest-facing oblique air photograph of the escarpment edge, with the outline of the earthwork emphasized with white flour (Figure 22, see arrow). We sought to assess whether the drone offered effective plan-view imagery, or whether the obscuring vegetation and snow cover impeded DEM rendering. We also addressed whether the spatial configuration of features and markers documented in the drone mosaic remained consistent with the field measurements.

Since Ontario Parks has cut and maintained a trail along the old portage route, this site was comparatively easy to find (Fig. 21). It is in a small clearing surrounded by relatively open deciduous and coniferous forest. This tree canopy significantly reduced the extent of area available for flying (Fig. 23:B).

Compounding these challenging conditions, the GPS signal detected by the drone was rather weak and intermittent during our visit. It is not clear whether this reflects poor satellite geometry at that time of day, or whether the forest cover was impeding the signal. In any case, the drone began to drift upon launching, in sharp contrast to the stable hovering that characterized its operation at Boulevard Lake. Stephenson, with his superior flying skills, took over the controls and carefully maneuvered among the trees at mid-canopy height in order to manually collect overhead images of the clearing.

The circumstances did not permit use of the Map

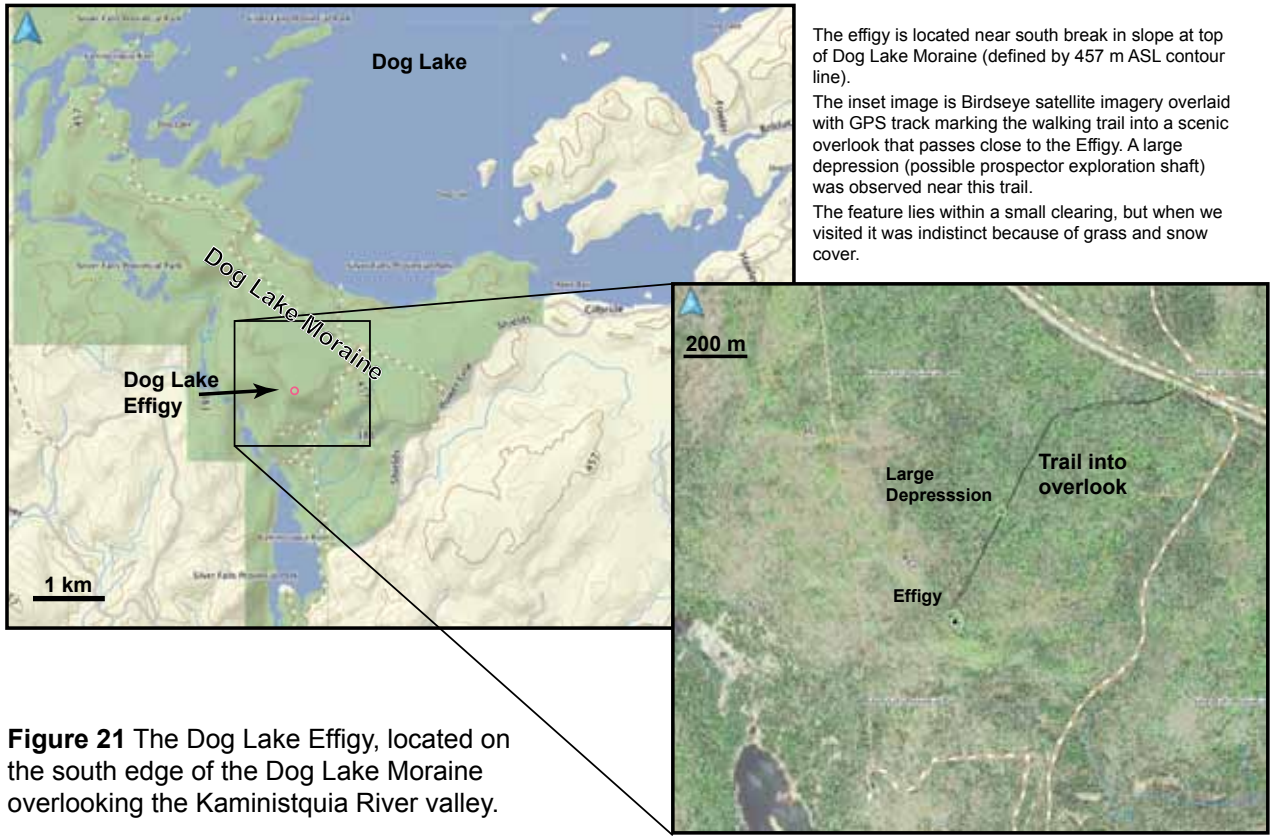

The effigy is located near south break in slope at top of Dog Lake Moraine (defined by 457 m ASL contour line).

The inset image is Birdseye satellite imagery overlaid with GPS track marking the walking trail into a scenic overlook that passes close to the Effigy. A large depression (possible prospector exploration shaft) was observed near this trail.

The feature lies within a small clearing, but when we visited it was indistinct because of grass and snow cover.

Figure 21 The Dog Lake Effigy, located on the south edge of the Dog Lake Moraine overlooking the Kaministqua River valley.

Pilot flight planning software. We did not have a precise GPS location for the site and could not 'see' the feature in any of the available satellite images. The area in question is also much smaller than the required 50 metres between corners of the flight polygon. We also needed to fly at a low elevation in order to capture maximum resolution of the subtle earthwork covered with low vegetation and snow. Since we had to fly over the clearing within the tree canopy, we relied to the *ad hoc* flight transect approach used with the Blade drone. Initial review of the DEM and 3D models yielded better than expected results.

Prior to undertaking the flight over the earthwork, we laid out orange pylons at strategic corners of the feature, coupled with 1 metre range poles (to provide a direct scale) (Fig. 24). Given the small area to be considered, we took (averaged) handheld GPS readings at each of the four pylons, and used 60 metre tapes to produce a sketch map of the spatial relationships between pylons relative to the effigy. This sketch was to aid assessment of the consistency of the overhead drone photograph with conventional sketch mapping. Since the GPS-generated coordinates proved insufficiently precise for our purposes, Hamilton manually adjusted those for Pylon 2 and 4 to more realistically reflect the orientation and size of the feature as indicated by both the sketch plan and the overhead photos. The sketch plan and the Dawson isocline (Fig. 22) were rescaled and reoriented, and then overlaid on top of the drone photograph in Figure 24.

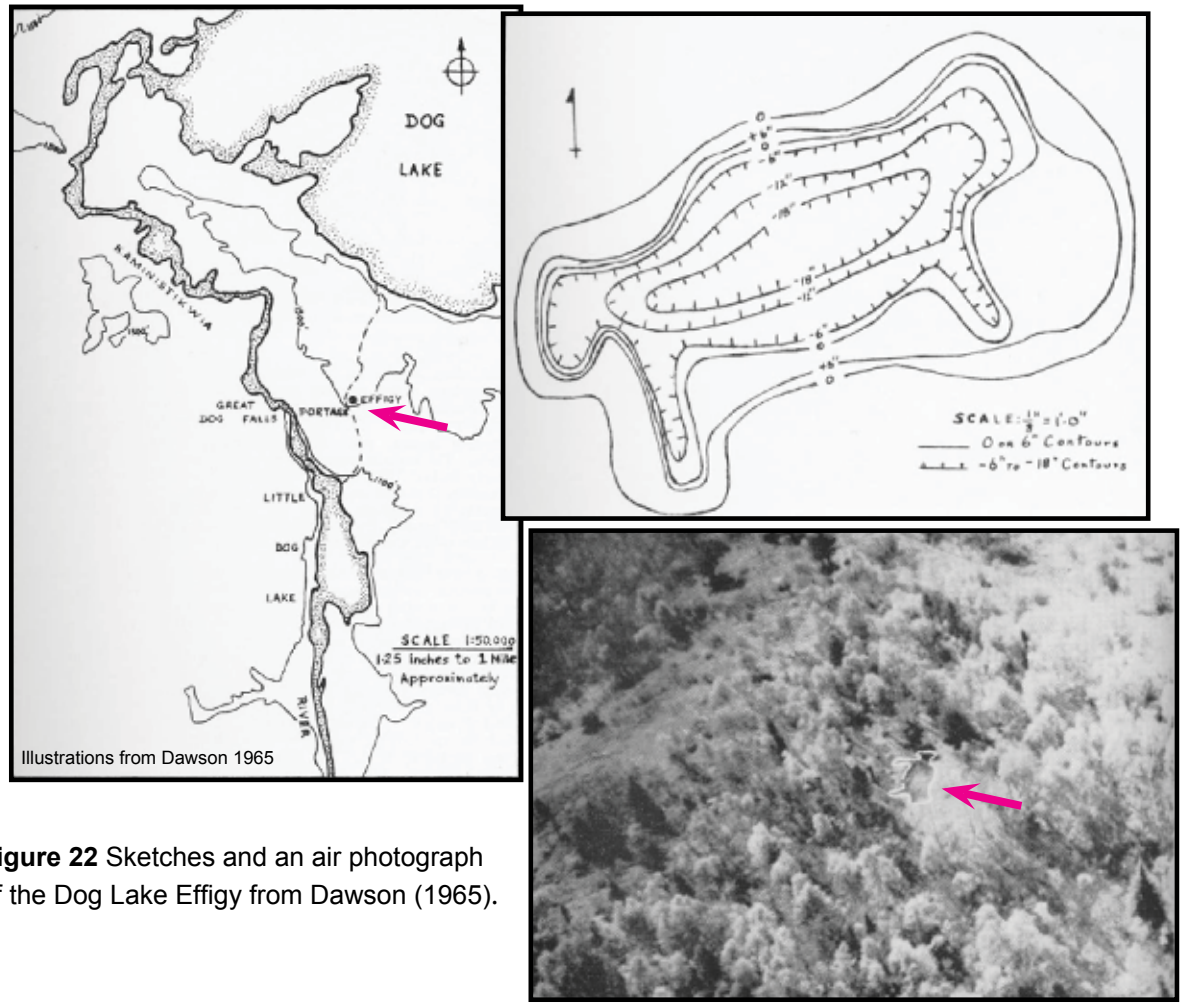

Figure 22 Sketches and an air photograph of the Dog Lake Effigy from Dawson (1965).

Given the small area considered, we used an alternative method for ortho-rectifying the imagery. This involves use of the Cartesian coordinates for pylons 2 and 4 that are visible in several discrete photographs. The photogrammetry service utilized these known coordinates rather than the GPS tags on the photographs (that are likely rather inaccurate given the poor GPS satellite reception). This maximized the precision of the GeoTIFF image generated by the photogrammetry service.

While our flight was rather rudimentary, we generated sufficient well-placed and overlapping images to create a mosaic. Contrary to initial expectations this documented the rather subtle relief defining this earthwork (Fig. 23:A) in the DEM (Fig. 24). This was in spite of the overburden of snow on grassy vegetation, the mix of sunlight and shadows running across the earthwork, and the obstructing tree canopy surrounding the clearing (Fig. 23, 24).

The Dog Lake Effigy is clearly the most challenging test for data collection and photogrammetric processing. To evaluate the geometric precision of the mosaic, we manually measured the distances between each of the four orange plastic pylons illustrated in Figure 24. After scaling the mosaic image using the one metre range poles, we measured the distances between pylons on the photo mosaic, and placed a yellow circle where the taped measurement indicated the pylon location. As Figure 24 demonstrates, three of the four yellow circles coincide quite precisely with the orange pylons, while the yellow circle over pylon 3 is displaced by 10-15 cm (Fig. 24). As this represents the longest taped distance, and runs across (and probably slightly down into the centre of the earthwork), we suspect that this displacement might be a tape measurement error on our part. This demonstrates that the spatial integrity

of the photo mosaic is quite good, and may exceed the precision of the field measurements. Clearly, in situations of good visibility, low elevation drone photography is sufficiently accurate to create large-scale cartesian maps of archaeological sites and features.

Finally, the drone is also effective for 'viewshed' site interpretation. In Figure 23:C we include an oblique angle photograph that includes the clearing containing the effigy (a in Fig. 23:C) perched along the top brink of the Dog Lake Moraine overlooking the Kaministiquia River valley. While the vegetation cover prevents any sense of the effigy 'viewshed' from ground height, the drone image effectively demonstrates it. As the effigy is positioned near what Dawson (1965) identified as one of the portage paths

A View from ground height looking east along length of earthwork.

B View up from clearing containing earthwork, revealing the limited airspace within which to fly the drone.

C View ssw from top of Dog Lake Moraine into Kaministiquia R. valley. Note effigy location in photo C (a).

Figure 23 Photographs of the Dog Lake Effigy feature and area. The earthwork itself is difficult to detect in photo A, but is located within 20 metres of the break in slope overlooking the river valley. It would have had a commanding view of the area to the south if the forest vegetation was cleared back.

Right: Google earth satellite image of clearing containing the effigy feature. It was invisible in the satellite image and the clearing (arrow) could only be identified with reference to the GPS coordinates calculated for Pylons 2 and 4.

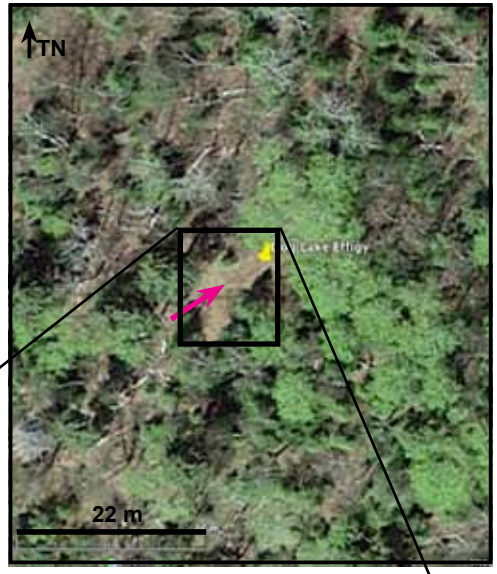

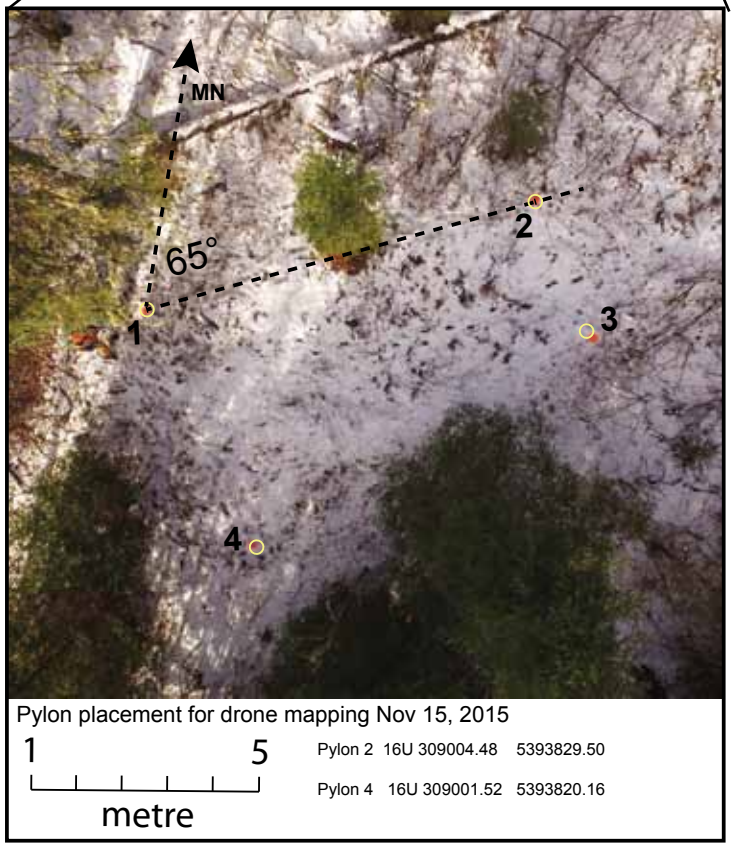

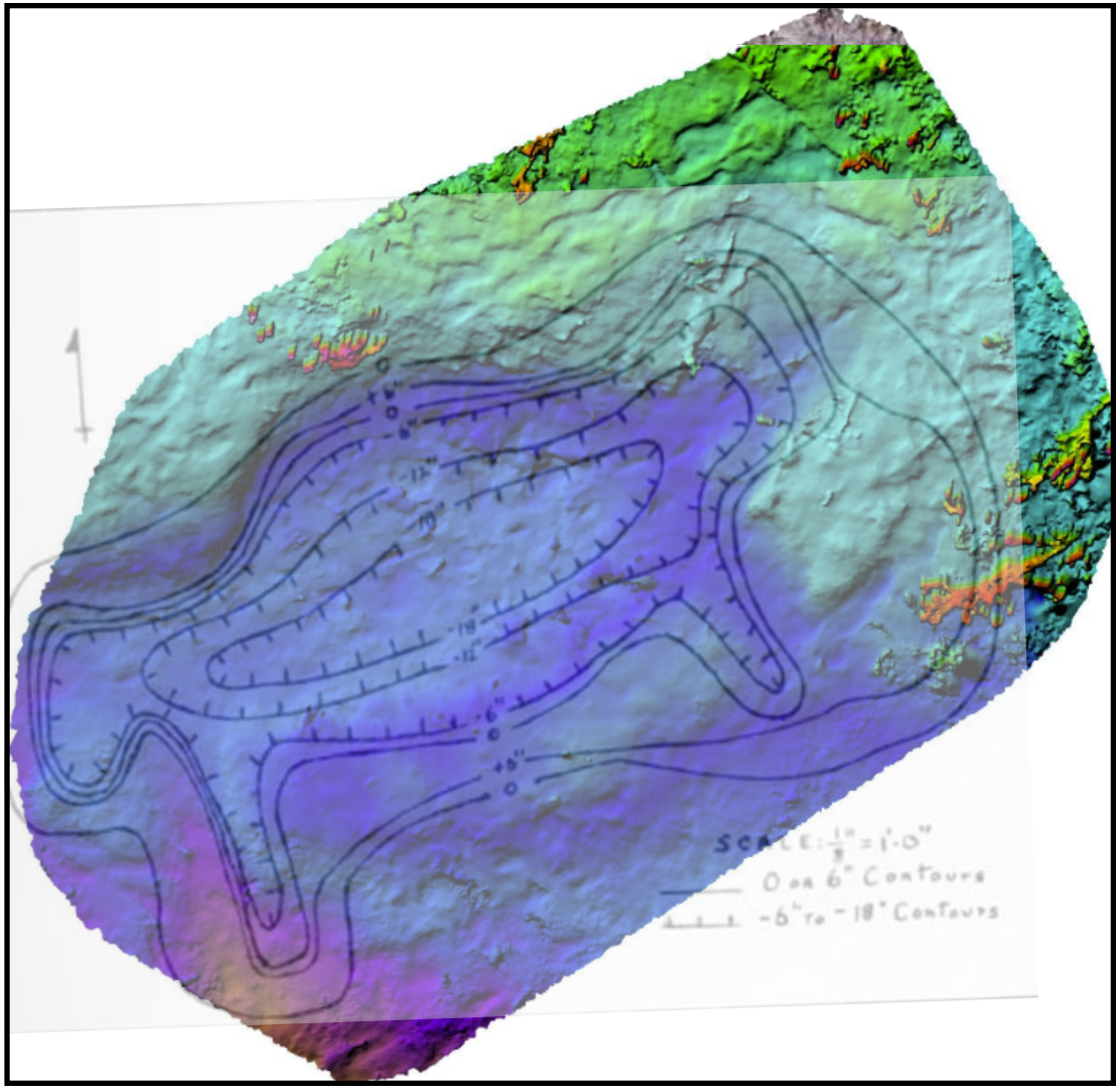

Up: DEM (colour image) of effigy, approximately overlaid with re-scaled isocline map produced by Dawson (1965). 'Head' of effigy is cut off the DEM because of obstructing trees.

Left: Photo mosaic of the Dog Lake Effigy. The orange pylons were measured with 60 m tapes to independently define their spatial configuration. The yellow circles mark the calculated position of the pylons based on the measurements. Note only pylon 3 diverges slightly from actual location.

Figure 24 Drone photomosaic and DEM of Dog Lake Effigy. The DEM is overlaid with Dawson's sketch map. The Google earth satellite imagery is offered in contrast to the resolution offered by the low elevation photograph and DEM.

over the moraine to Dog Lake, the photo draws attention to the strategic positioning of the effigy.

Kaministiquia River Delta lithic sites

In 1994 Hamilton (1996, 2000) conducted an archaeological survey of agricultural fields within the Kaministiquia River delta. This project was conducted on behalf of the Ontario Ministry of Natural Resources to assess the feasibility of GIS-assisted archaeological predictive modelling as part of timber harvest planning. This reconnaissance was one of several field surveys conducted, and focused on freshly cultivated fields in search of archaeological materials in situations of maximum site visibility. The discovered sites were then considered in light of associated landscape features to determine which ones might have utility for predicting archaeological site distribution.

Lithic scatter sites were intercepted on a number of the fields, many of which seem to be associated with subtle relief change, now-dry stream channels and relict lakeshores, and other landscape features. However many such features were not mapped on the available maps of the time. With the passing of over 20 years, and despite the availability of much improved satellite imagery, it is still difficult to remotely detect these features until LIDAR imagery is readily available.

In order to assess whether drone photography effectively documents features associated with possible Paleoindian lithic scatters, several localities were re-investigated. This includes the area located within the square labeled 3 in Figure 14. It contains a mix of cultivated fields, mature forest and wetlands, with the Kaministiquia River to the south. The most widely recognized Glacial Lake Minong shoreline bisects the area (defined here by the 750 foot contour line in Fig. 14 and 25), and appears important in explaining the site distribution.

Figure 25 illustrates the Rosslyn Village area, and the area below the 750 foot contour line is coloured blue to suggest Glacial Lake Minong. This elevation coincides with many of the best known and well-published Lakehead Complex sites (i.e. Cummins Site) (Julig 1994). While glacial meltwater achieved higher elevations, and by 8,000 years ago drained to levels lower than the current Lake Superior (Glacial Lake Houghton), this contour line is a useful local proxy for a relatively stable phase of Glacial Lake Minong. Within Figure 25, the 750 foot contour also marks an abrupt break in slope that coincides with aeolian reworked sand (dunes), coupled with silts at higher elevations and poorly drained muck and peat below (see the 1929 soil map included as a inset in Figure 25).

A series of lithic scatters were noted within the Breukelman Evergreen field and another group in the Halow C field in Figure 25. These localities are identified as Field A and Field B respectively in Figure 26 that includes Google earth satellite imagery at various scales. While this imagery is much higher resolution than what was available in 1994, it is still insufficient to detect the subtle landscape characteristics associated with the sites. During the original inspection we noted that lithic debitage clusters (virtually all composed of Gunflint Formation taconite) were often associated with localized sandy knolls. These subtle undulations were only visible when walking across the fields, and were not apparent on any of the maps or air photos available at that time. Hamilton (1994) hand-sketched some of these subtle features on the site maps to draw attention to them (Fig. 25).

It was speculated that the sites in Field A (Fig. 26) coincide with localized well-drained knolls found around what might have been a shallow embayment of Glacial Lake Minong. It is approximated by the 750 foot contour line, with low elevation wetlands to the east coinciding with a poorly drained glacial lake bottom (Fig. 26).

The first effort at drone photography of Field A involved a flight plan that encompassed all of the lithic recovery areas within the field. It specified an elevation of 50 metres, and with 70% overlap between adjacent images. This was calculated to complete the mission using one battery, leaving sufficient power to safely return HOME to land. The flight plan is illustrated in an inset in Figure 27, and was rather ambitious given the size of the field. Hamilton flew this flight alone, compounding some of the problems encountered during the flight.

Upon launch, the drone rose to the proscribed elevation and flew northeast from HOME (purple dot) to the mission start point (Fig. 27:2 or green dot). As the drone flew away, it rapidly was lost from sight against the grey overcast sky. Hamilton was able to monitor its progress using the downward pointing camera, and the red triangle on the iPad that marked the drone's location.

After reaching its start point, the drone paused momentarily to reorient itself, and then began flying northwards along the first flight line, taking the first two photographs defined by red and green bordered rectangles in the flight plan illustration (see also the two air photos of the east edge of the field in Figure 27). At that point the Map Pilot screen froze, and no more imagery or updated telemetry information appeared on the iPad screen. The drone was not visible in the sky, nor was there flight status information available. It was not known whether it had crashed, was continuing its flight plan (with a temporary loss of radio communications), or whether it was uncontrollably flying off in a random direction (the dreaded 'fly away' that sometimes affects UAVs). None of these alternatives is good news.

After momentary indecision, Hamilton aborted the mission by hitting the 'COME HOME' button on the radio controller. After an interval (probably about 3-5 minutes), he observed the drone flying back to the HOME position, whereupon it hovered momentarily before beginning a controlled descent and a safe landing.

We do not know what caused this mishap. The distance between the HOME point and the start point was about 425 metres (well within the rated performance range of the Lightbridge video-streaming system), but the machine clearly lost communications with the radio controller. This might be due to several

issues.

The Lightbridge antennae on the drone are installed in two of the landing legs. Perhaps the orientation of those legs resulted in brief loss of signal reception, and the drone followed the fail-safe protocol and returned HOME. The radio-controller antennae should always be deployed to point approximately towards the drone. Perhaps momentary inattention on Hamilton's part (or inability to see the distant drone) disrupted this orientation, causing communication loss. It is reassuring to note that when such communications loss occurs for more than a few seconds, the drone is automatically programmed to return to the HOME position and land. It is not clear whether this happened because Hamilton hit the COME HOME button, or whether the drone automatically returned HOME upon losing communications. Efforts to map Field A were suspended until further flight testing and error checks were completed.

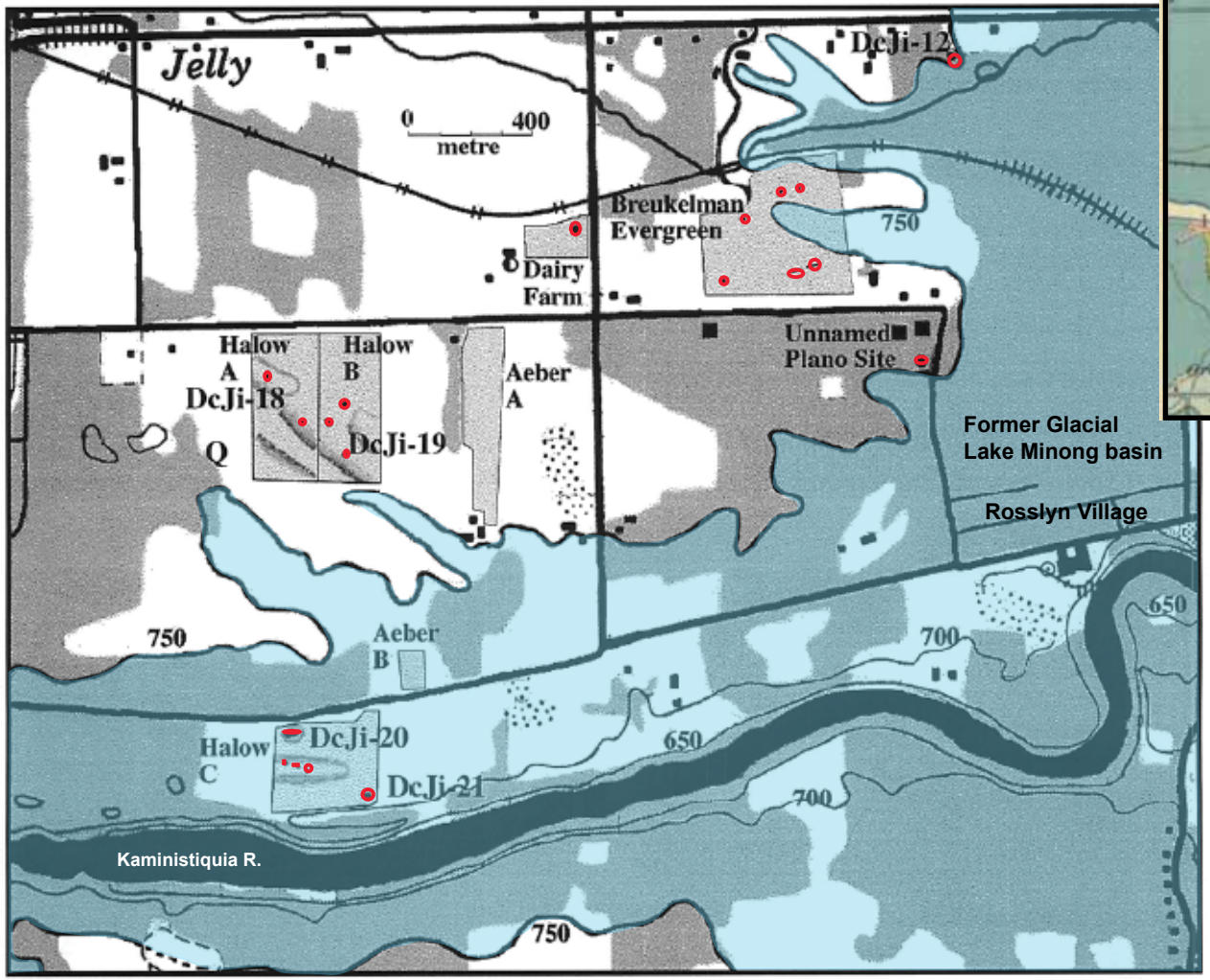

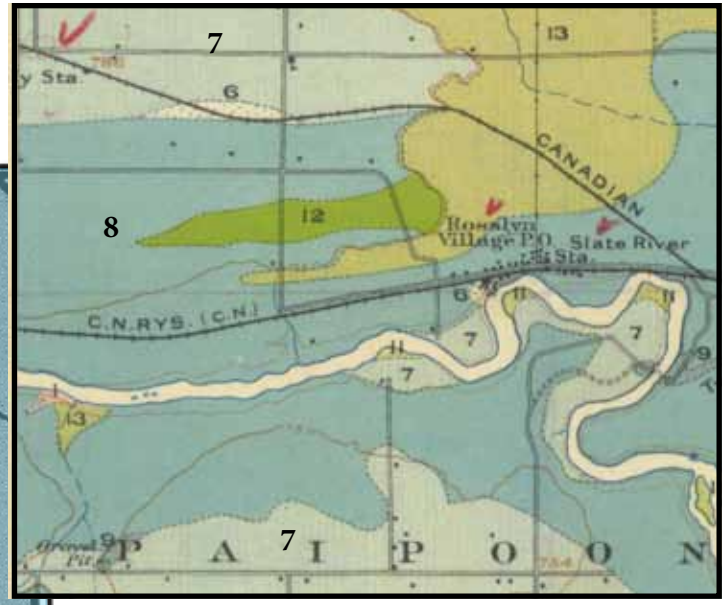

Figure 25 Map of the Rosslyn Village area, with the 750 foot contour line reflecting former Glacial Lake Minong water levels. The red dots and ovals mark archaeological site locations. The inset soils map is a detail from the 1929 Canada Dept. of Mines Geological survey map 197A showing the Rosslyn Village area. The sediments reported on this map are coded as follows: **6**) Clay; **7**) Silt; **8**) Fine Sand; **9**) Gravel and Stoney Sand; **11**) Alluvium of present streams; **12**) Dune Sand; **13**) Muck and Peat. The patterned distribution of these sorted sediments is consistent with our current understanding of the Glacio-lacusturine and fluvial history of the region.

Field A was subsequently flown with no difficulties. The DEM output is represented in Figure 28. This overview map includes a Google earth image of the survey area in the background, and overlaid with the DEM generated by the drone flight in the foreground. The estimated elevation (in feet) of the colour spectrum is represented in the bottom of the image. Additional information added to the image include a tracing of the 750 foot contour line (from NTS map) thought to approximate the former Glacial Lake Minong shore, and the location of the small lith-

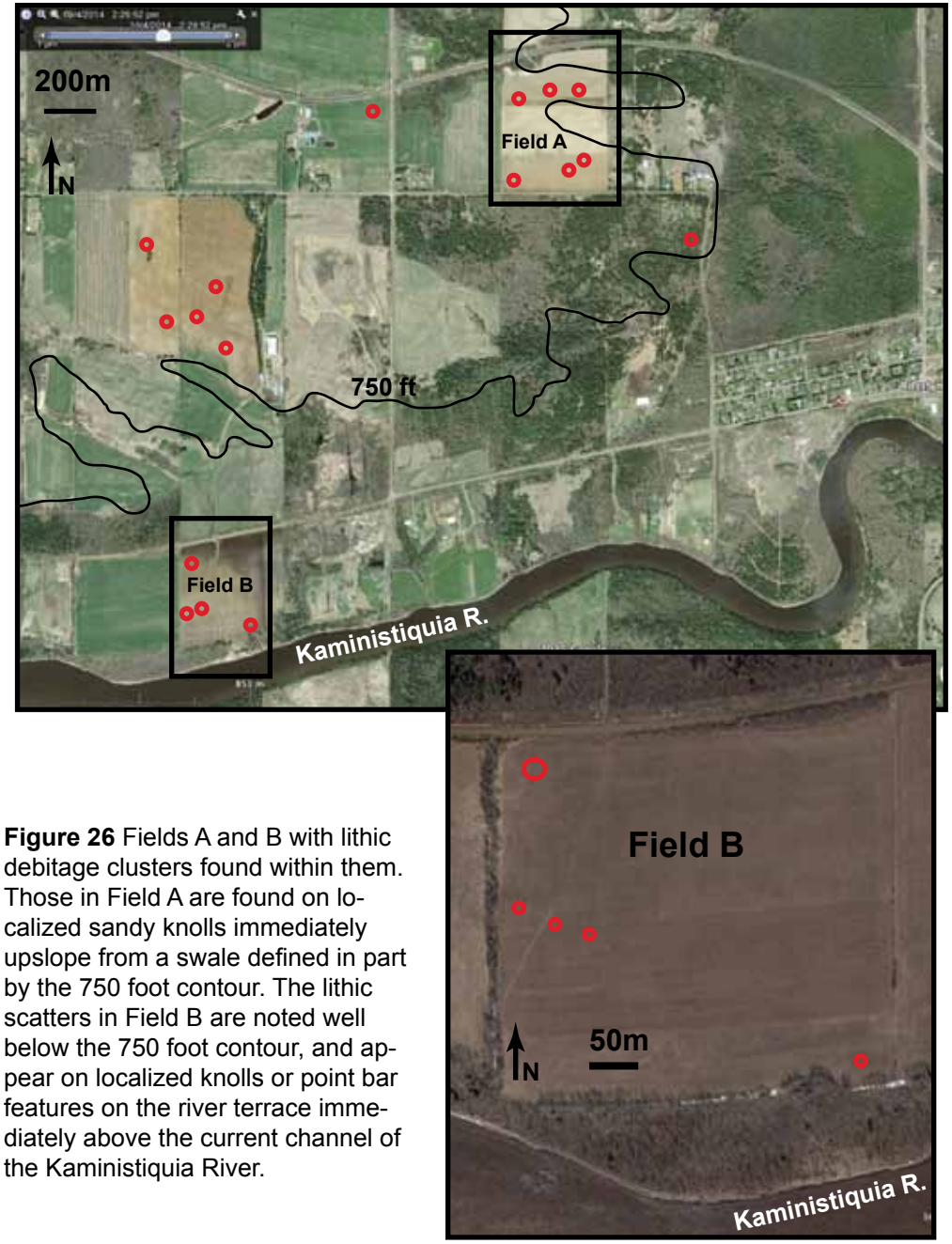

Figure 26 Fields A and B with lithic debitage clusters found within them. Those in Field A are found on localized sandy knolls immediately upslope from a swale defined in part by the 750 foot contour. The lithic scatters in Field B are noted well below the 750 foot contour, and appear on localized knolls or point bar features on the river terrace immediately above the current channel of the Kaministiquia River.

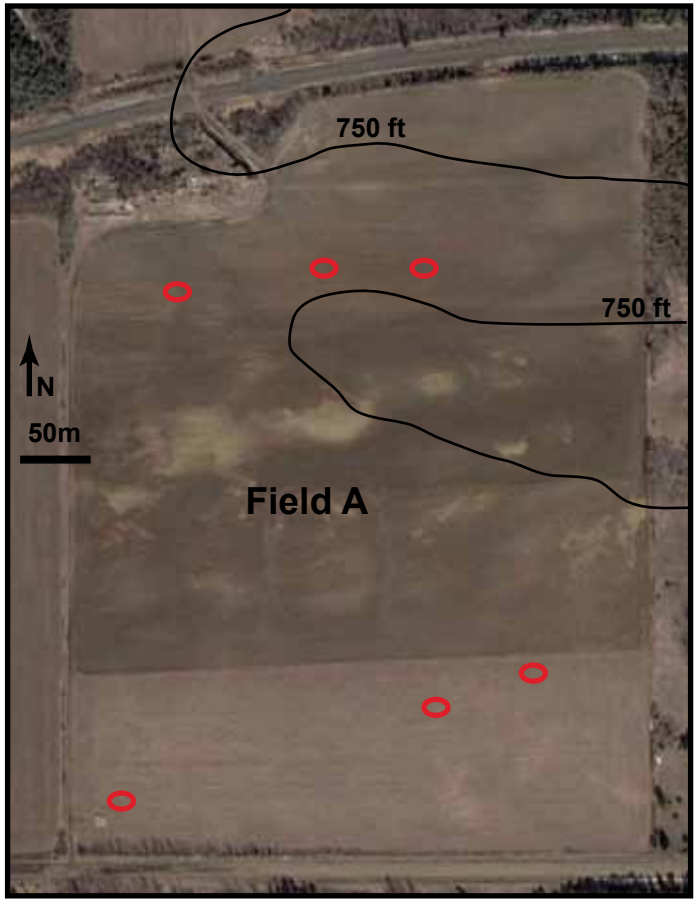

Cultivated fields in the Kaministiquia River delta that contain lithic scatter sites (red ovals) that are predominantely taconite.

These deposits are sometimes found immediately upslope from the 750 ft contour line, generally accepted to mark mid-Glacial Lake Minong shoreline levels.

Lithic scatters within Field A appear on localized sandy knolls overlooking a swale defined in part by the 750 ft contour.

Recoveries in Field B are also found on sandy localized knolls, but topographically below the 750 foot contour line.

These subtle landscape features are not visible in existing maps, and at issue is whether low elevation UAV photography will reveal them more clearly.

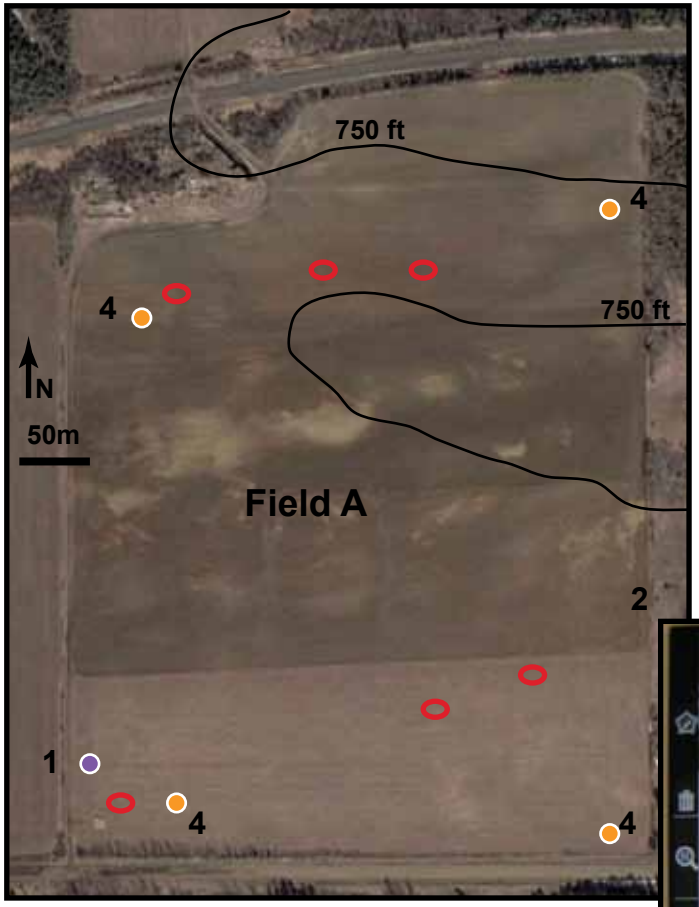

Right: Flight planning window on iPad generated with 'MapsMadeEasy' app. This allows flight planning to maximize efficiency, and to ensure uniform information collection.

The first two images reduced to 20% of original size. Note the degree of overlap between adjacent images to enable photogramatic interpretation. If flight was completed, a mosaic would have been generated of the whole field.

Left: Satellite image of Field A. While much more detail is apparent than was case in 1994 when the survey was completed, it is still insufficient to reveal the relevant landscape features.

1 UAV launch point

2 start of photo transect

3 end of photo transect

4 points marking corners of photo area defined by flight paths (white lines) designed to collect images with 70% overlap.

Flight plan specified an elevation of 50 metres with 70% overlap in order to ensure completion of the flight within the life of one battery.

After flight initiation and capture of two images, signal was lost between UAV and controller. Flight was aborted, and drone returned to 'start point' (1) whereupon it was retreived without damage.

Figure 27 The initial failed effort at mapping Field A.

ic scatters observed in the cultivated field. The DEM represents the swale running e/w through the centre of the field, with sandy upland knolls located around its margins. It effectively demonstrates the distribution of archaeological material relative to the hypothesized small cove along the glacial lake shoreline in more detail and precision than the conventional maps. It highlights errors in air photo interpretation made during the production of the NTS contour map of the area. In the absence of better-quality satellite or LIDAR imagery, low elevation drone mapping clearly offers analytic value.

Photo-documentation of the Halow C (Field B) locality (Fig 25, 26) was completed with none of the problems apparent at Field A. The drone was no further than 250 metres from the radio-controller during this flight, and care was taken to orient the antennae appropriately at all times. Perhaps this was sufficient to ensure flawless automated flight. While appearing a minor point, undertaking semi-autonomous flights requires focus, concentration and attention to detail. Two person flight missions, reference to a flight check list, and regular practise may be the best means of avoiding problems.

When investigating Field B, we sought to address a localized taconite lithic scatter found upon an sandy knoll in its northwest corner (Fig. 26). There is no more than 1 metre elevation difference between the knoll and the rest of the field. But its sandy sediment differs sharply from the silt making up the balance of field (Kaministiquia River flood plain). While a few flakes were found in other locations (notably on point bar terraces Fig. 26), the one associated with the sandy knoll was quite productive and very localized (likely less that 30 to 50 m^2). While it was readily evident while walking the field surface (Fig. 29), it is not detectable on any of the available maps, air photos or satellite images (Fig 26).

Figure 30 includes the best available satellite imagery, the Map Pilot flight plan, and a low resolution version of the geo-referenced photo mosaic overlaid upon a Google earth backdrop. The flight was flown at 40 metres elevation at a speed of 2 m/s, and with 70% image overlap. Weather conditions were good, with low winds, but with sunny skies that cast shadows.

The geo-referenced photomosaic image output is 285 by 182.6 inches (724 by 474 cm) at 72 DPI and requires 586.8 MB of storage space. This massive file captures very good detail of the field surface (Fig. 30). The inset image in Figure 31 offers sufficient resolution to show the tractor tire treads near the approach to the field, small stones on the edge of the road, as well as Hamilton as he operated the radio controller. The sharpness and clarity of the ground surface evident in Figure 31 appears better than the Boulevard Lake output (Fig. 20) that was flown at the same elevation and speed. The only real difference

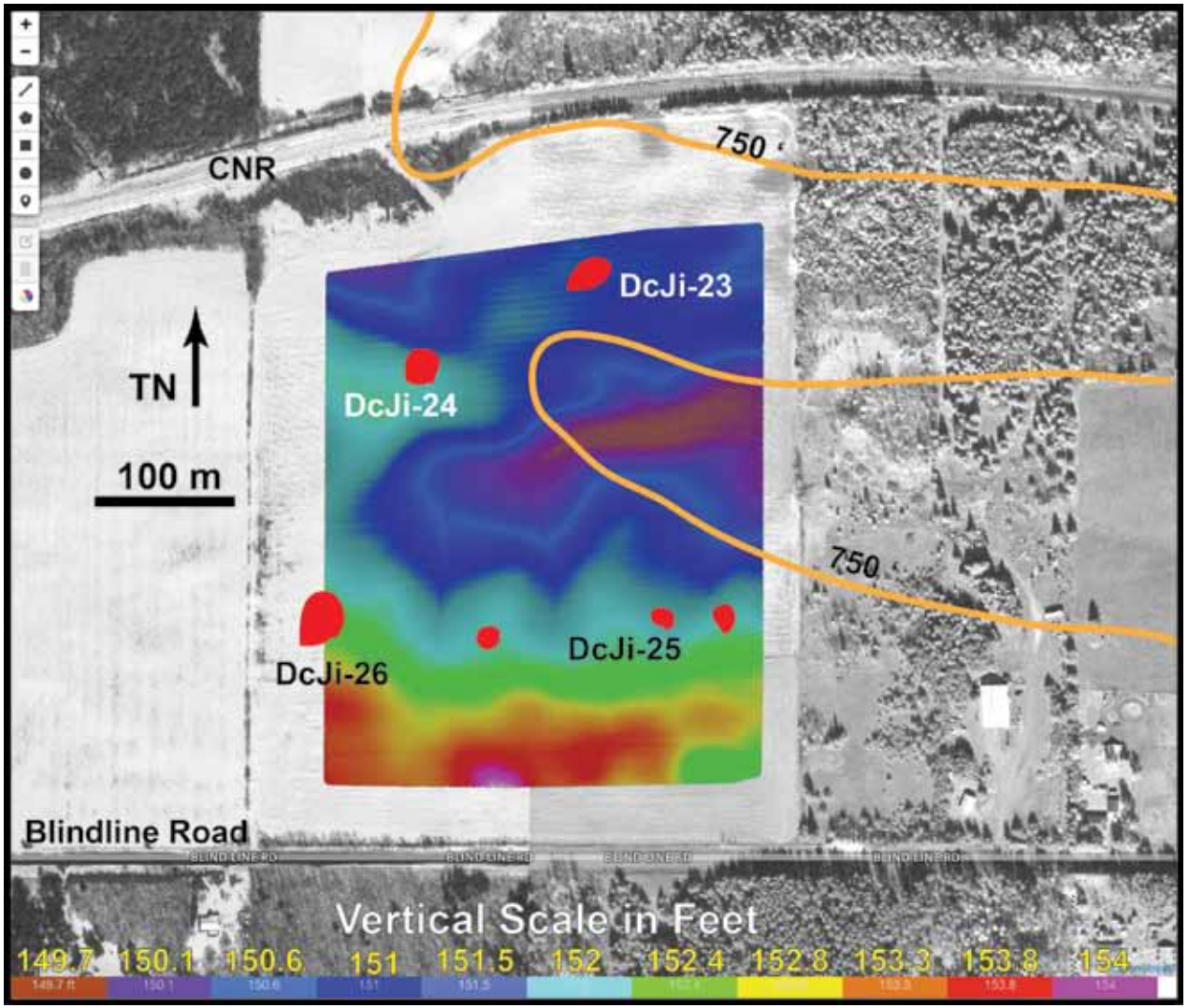

Figure **28** DEM of a successful flight over Field A documenting subtle landscape features thought to be conditioning archaeological site distribution.

was the lighting (Boulevard mission was cloudy while Field B was sunny).

Examination of the forest canopy around the north and northwest margins of Field B demonstrates that the software had difficulty generating the mosaic in these localized areas (Fig. 30). This is because the individual boughs and trunks of the trees were too complex for the software to find 'matches' from one overlapping photograph to the next. This is an impediment when documenting sites with a significant degree of vegetation cover.

Representing the imagery in a conventional 8.5 by 11 inch print format greatly impedes ability to interpret surface features compared to what can be observed in the original electronic imagery. The electronic output allows detection of quite small and subtle surface features which can only be 'seen' when one zooms to a large scale. Of course this means loss of perspective and broader spatial context. When examining such features electronically, one can readily zoom in and out to detect and interpret the relevant features, but this is not possible with static printed images. The most viable alternative is to provide large scale detail images of specific areas of interest that are referenced in a smaller-scale orientation image (see Fig. 31).

Figure 32 includes a reduced version of the Digital Elevation Model (DEM) generated from the geo-referenced photo mosaic of Field B. While our analysis of the precision and accuracy is incomplete, it effectively represents the low knoll located in the northwest corner of the field. The approximate location of the lithic scatter is marked by the red oval (Fig. 31). Given that only one mission was flown over this site with 70% image overlap (and with sunny conditions casting shadows), the DEM exceeded our expectations.

The high quality of the ground surface detail presented in Figure 31 offers possibilities for documenting the spatial distribution of archaeological objects in cultivated fields. For example, the Ontario Ministry of Tourism, Culture and Sport (MTCS) *2011 Standards and Guidelines for Consulting Archaeologists* specify controlled surface collection of freshly 'plowed' fields as a standard method for delimiting disturbed sites prior to subsurface testing. This often involves walking survey transects, with pin flags used to mark observed artifact locations. The distribution of these pin-flagged artifacts are then plotted using a total station or other GPS-assisted method. Perhaps drone-generated low elevation aerial photography might offer a cost-effective alternative, particularly with production of geo-referenced photo mosaics and DEMs. These high resolution (and geo-referenced) aerial images can be examined within a GIS, and may enable an alternative means of identifying artifact spatial patterns in cultivated fields as a prelude to subsurface testing.

While not readily visible in the small-scale version presented in Figure 32, the shadows cast across the road by the tall trees appear to be interpreted by the software as shallow depressions running across the road. If the field was photographed under the optimal overcast conditions these 'false depressions' (linear shadows) may not have appeared. This offers an interesting point of contrast to the test flight over Old Fort William which as also flown under sunny conditions, but without exhibiting the same problem with pseudo-relief deriving from shadows. Perhaps this is because the latter flights documented dramatic local relief change represented by tall (sharp-edged) structures, thereby minimizing the impact of the shadows.

Old Fort William Heritage Site

Two flights were conducted over the main Officers' House complex at the Old Fort William heritage site that is operated by MTCS. It is a reconstruction of the original Fort William built in 1804, the main inland depot of the North West Company. This large complex contains an array of log structures within and immediately outside a log palisade that was the primary administrative, warehousing and industrial centre of NWC operations (Fig. 33). The Officer's House Complex consists of three large white painted buildings in the most visibly prominent location at the back of the open central courtyard.

Figure 33 offers a Google earth satellite image of the compound, with the inset representing the area

Figure 29 View west across DcJi-20 located on an isolated sandy knoll within Field B. (bit-mapped black and white image from Hamilton 1996:61).

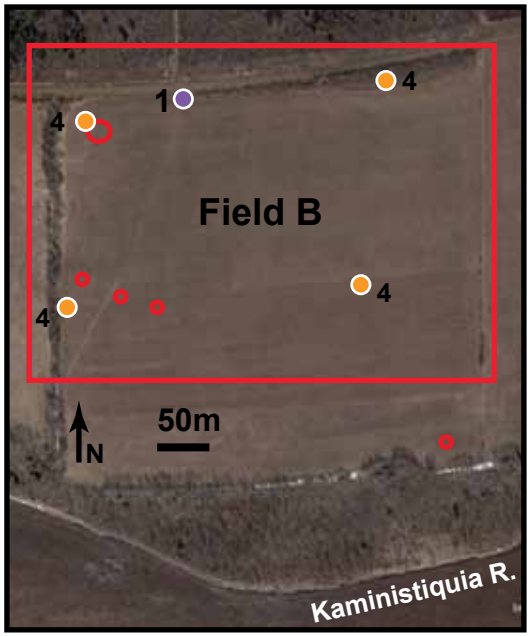

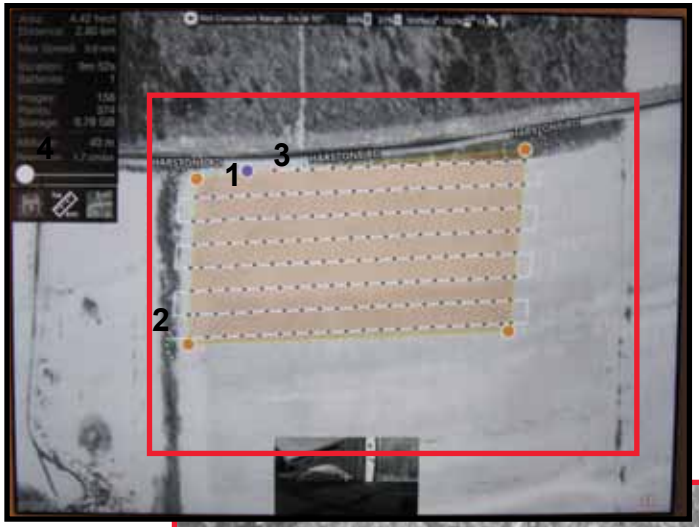

1 UAV launch point

2 start of photo transect

3 end of photo transect

4 points marking corners of photo area defined by flight paths (white lines) designed to collect images with 70% overlap.

Red ovals define lithic scatter locations.

Flight plan specified an elevation of 40 metres with 70% overlap in order to ensure completion within the life of one battery.

This automated flight plan was executed flawlessly, with 155 images (each 5.7MB) stored on the onboard mini-SD card. These images were uploaded to the 'MapsMadeEasy' photogrammetry service site, and rendered into a georeferenced orthomosaic.

While the photo mosaic below offers a much higher resolution image of the area of interest, the subtle relief associated with the distribution of artifacts is not readily apparent.

A Digital Elevation Model (DEM) was also generated. This proved much more effective in representing the site topography.

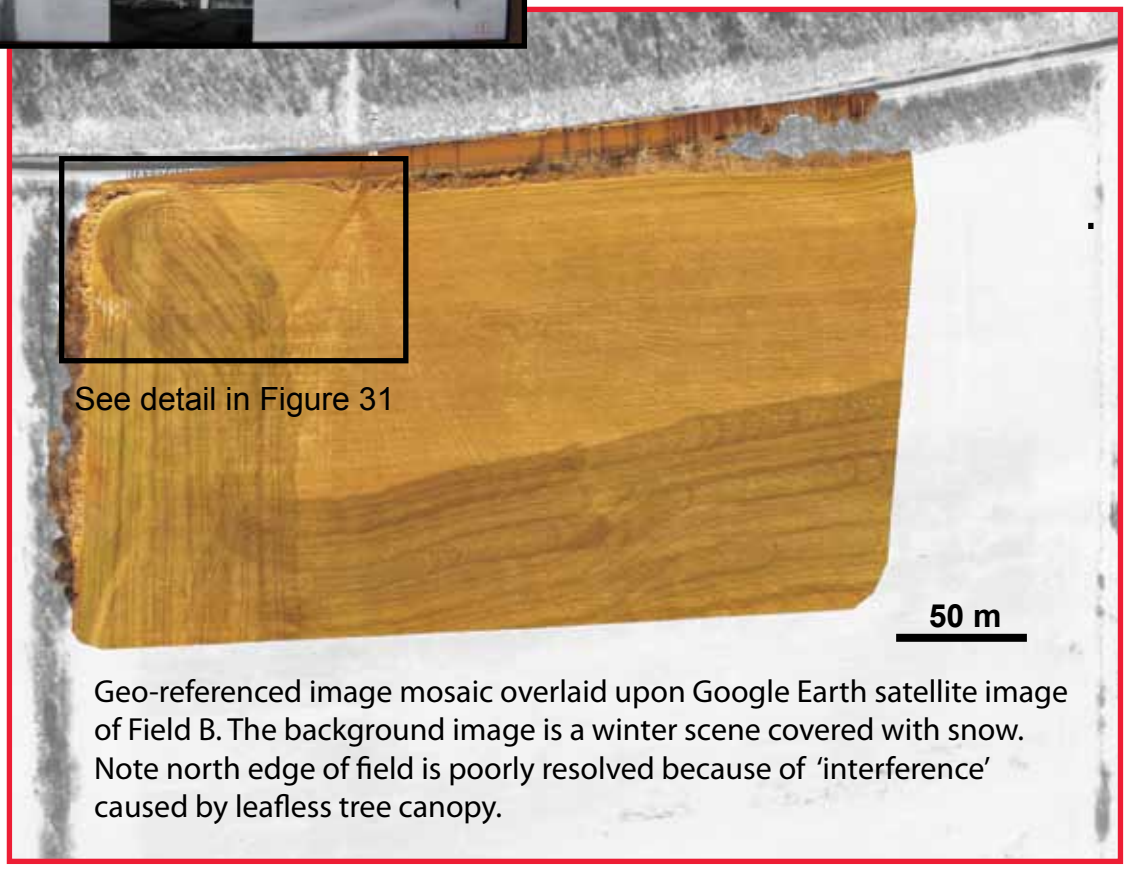

Geo-referenced image mosaic overlaid upon Google Earth satellite image of Field B. The background image is a winter scene covered with snow. Note north edge of field is poorly resolved because of 'interference' caused by leafless tree canopy.

Figure 30 Drone flight plan and georeferenced photomosaic for Field B.

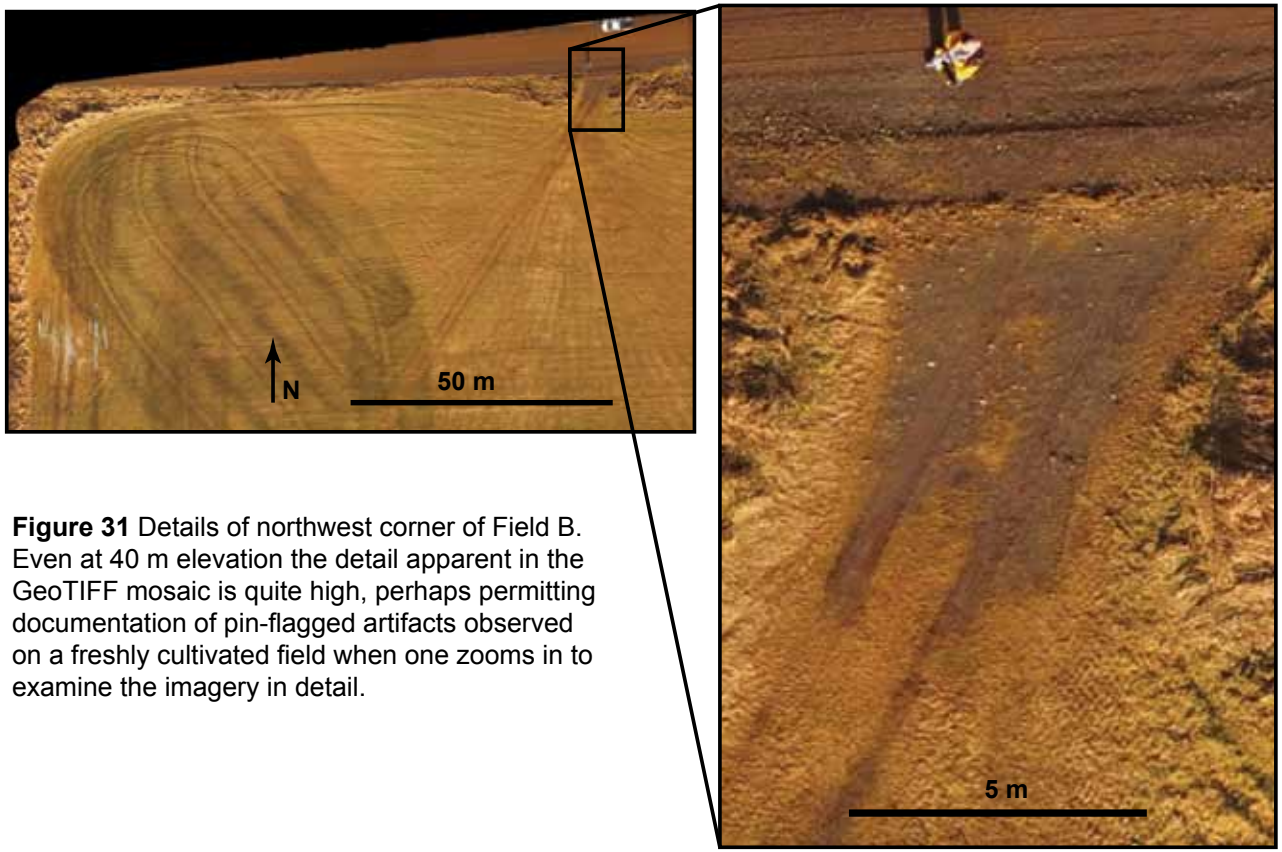

Figure 31 Details of northwest corner of Field B. Even at 40 m elevation the detail apparent in the GeoTIFF mosaic is quite high, perhaps permitting documentation of pin-flagged artifacts observed on a freshly cultivated field when one zooms in to examine the imagery in detail.

documented with the drone. While appearing quite detailed, it becomes grainy when viewed at larger scale, and offers insufficient detail of building features.

We received permission to fly the facility when no visitors were on the property to ensure safety and to minimize moving objects within the survey area. Two flights were completed: one with the camera pointing vertically down, and the second at approximately 30° from vertical. This was calculated to generate optimal imagery for a 3D model. These missions were flown using identical flight plans at an elevation of 40 m at a speed of 2 m/s, and with 70% overlap between adjacent images. The flights were conducted under sunny conditions and with a light wind from the west. Each flight was completed in succession using one battery each. Analysis of output indicates that the flight plan offered insufficient coverage of the front face of the Officers' House complex, resulting is poorer rendering of the front facade compared to back of the buildings.

Figure 34 is a scaled down version of the GeoTIFF photo mosaic of the survey area. The detail image inset demonstrates the ground detail recorded in the original image. The brick pavement surrounding the outdoor oven is readily interpretable, as is the utility vehicle parked nearby. The mosaic seems to address the isolated (leafless) trees found within the frame, but the DEM rendering is less satisfying.

Figure 35 is a scaled down version of the DEM, with red representing high elevation, orange-yellow and green representing mid elevation, and increasingly dark blue marking low elevation zones. Inset photos A, B and C illustrate discrete zones within the DEM that contain cultural features marked by localized relief change. Detail A represents small raised garden plots that are contained by 2 by 10 inch planks placed on edge. The 'waffle-iron' effect derives from the plank edges, raised planting areas and the natural ground surface. Detail B is firewood adjacent to the kitchen behind the Great Hall. It is stacked in rows about 3-4 feet tall, and the DEM is sufficiently precise to illustrate the depleted western row. Detail C marks objects and an outside fire hearth (with a steam box) located at the eastern entrance to the canoe shed. The circular objects forming a row along the east wall of the shed are upturned cast iron caldrons used for rendering pitch, with an outdoor fire hearth located nearby (Fig. 35). Even the gravel walkways that bisect the central courtyard are detected in the DEM (Fig. 35). The DEM is not measuring actual relief variation, but is photogrammetrically interpreting overlapping images, and relying heavily upon light patterns. The gravelled walkways likely stand out in contrast from the surrounding grassed lawn because of difference in light reflection. We also note in other flights that the white 60 m tape used to establish a scale on the ground is often miss-interpreted by the software as a very thin vertically oriented structure in the DEM. Despite these flaws, the DEM does represent a shallow swale that runs obliquely in a nw to se orientation behind the Officers' House Complex, and also the ne corner of the image that is a topographic low within the fort compound (Figure 35).

While visiting Old Fort William Park it was evident that the drone offered significant opportunities for cost-effective monitoring of such heritage structures. To that end we manually flew over the Great Hall and took several photographs of the roof line, gable ends and brick chimneys (Fig. 36). Such views of architectural details have great utility in evaluating the structural conditions (without the need of scaffolding or scissor lifts).

Finally, Figure 37 offers a screen capture of the

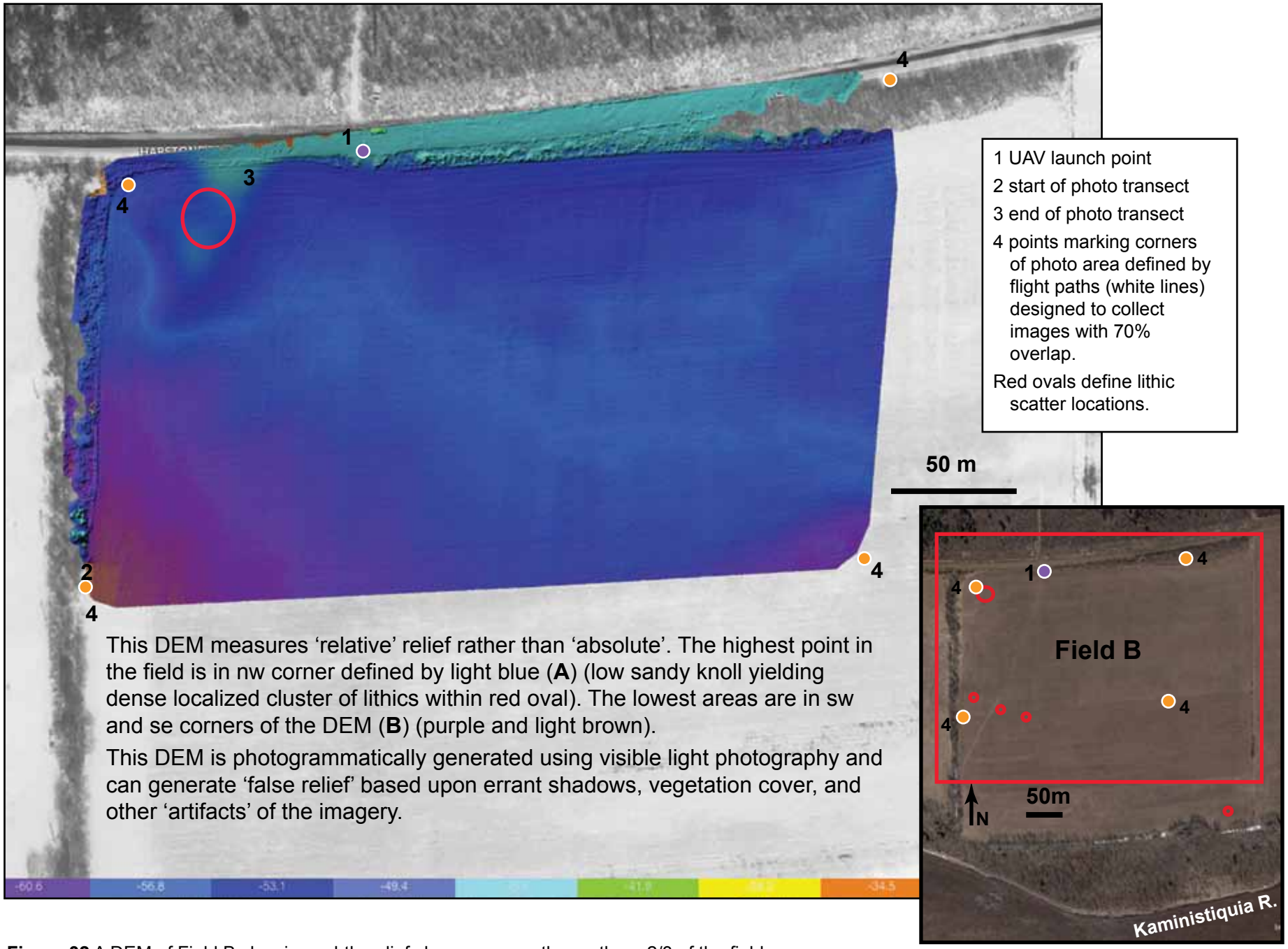

Figure 32 A DEM of Field B showing subtle relief change across the northern 2/3 of the field.

3D model of the building complex deriving from both missions. This image can be rotated and viewed from all directions and elevations within free software such as Google earth and Meshlab. Both of these programs allow dimension measurement of the features rendered within a 3D model. Ongoing research by Stephenson will assess the precision of this 3D model relative to direct measurements of the buildings.

While the interactive 3D model offers dramatic novelty value, it might also have analytic utility in viewshed analysis. For example, when considering cultural landscapes, medicine wheels, bison traps and other such features, interpretation might be greatly aided by viewing the area of interest from several angles and elevations. Consideration of the larger site locality might also be informative about the function of possible hunting blinds, outlooks and rock alignments. Such interactive consideration of site localities within 3D virtual reality is a largely unexplored aspect of Canadian archaeology, and is the subject of ongoing research.

Drones, Photogrammetry and GIS

UAV research throughout 2016 and 2017 has focused on information refinement using Geographical Information Systems (GIS) to aid application to Landscape Archaeology. Several case studies are briefly discussed here to illustrate the potential.

In the spring of 2016 Hamilton revisited fur trade posts located along the Assiniboine River of southern Manitoba (Fig. 38). They date from the late 1700s to the early 1800s and mark a time of intensive British fur trade competition. Hamilton initially documented these sites in the early 1980s (1982, 1983), and he sought to compare the original site maps with those deriving from UAV flights. This addressed issues of quality and resolution, and to estimate improved cost-effectiveness of low elevation photography and photogrammetry.

The 1980s investigations focused upon controlled surface collection of sites within cultivated fields, topographic mapping (optical survey instruments), and test excavation and proton magnetometer survey in undisturbed sites. The regional cartographic data available at that time consisted of paper-based maps and air photos, while now a great deal of electronic information is freely available from federal or provincial sources.

Figure 39 is an overview and detail map of a GIS project representing the best topographic and hydrological information available from Natural Resources Canada data sources (National Topographic Survey or NTS). The terrain visualization model represents relief change as a continuous variable ranging form green (lower elevation), through yellow, to light brown (higher elevation). These raster data are derived from interpolation of elevation points that also contribute to the contour lines (10 m contour interval) represented in Figure 39. For much of Canada, particularly rural and remote areas, this is the best data that is freely available from government sources, but now has been superseded by Google earth and other commercial imagery. It has limited analytic value because of its coarse resolution and overly generalized character, but remains useful for small-scale terrain visualization.

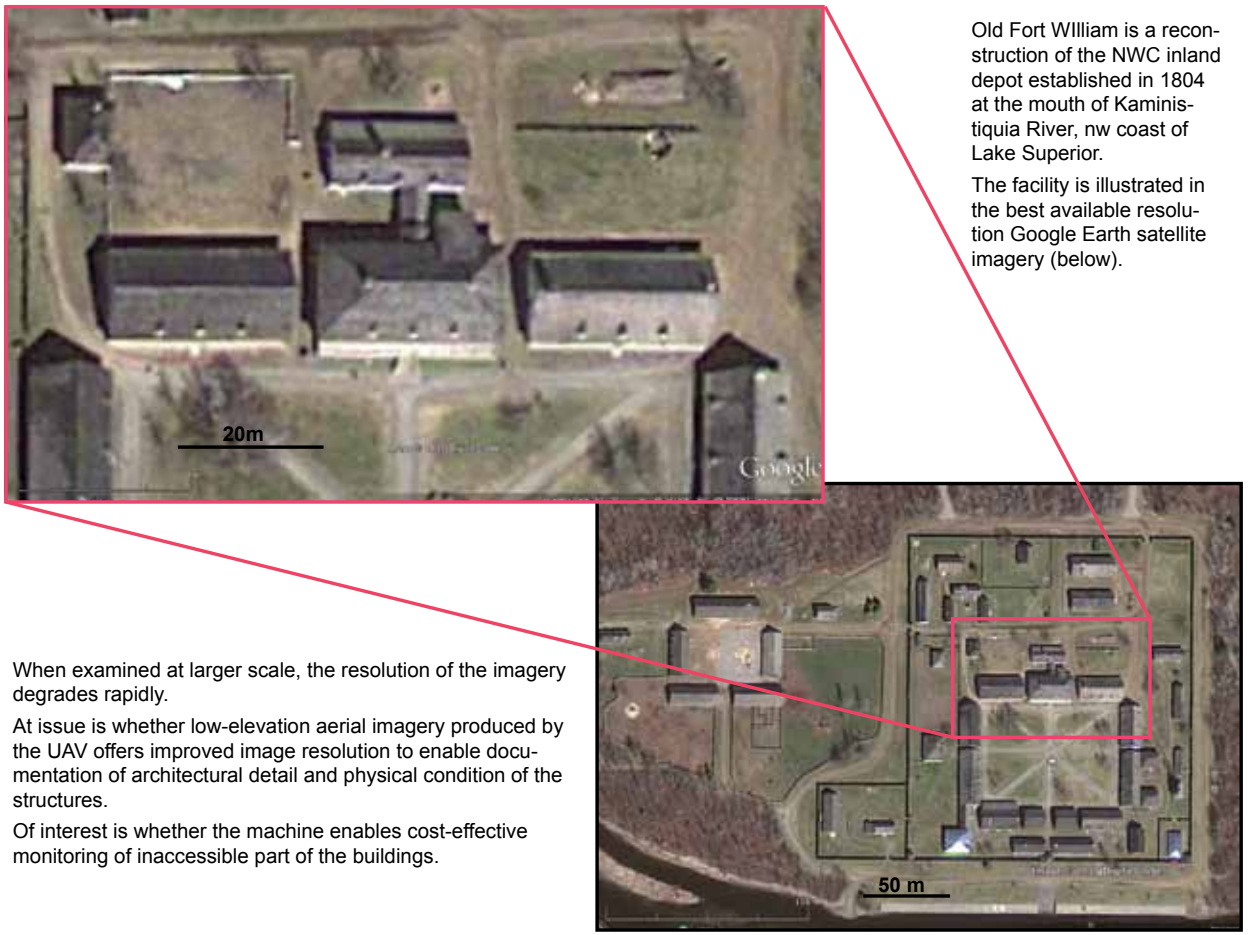

Old Fort WIlliam is a reconstruction of the NWC inland depot established in 1804 at the mouth of Kaministiquia River, nw coast of Lake Superior.

The facility is illustrated in the best available resolution Google Earth satellite imagery (below).

When examined at larger scale, the resolution of the imagery degrades rapidly.

At issue is whether low-elevation aerial imagery produced by the UAV offers improved image resolution to enable documentation of architectural detail and physical condition of the structures.

Of interest is whether the machine enables cost-effective monitoring of inaccessible part of the buildings.

Figure 33 Google earth imagery of Old Fort William at different scales.

Detail of original image illustrating brick pavement around outdoor oven behind the kitchen.

Georeferenced images stitched together in a mosaic. The original is 104.6 by 71.6 inches (72 dpi). This version is rendered at 300 dpi and 38% of original.

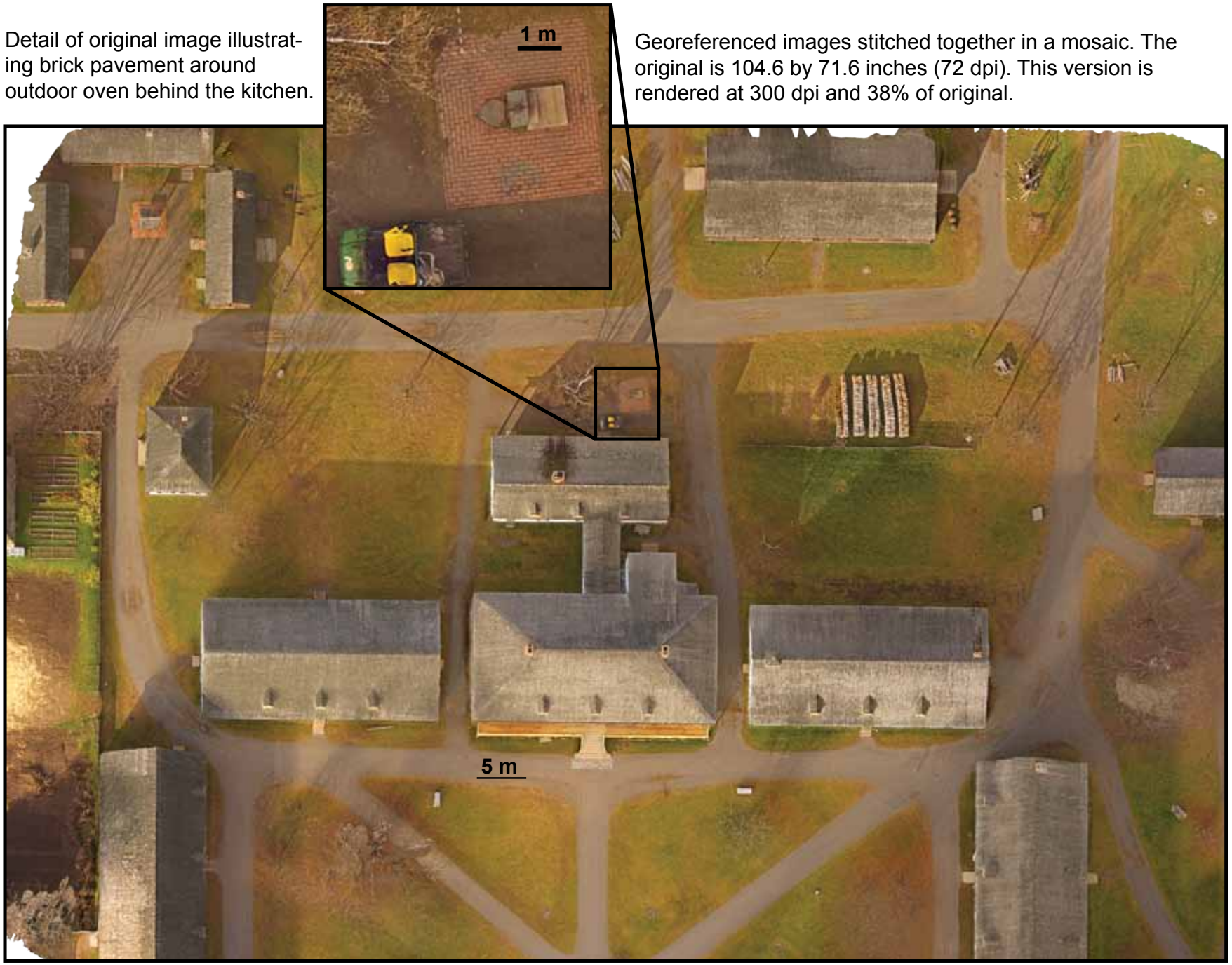

Figure 34 A scaled down version of the photo mosaic deriving from the two drone flights.

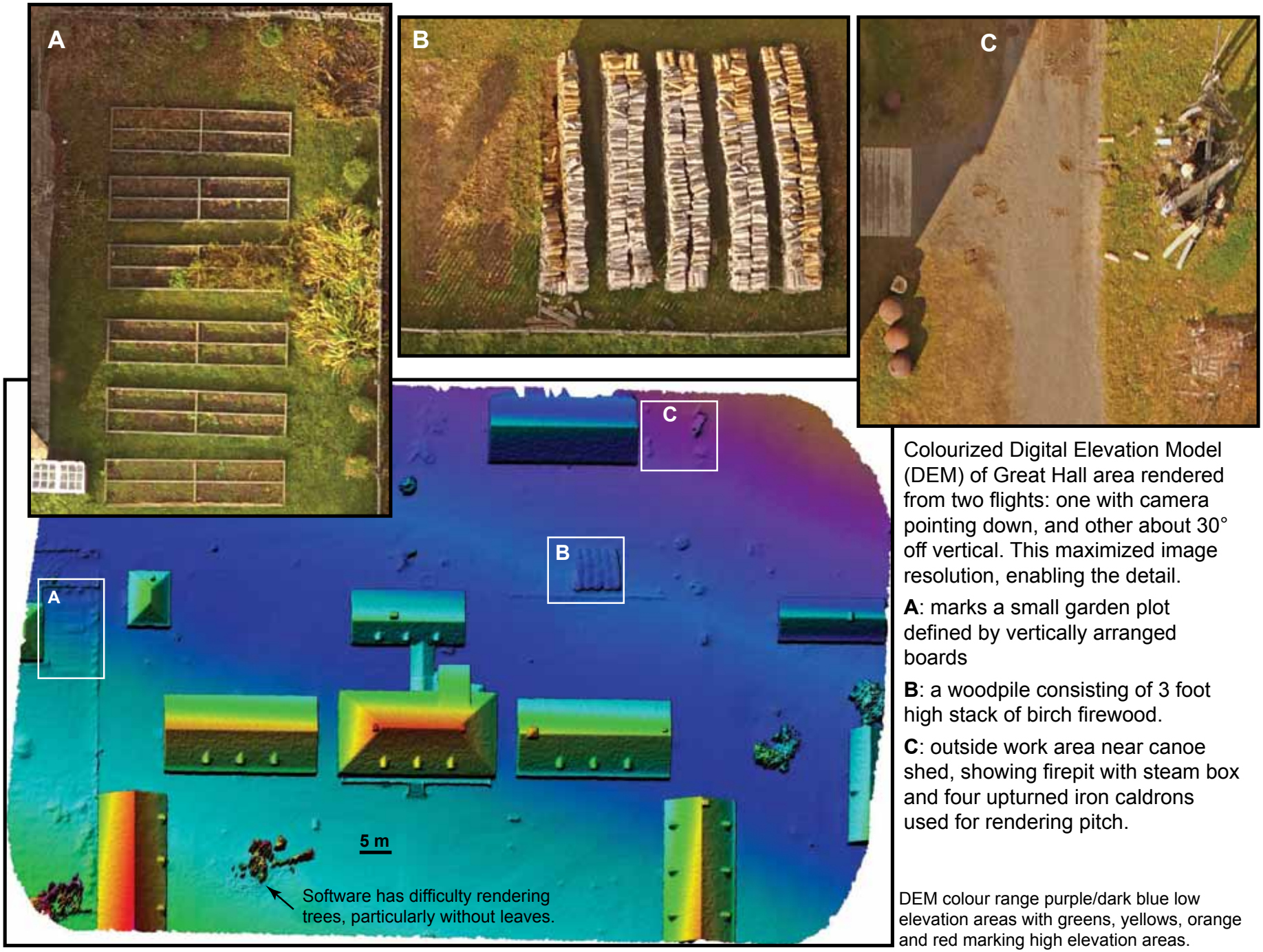

Colourized Digital Elevation Model (DEM) of Great Hall area rendered from two flights: one with camera pointing down, and other about 30° off vertical. This maximized image resolution, enabling the detail.

A: marks a small garden plot defined by vertically arranged boards

B: a woodpile consisting of 3 foot high stack of birch firewood.

C: outside work area near canoe shed, showing firepit with steam box and four upturned iron caldrons used for rendering pitch.

DEM colour range purple/dark blue low elevation areas with greens, yellows, orange and red marking high elevation areas.

Figure 35 Reduced version of the DEM of the Officers' House complex with inset photos detailing specific features within the compound.

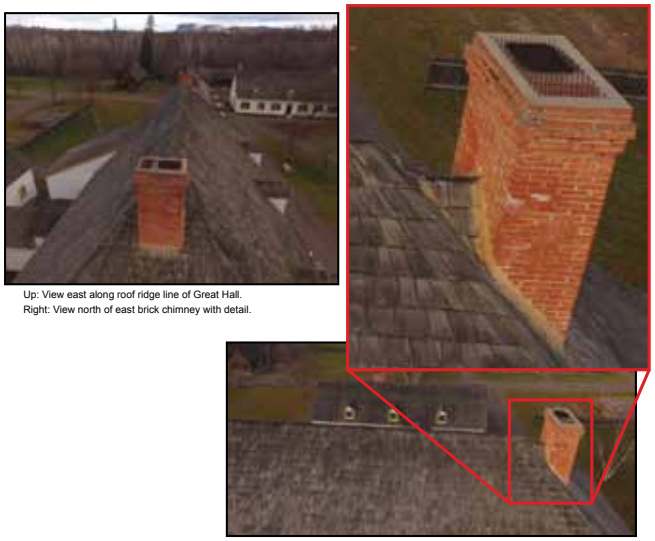

Up: View east along roof ridge line of Great Hall.
Right: View north of east brick chimney with detail.

Figure 36 Details of the roof and chimney of the Great Hall.

The primary value of these data is that it is geo-referenced, and within GIS software can be effectively customized, recoloured and turned on or off, or rendered as the cartographer desires. The UAV Digital Elevation Models produced for three of the known fur trade sites are also geo-referenced raster images, and can be uploaded to the layer 'stack' within the project. While presented at a small scale in Figure 39, the UAV images demonstrate superior topographic resolution. Examination of the imagery at a large scale reveals considerable detail that is lost when scaled to fit in conventional printed pages.

Figure 40 offers a similar GIS model featuring 2 m resolution black and white orthophotography made available by the Manitoba government in the early 2000s. This pre-dated the development of Google earth, and represented a significant improvement in landscape representation over the federal data, particularly when used in concert with the 1:50,000 scale NTS topographic and hydrological data. The UAV derived DEMs are overlaid upon these base layers after rendering them semi-transparent (Fig. 40). While the 2 m resolution orthophotos appear coarse-grained compared to better-quality Google earth coverage, the UAV data offers far more detail and resolution than both.

Figure 41 represents a detail plan of the Fort la Souris site (within Cluster 1). It includes the original topographic isoclines from 1981, and output from the controlled surface collection overlaid upon the UAV DEM. Remarkable consistency is evident between the legacy data and the UAV output. This illustration highlights both the strengths and weaknesses of the UAV approach. The software interprets the vegetation canopy as topographic high zones. This tends to obscure the more subtle ground relief variation that is of archaeological interest. Such interpretation of visible light photography is inferior to relief models deriving from LIDAR imagery. The latter penetrates the vegetation canopy to detect the actual ground surface. But until such imagery is widely available and affordable, UAV imagery clearly offers important advantages, particularly at more open site locations. The real advantage is evident with the time efficiency of a UAV approach. The drone flight was about 15-18 minutes long, with photogrammetric processing completed within 2-3 hours. This flight can be conducted repeatedly under different conditions at low operational cost. This sharply contrasts to the time and labour costs of the original site contour map produced through optical survey.

More intensive evaluation of UAV imagery was conducted at Brandon House 4 (Fig. 38), again comparing legacy data with UAV imagery subsequently

Two flights with different camera orientations provided enough data to render this 3D model. It can be spun, re-scaled and viewed from different perspectives to provide a sence of perspective. Continued research is required to determine whether the Z axis is accurately represented.

Figure 37 3D model of the back side of the Great Hall and the associated Officers' Quarters and attached kitchen.

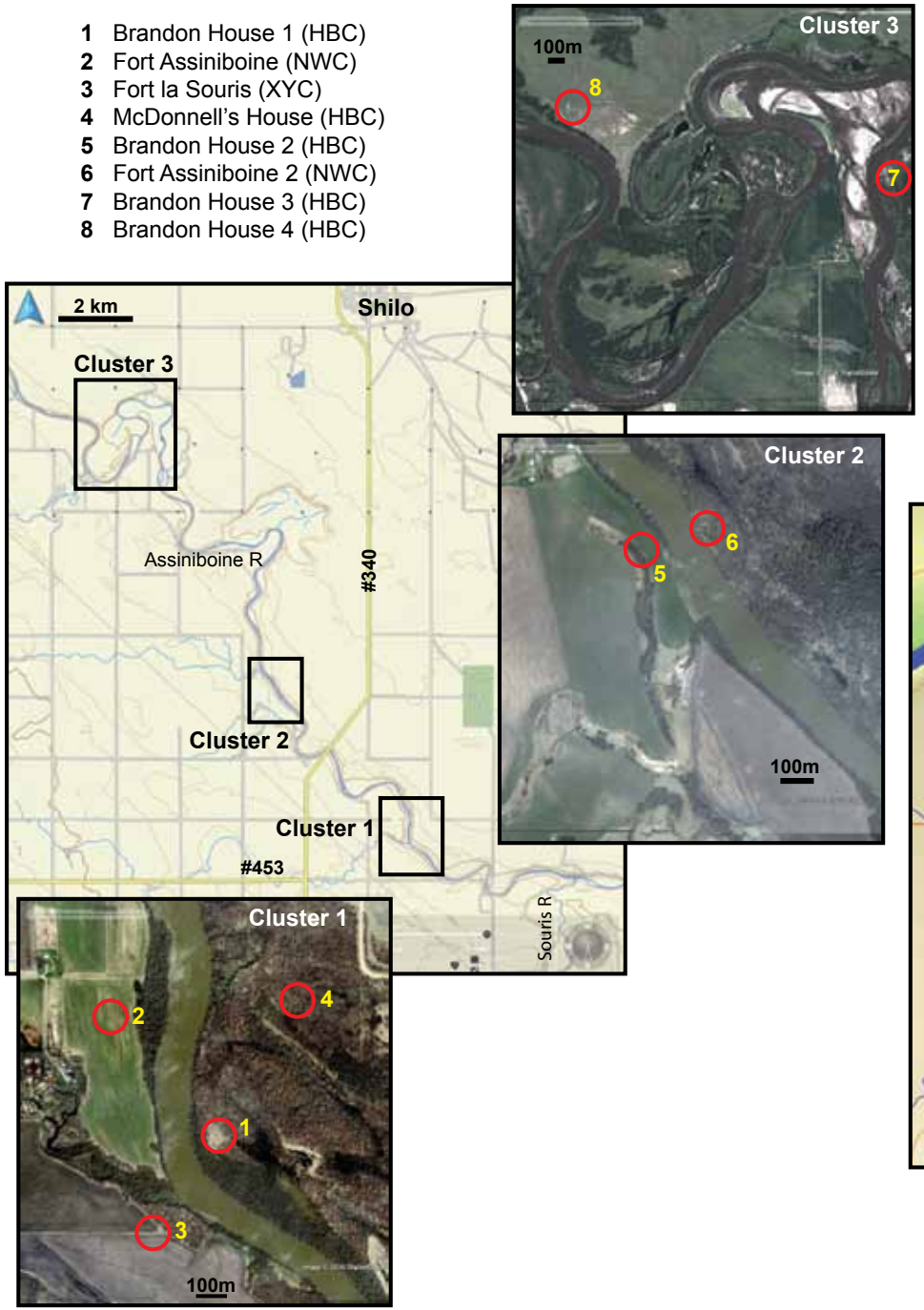

Figure 38 The Souris Mouth Forts along the Assiniboine R. in s. Manitoba.

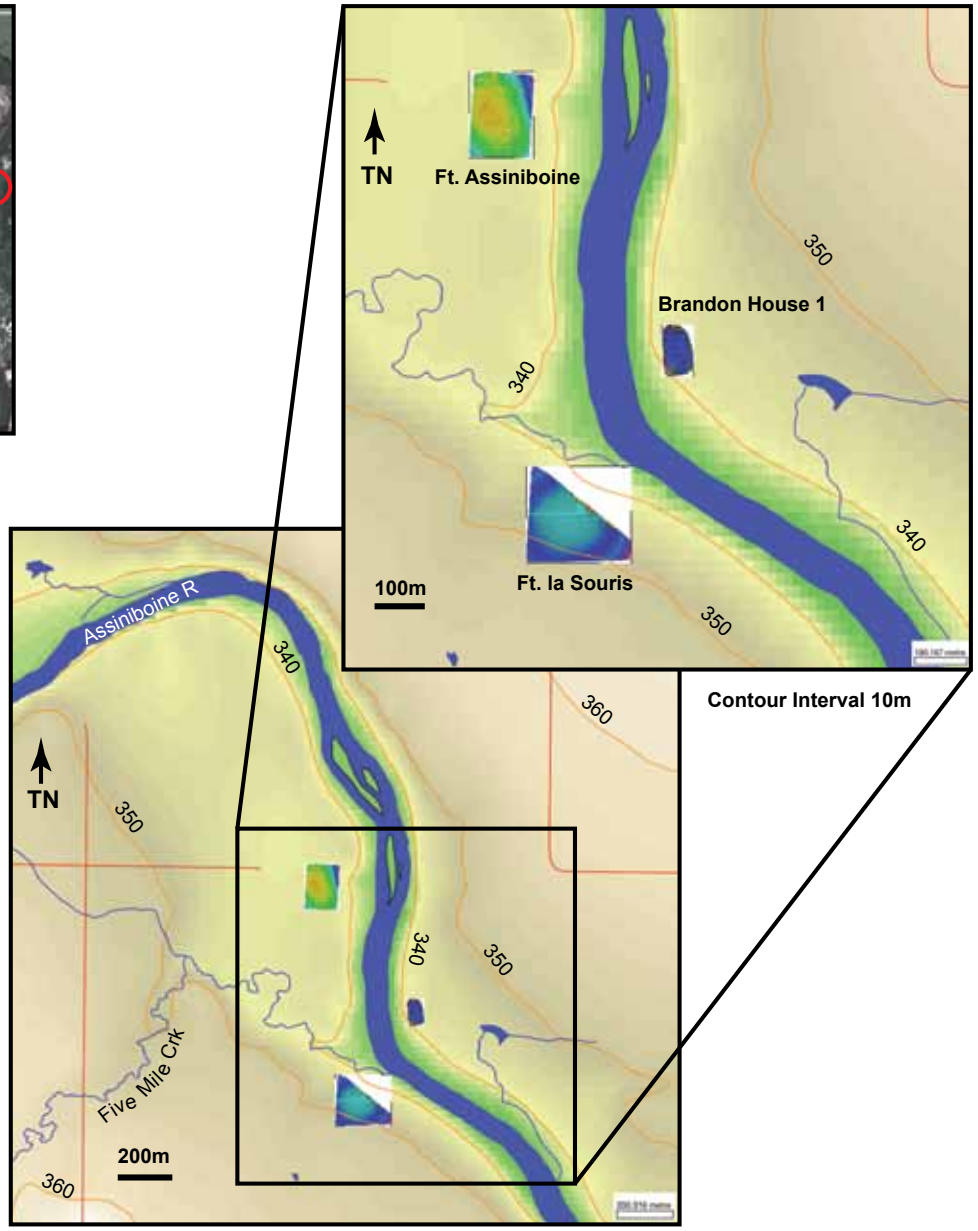

Figure 39 Some relocated fur trade posts within Cluster 1. The map derives from a GIS project that used terrain visualization, contours and hydrology layers (NTS) as a backdrop upon which the geo-referenced Digital Elevation Models are overlaid. Note the data generalization evident in the NTS data in contrast to the topographic detail evident in the drone data.

processed within a GIS (Hamilton in press). This fort site is located on rolling short grass prairie overlooking the Assiniboine River valley. Obscuring vegetation is limited to short grass prairie and low woody shrubs, with much more anthropogenic relief visually evident (Fig. 42). The UAV imagery used to produce this mosaic was collected in less than 20 minutes with a single flight, and was processed within a few hours. Subsequent processing and data refinement within GIS software took somewhat more time as it is an iterative process to find the most effective data representation.

Upon receiving the products of photogrammetric processing, the geo-referenced imagery was imported into GIS software and inspected. The original DEM interpreted the truck, the commemorative cairn, fence posts, and low woody shrubs as topographic high points (Fig. 42). The vegetation is problematic as it sometimes obscures and minimizes subtle evidence of former structural outlines and internal features. Topographic low areas defining hillside slopes below the fort compound are also captured and represented in the colour coding. In the original DEM the colour palette was expended to represent the full topographic range, much of which is not of archaeological interest. This obscures the micro-topography of analytic interest. Further problems derive from subtle colour variations representing archaeologically important relief that is not readily evident to the naked eye, particularly when the data output is reduced for publication.

To help resolve interpretation problems, the original DEM was reprocessed within the GIS to interpolate contour lines. To maximize possible micro-relief interpretability, a 5 cm contour interval was specified (Fig. 43). These isoclines were closely examined and manually modified to aid interpretation. No GIS smoothing functions were applied to them. While the lines are somewhat 'noisy' and affected by vegetation cover, analysis confirmed the topographic range that is of archaeological interest. That is, relative elevations greater than 5.8 m (dark orange to red) and less than 3.75 m (dark blue) are not of archaeological in-

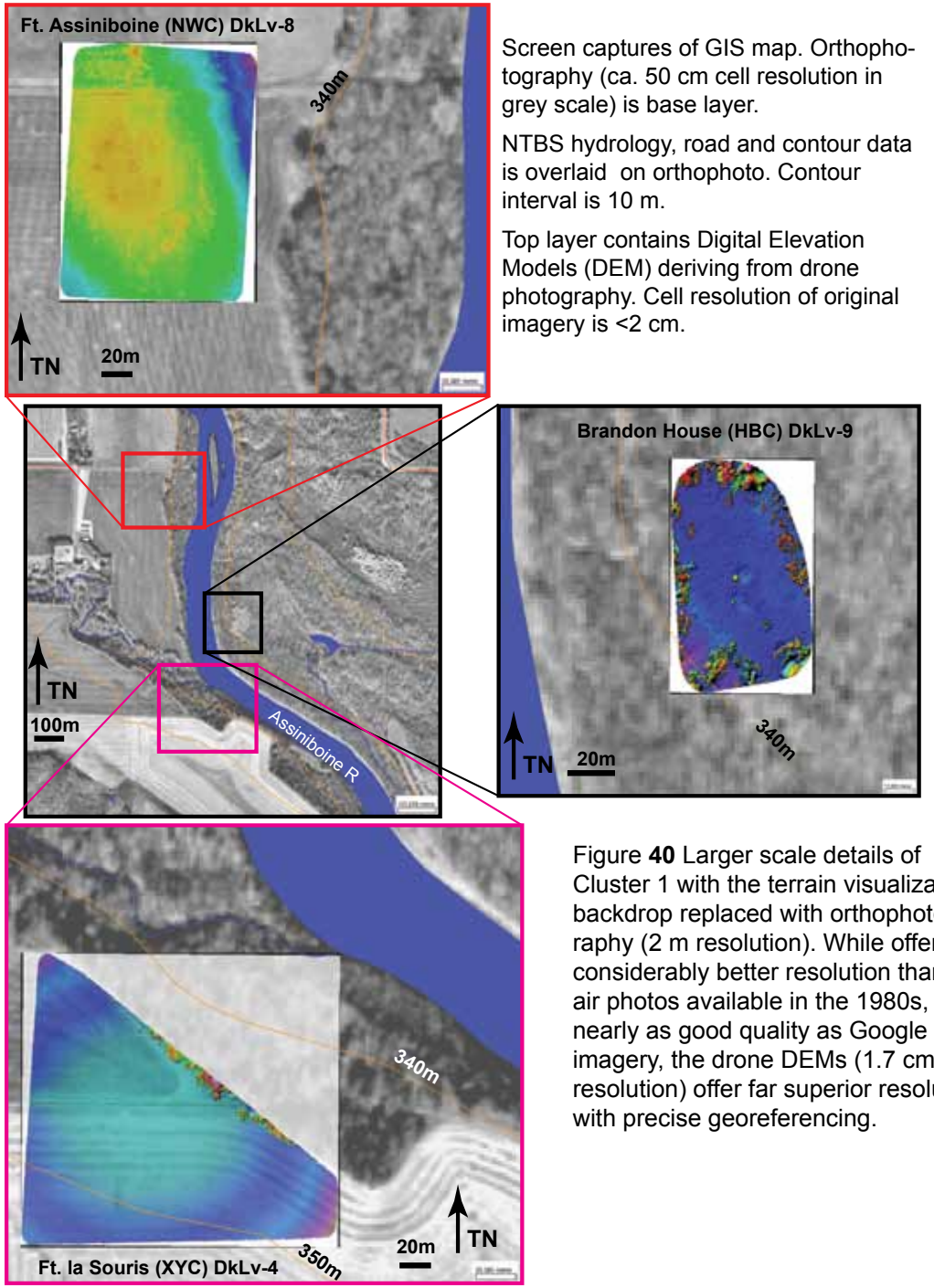

Screen captures of GIS map. Orthophotography (ca. 50 cm cell resolution in grey scale) is base layer.

NTBS hydrology, road and contour data is overlaid on orthophoto. Contour interval is 10 m.

Top layer contains Digital Elevation Models (DEM) deriving from drone photography. Cell resolution of original imagery is <2 cm.

Figure **40** Larger scale details of Cluster 1 with the terrain visualization backdrop replaced with orthophotography (2 m resolution). While offering considerably better resolution than the air photos available in the 1980s, and nearly as good quality as Google earth imagery, the drone DEMs (1.7 cm resolution) offer far superior resolution with precise georeferencing.

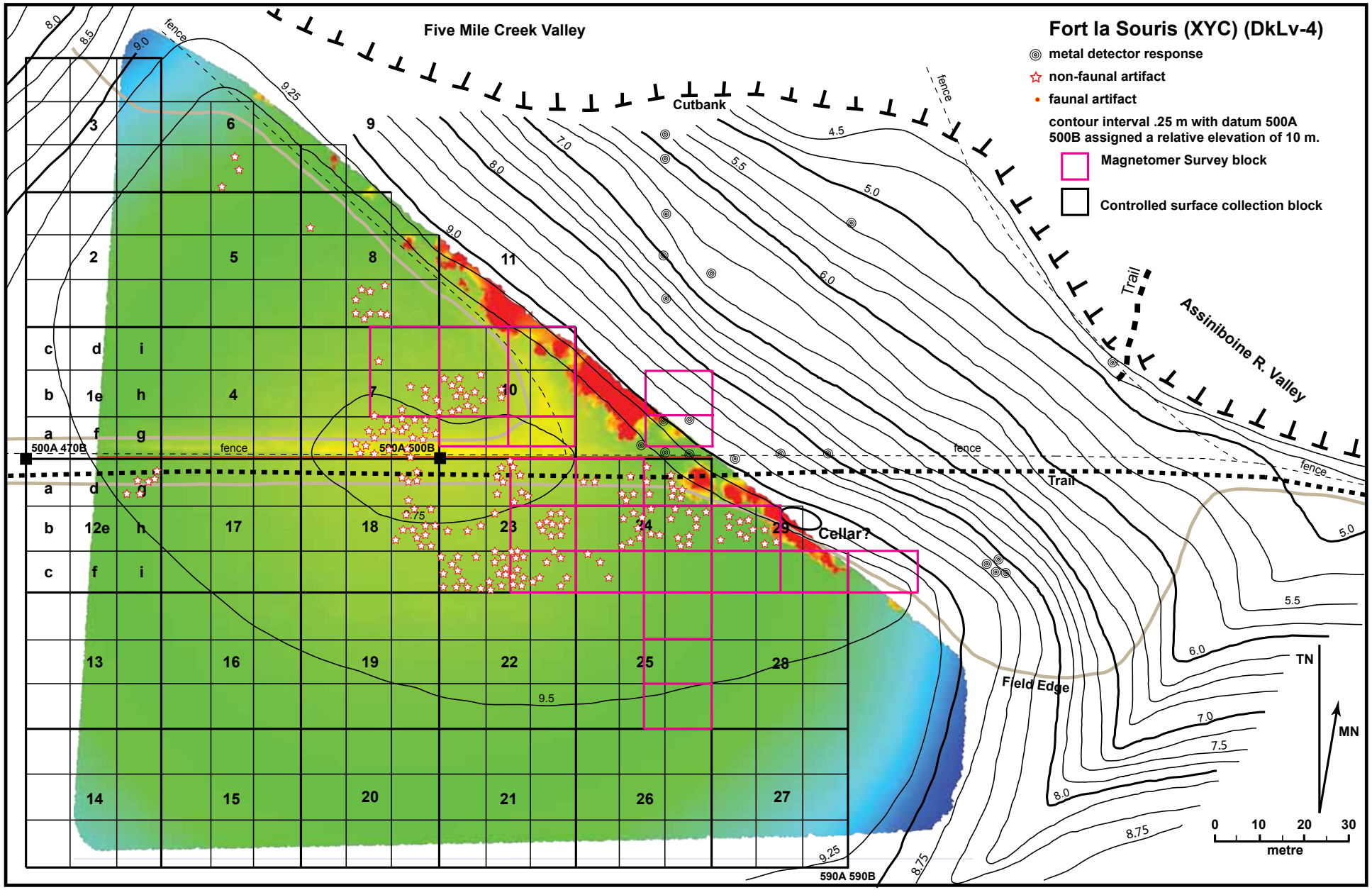

Figure **41** The Fort la Souris site, located on the south bank of the Assiniboine R. within Cluster 1. This site is partially cultivated and partially intact within the forest grove along the field edge. In 1981 it was contour mapped (the black isoclines) and subjected to controlled surface collection. The original map was redrafted and integrated with a appropriately scaled and reoriented version of the DEM deriving from a 15 minute drone flight. The bright red zones mark the tree canopy, while the yellow, green, blue colour spectrum marks topographic variation (affected by vegetation cover). This version of the DEM has been modified within GIS to emphasize the relief variation that is archaeologically relevant.

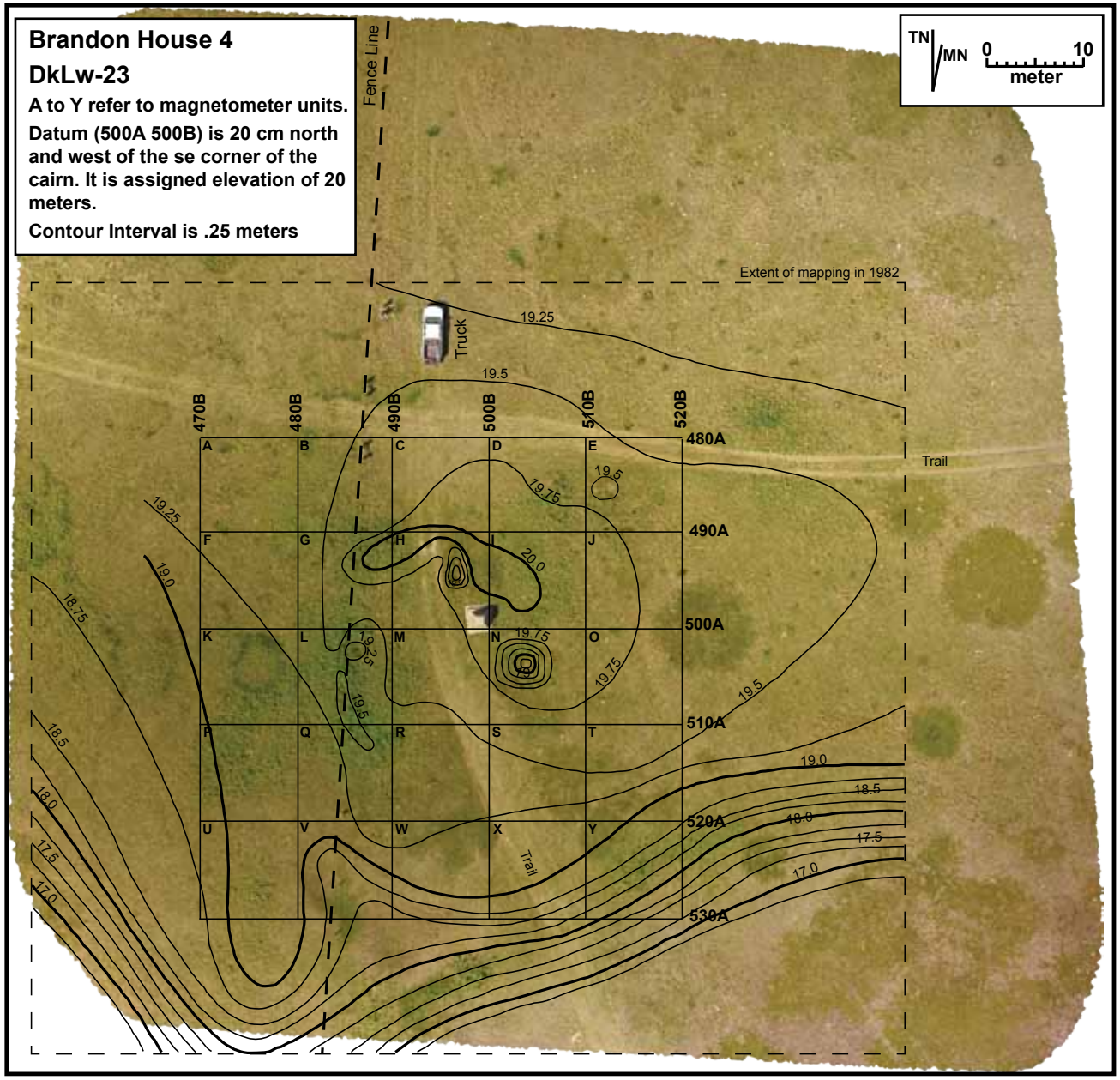

Figure 42 Aerial photo mosaic of Brandon House 4. This image is overlaid with the original isoclines deriving from conventional optical survey which are sufficient to represent some depressions and mounds representing building features.

terest (Fig. 43). These elevations were used to define 'break points' to minimize the colour range expended on archaeologically irrelevant relief, leaving the remaining colour range to represent more subtle relief change (between 3.75 and 5.8 m). Coupled with the contour lines, this provided an effective (and analytically robust) means of drawing attention to analytically relevant relief variation. These data were then compared to the results of the proton magnetometer survey conducted in 1982 by Dr. Terry Gibson (Western Heritage Services). This sought to address the utility of multi-proxy remote sensing methods (including UAV) to aid in non-invasive interpretation of the structural layout and use of space within and around the fort compound (Hamilton in press, Fig. 44).

The refinement of UAV output within GIS software proved useful at Brandon House 4 in the ideal circumstances of good ground visibility. This degree of visibility is not common without first clearing vegetation cover. Our ongoing experimentation using these approaches to site documentation have proven sufficiently useful to justify the effort at site preparation.

The final case study presented reflects efforts to amplify documentation of the Brockinton Bison Kill site, first investigated by E. Leigh Syms in 1971. This site is located along the east bank of the Souris River about 8 km south of Melita, Manitoba (Fig. 45). This late pre-contact communal bison kill is on the lower terrace overlooking the river at the base of the valley wall, and is deeply buried by subsequent sediment accumulation. While focusing upon test excavation of the area eroding from the cut bank, Syms sketched the slopes and gullies draining down from the top prairie level to the kill zone in an effort to understand communal kill operations. The UAV flight sought to determine whether it could add substantive detail to this interpretation despite the mature forest that currently mantles the valley wall (Fig. 45). The image mosaic depicts the deciduous forest vegetation (in its fall colours), with Syms' excavation and interpretative information overlaid.

Figure 45 demonstrates remarkable consistency

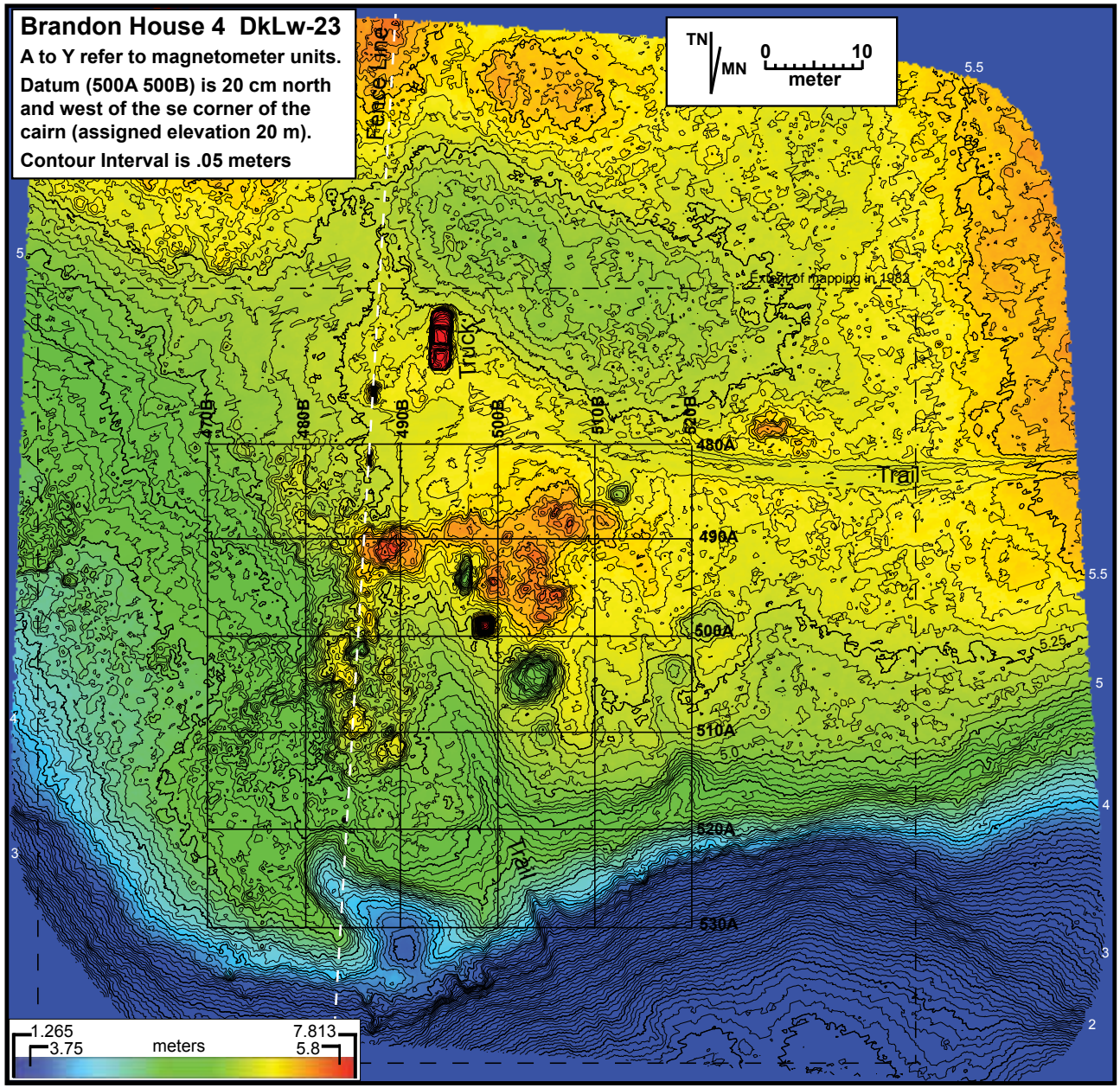

Figure 43 The DEM of Brandon House 4. It was further processed within GIS software to interpolate contour isoclines (5 cm contour interval), and then the colour coding of the DEM was modified to minimize analytically trivial relief and emphasize that reflecting archaeological features. This identified subtle landscape features of anthropogenic interest that were undetected during ground inspection and optical survey mapping.

between the sketch map and the geo-referenced drone output. Since the drone image derives from relatively brief time investment in data collection and processing, it has considerable utility compared to that required to produce similar output using conventional mapping methods. Figure 46 contains the DEM deriving from the original photogrammetric processing. The colour palette is automatically assigned to document relief change from the lowest detected surface (dark blue) to the highest (red, purple). Again, subtle undulations in the ground surface are obscured as the software uses much of the colour palette to document the tree canopy. While visually effective, the analytic value of the elevation model is obscured.

In an effort to 'correct' this negative effect, the Brockinton output was reprocessed using GIS (Fig. 47). The isocline operation was used to arithmetically document relief, and more systematically identify that of analytic interest. These elevations were again used as 'break points' to electronically stretch the colour palette to minimize the colour range used to represent analytically trivial relief, and to emphasize that of archaeological interest. This improves the interpretability of the imagery, and renders more explicit the rationale behind site interpretation. That said, we note the gully reported by Syms which he identified as important for understanding how the animals were directed down the valley wall and into the kill zone. This insight derives from ground inspection, but it is obscured and rendered 'invisible' in the UAV imagery (Fig. 45, 46 and 47). That said, the DEM interpretation represented in Figures 46 and 47 offers more detail and corrects scaling and interpretative errors evident in Syms' sketch of the valley wall. Clearly, UAV-derived remote sensing serves to supplement, amplify and validate conventional field archaeological inspection.

Summary and Conclusion

Over the past 3 years of testing UAV application to archaeology we have experienced mixed success, including a crash that rendered the first drone inoper-

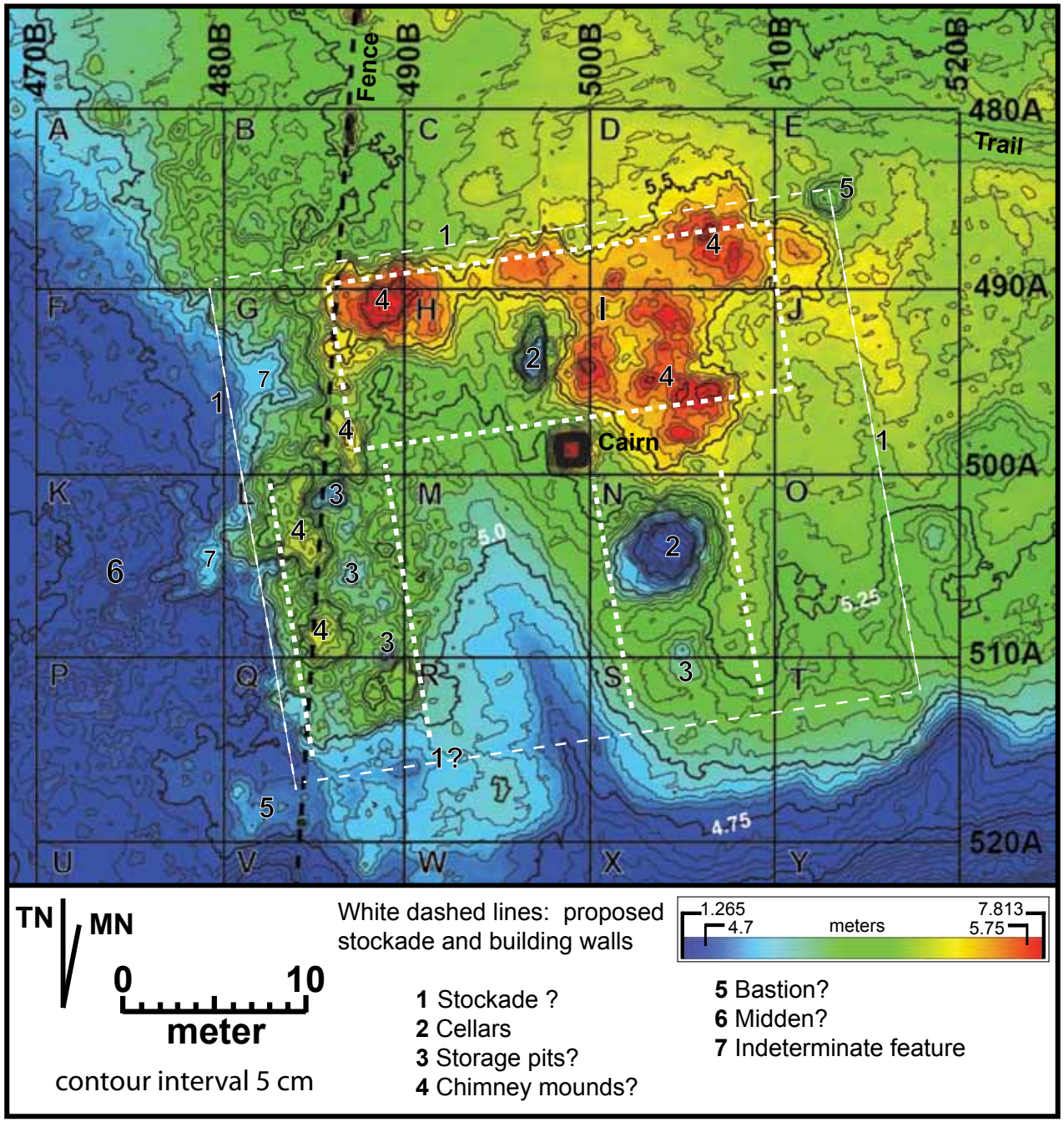

Figure 44 Interpretation of the DEM of Brandon House 4.

able. Hindsight indicates that this should be expected as we were simultaneously developing piloting and photography skills, while also evaluating UAV utility for archaeological documentation.

Purchasing a mid-range drone is a costly undertaking. While vulnerable to currency exchange rates, investment of between $1500 and $3500 should be anticipated for a drone, extra batteries, a tablet, spare parts, a carrying case, and extra mini-SD cards. Also of consideration is the intended purpose of the imagery. If still and video photography is the primary outcome, then a standard computer with image and video processing software is sufficient. If photogrammetry software is to be used, then one should expect additional costs related to software licences and high speed computers. We chose to use a photogrammetry service to reduce these short-term costs, but we have subsequently invested in equipment and software to aid in-house photogrammetry and 3D modelling.

Important improvements were noted between the Blade (purchased in the fall of 2014) versus the Phantom 3 (purchased in the fall of 2015). The removal of the 'fish eye' distortion problem is particularly important development.

Another important development derives from the improved telemetry control that provides in-flight information to reduce crash risks, and to generate more accurate image metadata. The more recent generations of UAVs feature enhancements that render the Phantom series obsolete. Automated collision avoidance capacity is one important development. The sharply improved flight range associated with the Phantom 3 is also noteworthy, as is gradual improvement in battery life. Finally, the development of automated flight Apps to enable more effective and stable flight missions and maximizing battery use represents a major innovation. It greatly improves the planning and execution of flights, and enables production of high quality photo mosaics, DEMs and 3D output.

Issues that remain to be addressed with most

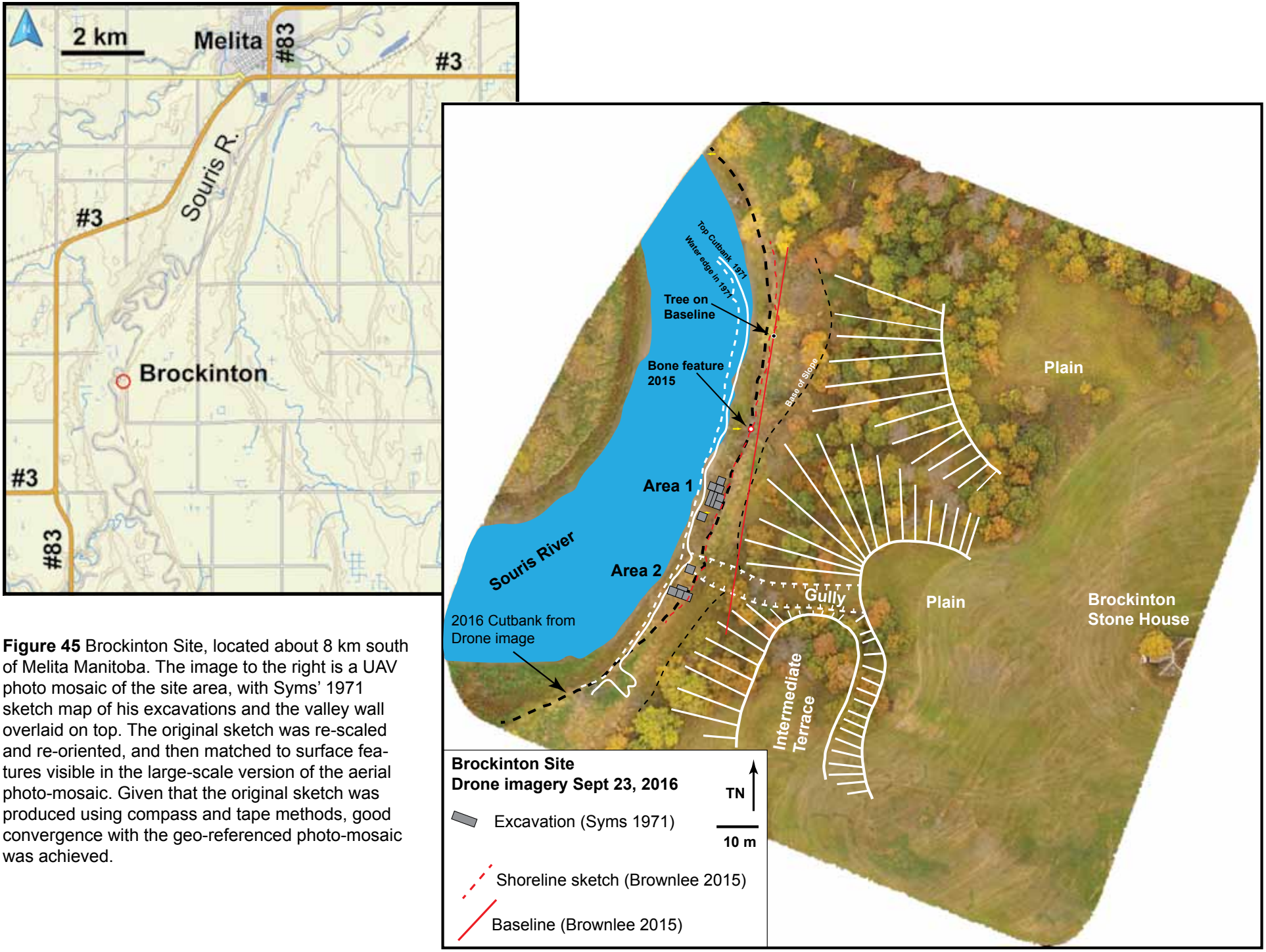

Figure 45 Brockinton Site, located about 8 km south of Melita Manitoba. The image to the right is a UAV photo mosaic of the site area, with Syms' 1971 sketch map of his excavations and the valley wall overlaid on top. The original sketch was re-scaled and re-oriented, and then matched to surface features visible in the large-scale version of the aerial photo-mosaic. Given that the original sketch was produced using compass and tape methods, good convergence with the geo-referenced photo-mosaic was achieved.

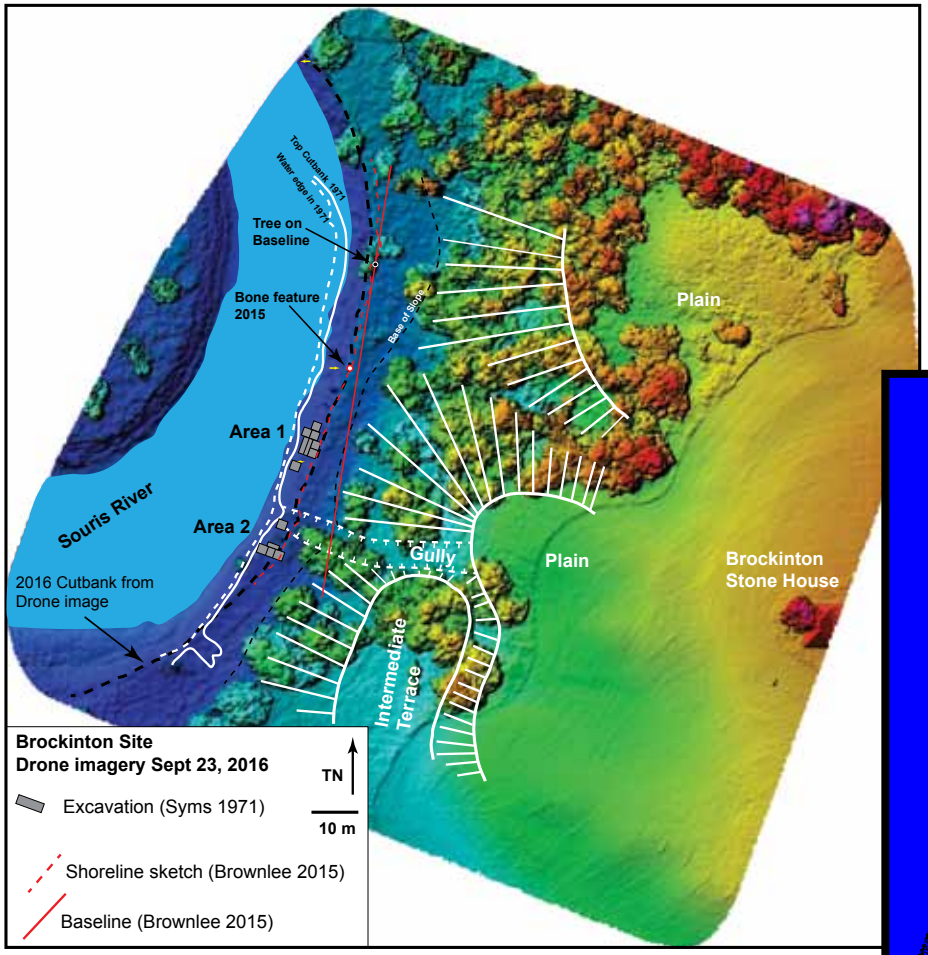

Figure 46 Original DEM of the Brockinton Site overlaid with Syms' sketch map. Topographic low areas are defined by dark blue, while high areas range from green, yellow, red and to purple. Gaps in the tree canopy reveals the relative elevation of the ground surface trending downwards from the top prairie level (yellow-orange), while much of the red and purple colour range represents the top tree canopy.

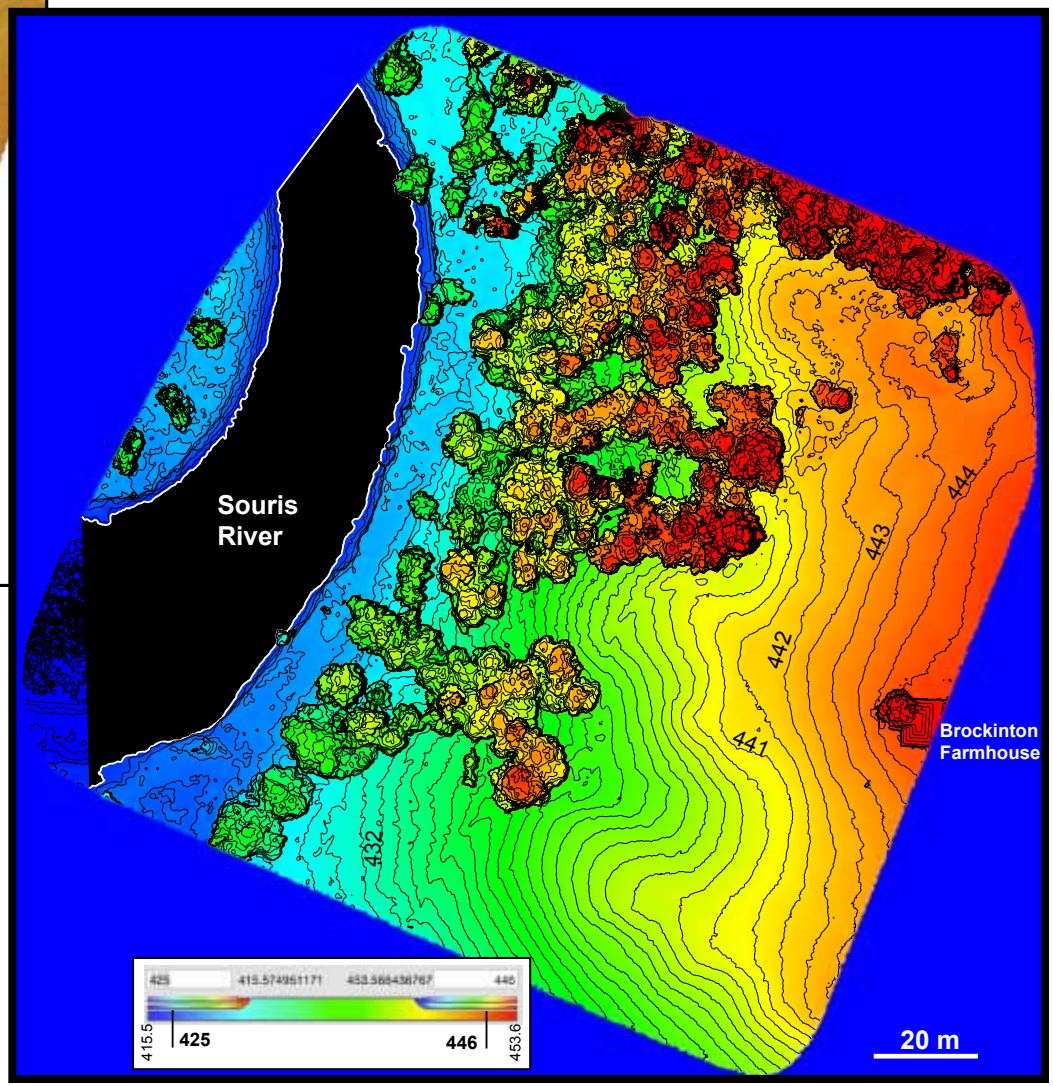

Figure 47 The Brockinton DEM rendered and modified using GIS. Elevations below 425 are uniformly coloured dark blue, while those above 446 are shaded red. This leaves the balance of the colour spectra available to symbolize elevations between 425 to 446 m. These modifications were undertaken after first subjecting the DEM to interpolation to define contour lines (.5 m intervals). The resulting map offers both visual and arithmetic representation of the landscape to aid interpretation of how the valley wall was employed for communal capture and killing of bison.

prosumer drones is the comparatively short battery life that limits flight time, and some limitations on camera adjustments to address difficult lighting conditions. The latter issues can be addressed with more 'trial and error' experimentation. We also note continued challenges with temperature and wind related limitations upon flights.

Another emerging innovation will be the ability to mount interchangeable cameras/sensors on the prosumer drones so that collection of imagery beyond the visible light spectrum is possible. As the market for consumer drones continues to grow, ongoing research and development of lithium batteries, more power-efficient micro-processors, radio-transmitters and engines may alleviate to some of the power management issues.

UAV technology continues to evolve as a growing number of manufacturers improve the capacity and flying ease of their equipment, and market to hobbyists and professionals. Not unlike the consequences of micro-computers 30 years ago and GPS technology 15 years ago, we expect a revolutionary transformation of UAV technology and its application over the next 2 to 5 years. This will be represented by improved capacity and broader application, coupled with sharp price declines. This makes it difficult to justify early purchase of expensive technology that will quickly become obsolete, but this is the price of early experimentation and application of technology. Notably we observed continued utility of the Phantom 3 series long after the development of models with new features

Perhaps the greatest impediment to widespread integration of UAV technology into routine archaeological site documentation is the increasingly complex regulatory environment affecting drone operations in Canada and the USA. This is coupled with the requirement for insurance coverage for those seeking to use UAVs for research and commercial purposes. Such non-hobby flying requires the operator has certification issued by Transport Canada (Special Flight Operations Certificate or SFOC). While both of us gained this certification in 2016, changing regulations resulted in Hamilton failing to get his licence renewed in 2017. While frustrating, this is indicative the gradual refinement of regulatory expectations for drone operations to support research or commercial application. Inappropriate use of drones can represent a real risk to property and people, particularly in crowded airspace, or if they are flown over urban or populated areas. Routine use of drones to collect low elevation imagery requires operators to professionalize their skills, and become aware of their responsibilities as aircraft pilots even though we have our feet firmly planted on the ground.

References

Dawson, K.C.A.
1965 'The Kaministikwia Intaglio Dog Effigy Mound' *Ontario Archaeology*, No. 9, p.p.25-34.

Hamilton, S.
1982 '*1981 Archaeological Reconnaissance of the Souris Mouth Area.'* Unpublished field report submitted to the Manitoba Historic Resources Branch, Manitoba Dept. of Culture, Heritage and Recreation, Winnipeg.

1983 '*The Remote Sensing Activities at the Souris Mouth Forts: A Summary'* Unpublished field report submitted to the Manitoba Historic Resources Branch, Manitoba Dept. of Culture, Heritage and Recreation, Winnipeg.

1996 *Pleistocene Landscape Features and Plano Archaeological Sites upon the Kaministiquia River Delta, Thunder Bay District*. Unpublished site report, Dept of Anthropology, Lakehead University.

2000 'Archaeological Predictive Modelling in the Boreal Forest: No Easy Answers' *Canadian Journal of Archaeology*. Vol. 24, issues 1 and 2 pp. 41-76.

2017 'Drone-based air photography and photogrammetry trials at archaeological sites in southern Manitoba.' Unpublished license report submitted to the Manitoba Historic Resources Branch, Winnipeg.

in press 'Drone mapping and photogrammetry at Brandon House 4" Paper accepted for publication by Society for Historical Archaeology.

Hamilton, Scott and Jason Stephenson
2016 'Testing the utility of UAV (quadcopter) aerial photography and photogrammetry for archaeological documentation'. Unpublished discussion paper for electronic redistribution on ResearchGate https://www.researchgate.net/publication/299503960.

2017 'Archaeological case studies of drone photography and photogrammetry' Newsletter of the Manitoba Archaeological Society, Winnipeg, also available through ResearchGate https://www.researchgate.net/publication/315736037.

Julig, Patrick J.
1994 *The Cummins Site Complex and Paleoindian Occupations in the Northwestern Lake Superior Region* Ontario Archaeological Reports 2, Ontario Heritage Foundation, Toronto.